Processing Report

MDM – Beaufort Cable Route

GR-GEO-REP-24G01 Beaufort

Confidential - Draft prepared for Client review

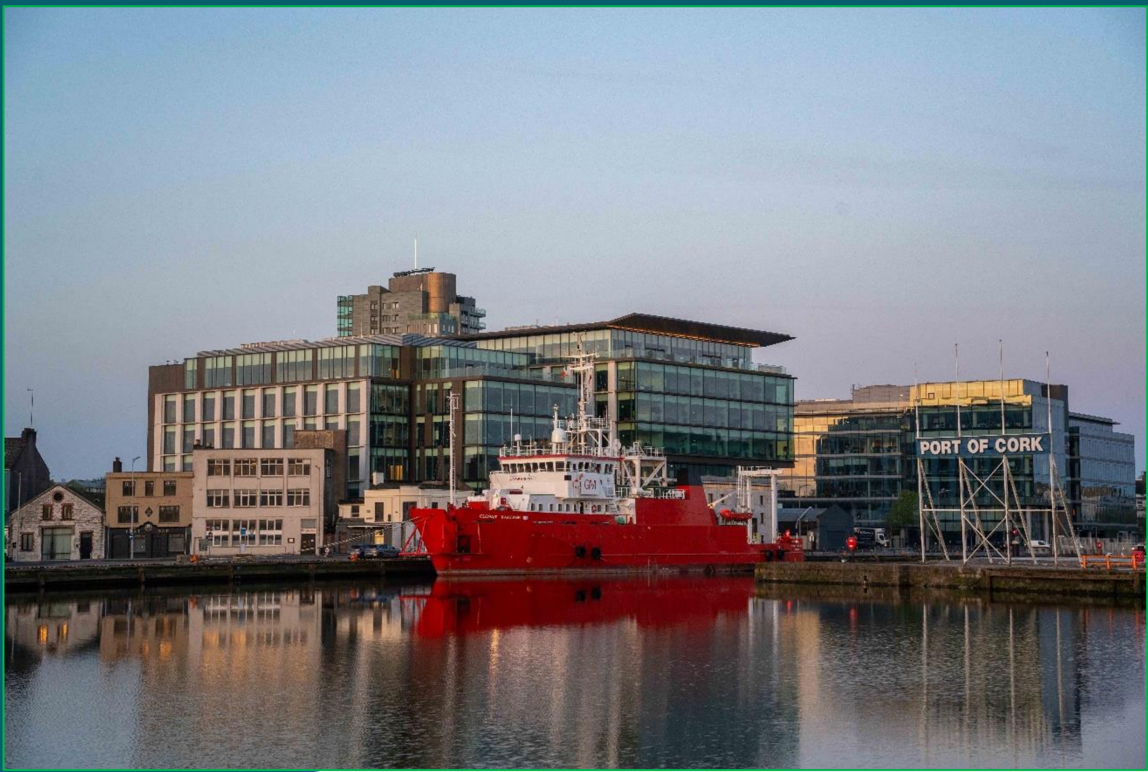

Prepared for: MDM McMahon Design & Management Ltd

By: GREEN REBEL

25 November 2024

Document Information Summary:	
Document Title:	Processing and Interpretation Report – Beaufort Cable Route
Document Reference Number:	GR-GEO-REP-24G01 Beaufort
Document Confidentiality:	Confidential - Draft prepared for Client review

Document Control:

Date:	Revision:	Revision Description:	Prepared By:	Reviewed By:	Approved By:
25 November 2024	002	Revision 2	SB, JM, LOH, BÓG, OMcC, EB, ER	EOM	JP

Contents

Executive Summary

Green Rebel Ltd was contracted by McMahon Design and Management Ltd (referred to herein as 'the client') to complete a reconnaissance grade geophysical and hydrographic investigation of a new potential cable route, in the Irish Sea, spanning from the UK, Welsh coast to the territorial waters of Ireland, roughly adjacent to the Wexford Coast. The investigation consisted of the acquisition, processing and interpretation of sub-bottom profiler, multibeam bathymetry and backscatter, side-scan sonar, and magnetometer data. The purpose of the investigation is to underpin and support the development of the cable route through:

- The identification and mapping of potential geohazards.
- The facilitation of the development of a ground model.
- The provision of data and information to inform Cable Burial Risk Assessment (CBRA).

To this end, Green Rebel commenced Beaufort geophysical and hydrographic survey operations on the 1st of July 2024. Total Beaufort survey operations with all infills before demobilisation were completed on the 16th of July 2024. Data were processed, analysed, and interpreted; the results are presented herein.

This report presents background information that includes a summary of the Beaufort project objectives and variations from the scope of work. Following this, the acquisition and subsequent processing steps for each type of geophysical data (multibeam, side-scan sonar, magnetometer and sub-bottom profiler) are described. The classifications used for analyses are described. Finally, the results of the data analyses are documented; these are organised by the type of data.

Definitions, Symbols and Abbreviations

AOI	*Area Of Interest*
ARA	Angular Range Analysis
BIIS	British-Irish Ice Sheet
CTI	Chesapeake Technology International
DEM	Digital Elevation Model
DOP	Dilution Of Precision
EGN	Empirical Gain Normalisation
EIAR	Environmental Impact Assessment Report
ETRS89	European Terrestrial Reference System 1989
FOM	Figure of Merit
GIS	Geographic Information System
GNSS	Global Navigation Satellite System
GPS	Geographic Positioning System
GSI	Geological Survey of Ireland
HDOP	Horizontal Dilution Of Position
IHO	International Hydrographic Organization
ISIS	Irish Sea Ice Stream
ka BP	thousand (calendar) years Before Present
LAT	Lowest Astronomical Tide
MAG	Magnetometer
MBES	Multibeam Echosounder
NaN	Not a Number
NMO	Normal Move Out
pUXO	Potential Unexploded Ordinance
QC	Quality Control
QINSy	Quality Integrated Navigation System
SBP	Sub-bottom Profiler
SSS	Side-scan sonar
THU	Total Horizontal Uncertainty
TVU	Total Vertical Uncertainty
USBL	Ultra-short Baseline
VDOP	Vertical Dilution Of Position
VORF	Vertical Offshore Reference System

List of Tables

List of Figures

1 Introduction

1.1 Survey objectives and Scope of Work

The objectives of the survey are described in the "Purpose of Investigation" in the Scope of Work (SoW). The desired outcomes of the project as stated in the SoW include:

- Identify and map potential geohazards.
- Provide data and information in support of Environmental Impact Assessment reporting.
- To provide relevant seismic information to inform Cable Burial Risk Assessment (CBRA).

To achieve these outcomes, the data deliverables outlined in Table 1 were stipulated by the technical specifications.

TABLE 1: LIST OF MAIN DATA DELIVERABLES (ADDITIONAL DELIVERABLES SPECIFIED IN THE DATA MATRIX).

Type	*Description*	*Resolution (m)*	*File*
Kingdom projects	Projects containing SBP horizon files and data	NA	NA
Position	Tracklines for each sensor	NA	*.shp
Multibeam Bathymetry	LAT-corrected, post-processed, IHO 1a bathymetric grid	1.0, 0.25	*.tif, *.xyz
Multibeam backscatter	Multibeam backscatter grid	1.0	*.tif, *.xyz
Side-scan sonar data	Single line data corrected for navigation (including heading) with no additional processing applied	NA	*.xtf
Side-scan sonar mosaic	Processed low-frequency side-scan sonar grid	0.2	*.tif
Magnetometer	Processed magnetometer track plots	NA	*.shp
Magnetometer	Picked magnetometer targets	NA	*.shp
Magnetometer	Processed magnetometer files	NA	*.csv, *.shp
Sub-bottom profiler data	Processed sub-bottom profiler data in time	NA	*.sgy
Sub-bottom profiler horizon files	Picked horizon files for the main reflectors	NA	*.csv
Side-scan sonar target list	Target list of selected contacts from side-scan sonar data to include Target ID, X, Y, Contact Type	NA	*.xlsx
Mobilisation Report	Presented to MDM representative within 48 hrs of mob completion.	NA	*.doc, *.pdf
Survey Operations Report	Completed within 1 week of survey completion.	NA	*.doc, *.pdf
Data Acquisition, Processing and Interpretation Report	To include full details of processing and interpretation results.	NA	*.doc, *.pdf

1.2 Variations from the SoW

Table 2: Summary of variations from the SoW.

Reference Number	Description	Cause
Var-001	Consolidation of Tuskar Routes and additional Kms	MDM request to GR
Var-002	Additional survey scope to below 5m LAT for Lady K	MDM request to GR
Var-003	Additional scope for Newport Connect (281 km) for Lady K	MDM request to GR
Var-004	Additional infill, standby and technical breakdown items	MDM request to GR
Var-005	Additional infill, standby, fishing gear, route development, weather, and technical breakdown items	MDM request to GR
Var-006	MMO, accommodation, Client rep, IT, additional scope	MDM request to GR

1.3 Reference Documents

Table 3: Summary of referenced documents.

File name	Title	Author
MDM Survey Clarifications - Scope	MDM Survey Clarifications	MDM

1.4 Summary of Findings

Table 4: Summary of findings, including metadata, quality, results, interpretations, and potential hazards.

Acquisition	
Survey Dates	1 – 16 July 2024
Geophysical systems used	MBES, SSS, MAG, SBP
Bathymetry	
Complex relief, with highs and lows. Depth range: -46.05 to -135.66 mLAT	
Seafloor Morphology	
Sediment waves, trochoidal sediment waves (small, medium, large and very large), possible tunnel valleys, iceberg plough marks and exposed bedrock outcrops identified in the MBES bathymetry data	
Seafloor sediments	
Fine, medium, coarse acoustic facies and bedrock outcrops identified in MBES backscatter data	
Seabed Targets and Potential Site Specific Hazards	
Wrecks	0
Boulders	3072

Acquisition	
Other Targets	9
Potential Hazards	
Steep gradients	Present, associated with sediment waves and bedrock outcrops
Mobile sediments	Present, sediment waves of various scales
Shipwrecks	0, no clear wrecks in MBES/SSS
Magnetic anomalies	49: 35 monopoles, 14 dipoles
Boulders	3072 boulders detected in SSS waterfall
Cables	2 extant cables identified in the dataset

Subsurface Geology	
Seismic Unit 1	Seismic Unit 1, referred to as SU1 (Table 12), is the shallowest (stratigraphically youngest) unit. SU1 is delineated by the discontinuous horizon H2 (top). Acoustically, SU1 is characterised by a high amplitude top reflection i.e.H1, and low to high amplitude base (Figure 46), displaying occasional stratification and cross bedding but typically appears as massive internally. As H2 sits at the seabed surface, it has a depth below seabed value of 0 m (Figure 46).
Seismic Unit 2	Seismic Unit 2 (SU2, Table 12) is laterally dis-continuous and is delineated by its top horizon H3 (Figure 46 and Figure 47). Acoustically, SU2 is described as having low to moderate amplitude reflectors with a chaotic internal reflection pattern. SU2 is predominantly found in the west of the site between KP46 – KP62. The depth below seabed values for H3 range from 0.00 - 6.48 m (Figure 46 and Figure 47) with an average depth of 1.24 m and a standard deviation of about 1.20 m.
Seismic Unit 3	Seismic Unit 3, referred to as SU3 (Table 12) is discontinuous and is delineated by its top horizon H4. SU3 is characterised as a massive unit of sediment, mostly transparent internally with moderate to relatively low amplitude chaotic reflections. Unit SU3 is similar to SU2, however the erosive top horizon H4 separates the two units marking an unconformity. The depth below seabed values for the top of SU3 (H4) ranges from a 12.93 - 2.68 m, with a mean depth of 8.34 m and a standard deviation of about 2.40 m.
Seismic Unit 4	Seismic Unit 4, referred to as SU4 (Table 12), is delineated by the H5 (top) and H6 (bottom) horizons. Internally, SU4 consists of low to moderate amplitude internal reflector displaying a well stratified sediment which appears conformable with the overlying unit SU3 but uncomfortable with SU5 (Figure 47 and Figure 49). The depth below seabed values for the top of SU4 (H5) range from 0.00 – 21.98 m (Figure 46), with an average depth of 12.10 m and a standard deviation of about 5.06 m.

Subsurface Geology	
Seismic Unit 5	Seismic Unit 5, referred to as SU5 (Table 12), is characterised by chaotic reflections (Figure 49) and is delineated by the discontinuous H6 (top) and H7 (bottom) horizons. SU5 is found throughout the survey site. Internally, SU5 displays mostly transparent or chaotic reflectors. SU5 is typically a sub-surface unit, however, it is identified at the seabed in several areas, particularly in the east. The depth below seabed values for the top of SU5 (H6) range from 0.00 - 30.20 m (Figure 49), with an average depth of 9.19 m and a standard deviation of about 7.98 m.
Seismic Unit 6	Seismic Unit 6, referred to as SU6 (Table 12), is characterised by the moderate to high amplitude reflection of H7 (top) (Figure 49). Its base is not observed in this survey. Internal reflections within the SU6 are poorly resolved with limited occurrences of low amplitude and chaotic reflections. The depth below seabed values for H7 range from 2.01 – 18.91 m, with an average depth of 6.90 m and a standard deviation of about 3.53 m. From bathymetry and backscatter data, cleavage and bedrock morphology are visible in the east of the site and consequently have been picked as such in the seismic interpretation. Seismic profiles do not display a clear distinction between this outcropping bedrock and the surrounding sediments as there is limited attenuation of seismic signal beneath the surface where this outcrop is identified. Internal reflections within SU6 appear transparent (Figure 51). Bedrock outcrops at the surface between KP 8 and KP 10.

2 Data Acquisition and Processing

2.1 Surface and subsurface positioning

2.1.1 Surface positioning

There were two independent global navigation satellite systems (GNSS) installed on top of the vessel's geotechnical gantry on the back deck. The antennae were mounted as high as possible to ensure optimal signal reception. Details of the GNSS systems are presented below in Table 5.

Table 5: Positioning system aboard MV Glomar Vantage.

GNSS	Antenna Type	Corrections	Output Interval
Applanix Oceanmaster	Trimble 540AP (x2)	Fugro Marinestar G4	50 Hz
C-Nav X1	C-Nav289	C-Nav LEO	5 Hz

An inertial navigation system (INS) attitude and heading reference system (AHRS) were mounted close to the MBES system on the lower moonpool hatch. A secondary AHRS is mounted close to the edge of the vessel moonpool. Details of these systems are presented below in Table 6.

Table 6: AHRS on board MV Glomar Vantage.

Attitude and Heading Reference System	Control
Applanix Oceanmaster IMU 65	Applanix POSView v11.43
iXblue Octans 3000	Web GUI

2.1.2 Sub-surface positioning

cNODE Micro ultra-short baseline (USBL) system was used for underwater positioning of towed survey equipment. The USBL transducer is mounted to a plate that is welded to the lower moonpool hatch. This hatch is deployed in a vertical orientation during survey operations. The system does not require infield calibration as there are inbuilt motion and heading sensors. This system receives time synchronised positioning input from the primary GNSS system.

2.1.3 Tidal Reduction Methodology

Vertical corrections were applied to the data in real-time via Quality Integrated Navigation System (QINSy) using the PPP and RTK systems. All data were then reduced specifically to Lowest Astronomical Tide (LAT). To do this, the UCL and UKHO product, Vertical Offshore Reference Frames (VORF) system was used. The VORF project allows to seamlessly transform vertical height information to other common coastal and offshore levels within the Irish and UK nautical zones.

2.2 Multibeam bathymetry data (including tidal reduction methodology)

2.2.1 Data acquisition

Bathymetric and acoustic backscatter data were acquired using a dual head Reson SeaBat T50-R multibeam echosounders (MBES). Each MBES transceiver produces 1,024 beams per ping and can operate from 190 to 420 kHz. During the Beaufort survey operations, the MBES was typically operated at a frequency of 400 kHz. Opening beam angles were dynamically adjusted to ensure sufficient coverage. The sonar heads were integrated with a real-time sound velocity sensor, an iXBlue HYDRINS inertial navigation system and two independent GNSS antennas (C-Nav and Hemisphere).

Data were acquired in a gridded survey design. Survey speed was approximately 4.5 knots. Sound Velocity Profiles were acquired at a minimum of every 12 hours but always whenever clear changes were observed in sound speed recordings (QINSy alarm set to sound velocity changes greater than 2 m/s). A Valeport Swift sound velocity profiler was used for SVP casts and a total of 14 profiles were recorded during acquisition. Data acquisition was managed in QINSy which was also used to visualise raw data and save *.db files with raw multibeam data. All data were stored on a dedicated offshore data server.

2.2.2 Processing workflow

Multibeam bathymetric data are interpreted to accurately measure water depth, capture seafloor features, geomorphology and other objects like shipwrecks. Raw multibeam echosounder data were acquired and stored in a series of QPS *.db files. These files contain the raw sounding, GNSS, altitude and applied sound velocity data. As such, data processing was required to merge these data, remove or correct anomalous data, create a bathymetric surface corrected to a defined vertical reference system, confirm that the data conforms with IHO standards and export the data in a GIS-compatible format. The general processing workflow is outlined in the Project Execution Plan (Table 3).

The *.db files were imported to QPS Qimera which converts the data to a proprietary (*.qpd) file format. From the *.db files, sound velocity, vessel and offset values are automatically read into the project. The processing parameters were defined to ensure that the sound velocity strategy is in accordance with the surveyed strategy, that the altitude values are applied from the correct source from the *.db file as well as GPS tide and the correct separation model. A raw surface was then created using these processing parameters. Vessel configuration was checked for any clear deviations from those set during acquisition. Nearest in time or nearest in distance sound velocity profile casts were selected for refraction corrections in Qimera, depending on the observed sound velocity variations.

Surface and profile sound velocity data and vertical positioning were then inspected for anomalous data values and spikes which were subsequently removed. Although vertical errors within the GPS heights were low (± 15 cm), navigation data were smoothed in QPS Qimera where appropriate. The raw bathymetric surface was then colour coded based on uncertainty (95% confidence interval) with a standard range of 0 to 0.4, to view areas where accepted soundings have considerable standard deviation. Weak filters (e.g., spline) were applied locally to areas with evident noise, ensuring that no possible contacts or bathymetric features were removed during the process. This was confirmed by performing visual inspections on each line or area before and after applying the filter. This strategy allows for a detailed examination of the dataset while at the same time removing the erroneous measurements.

Subsequently, the data were cleaned using the swath and slice editors, depending on the morphology of the seabed and the distribution of the anomalous data. In areas with complex natural or anthropogenic seabed features like wrecks, pipelines, infrastructure, the 3D editor is also implemented.

If high standard deviation values remained in the outer beams or line overlap, then the data were interrogated further. If this error was related to sound velocity, a series of checks were performed: i) re-inspection the surface and profile sound speed data and smoothing/despiking if required; ii) application of a refraction edit (± 1 ms-1 at 1 m water depth) and/or; iii) application of QPS's TU Sound Speed Inversion algorithm which utilises neighbouring soundings to determine the 'best-fit' sound speed refraction solution that minimises sounding mismatch in areas where there is sufficient overlap.

All data were corrected to LAT using the VORF separation model. Total Horizontal Uncertainty (THU) and Total Vertical Uncertainty (TVU) were computed for each sounding within the dataset. These were used for quality control purposes to ensure that the data is within client-specified limits. Another surface was created to ensure adequate sounding density (showing hit count per 1 m pixel). Finally, cross lines, which are independent of the surface grid were cross checked with the grid. This check, carried out in Qimera's cross check tool, generated a table of statistics that provide the results of the analysis of beam footprint values within the processed surface.

On inspection of the data and ensuring that the data meet the required IHO survey specifications, the data were exported. Initially, *.gsf as well as *.asc, *.tif and *.xyz files were exported comprising the backscatter and bathymetric surface data, respectively. The LAT-reduced, denoised bathymetric data was then inspected using GIS.

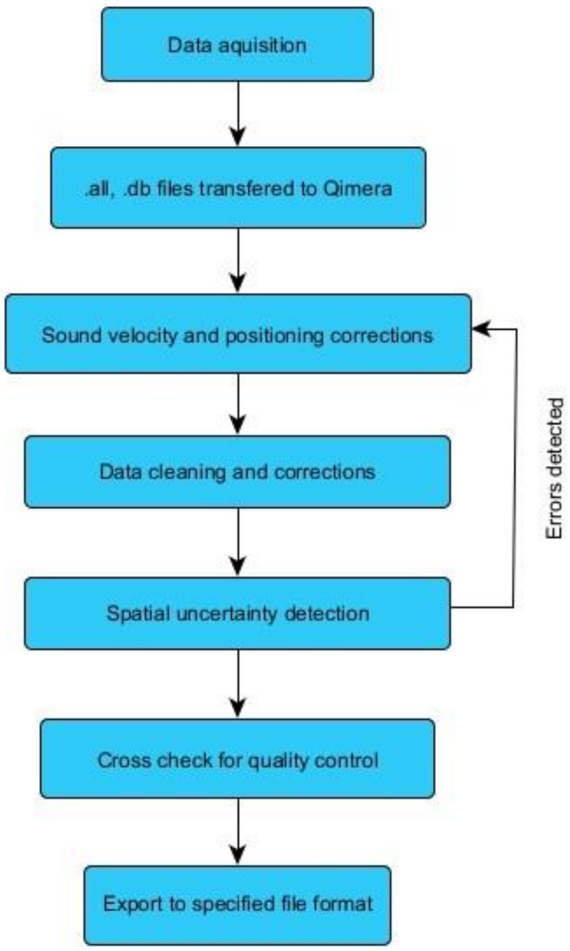

Figure 1: General multibeam echo sounder data processing workflow for corrected bathymetric grids .

2.2.3 Coverage

Multibeam echosounder swath coverage was optimised for sounding density to ensure that depth-induced swath width changes do not cause unnecessary fluctuations to sounding density. This ensures that all pixels on the final bathymetric surface were binned based on a similar number of soundings. Furthermore, it facilitates consistent data quality when sea state is less favourable.

To do this, an alarm was set in QPS QINSy to note considerable sounding density changes and the swath was subsequently adjusted based on the discretion of the senior surveyor. Given that water depth throughout the

Beaufort survey ranges from 46.05 mLAT to -135.66 mLAT, swath width was generally consistent. Figure 2 demonstrates swath width and water depth in cross track data.

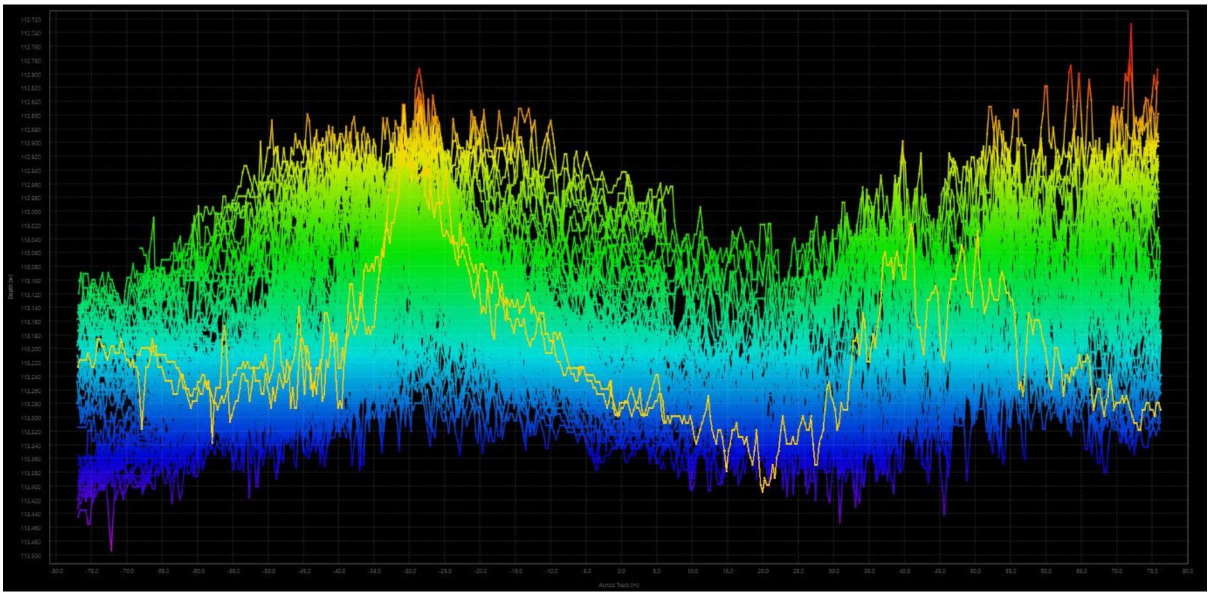

FIGURE 2: PLOT SHOWING TYPICAL CROSS TRACK PROFILE FROM SEVERAL MULTIBEAM ECHOSOUNDER PINGS DURING THE BEAUFORT SURVEY. NOTE: WATER DEPTH (113.4 M) AND SWATH WIDTH (160 M). DATA ARE COLOUR CODED BY DEPTH.

Using the swath coverage strategy outlined above, an area of c. 95.8 km2 was surveyed by multibeam in the Beaufort survey area (Figure 3). The coverage consisted of a series of parallel, broadly E-W oriented lines with crosslines perpendicular to these survey lines. Line spacing for the survey line plan was designed to ensure consistent data coverage depending on the water depth and generally ranges from 30 to 90 m for the mainlines and 1 to 3 km for the crosslines. These cross lines were used in the final assessment of the post-processed data to confirm product quality in terms of IHO accuracy.

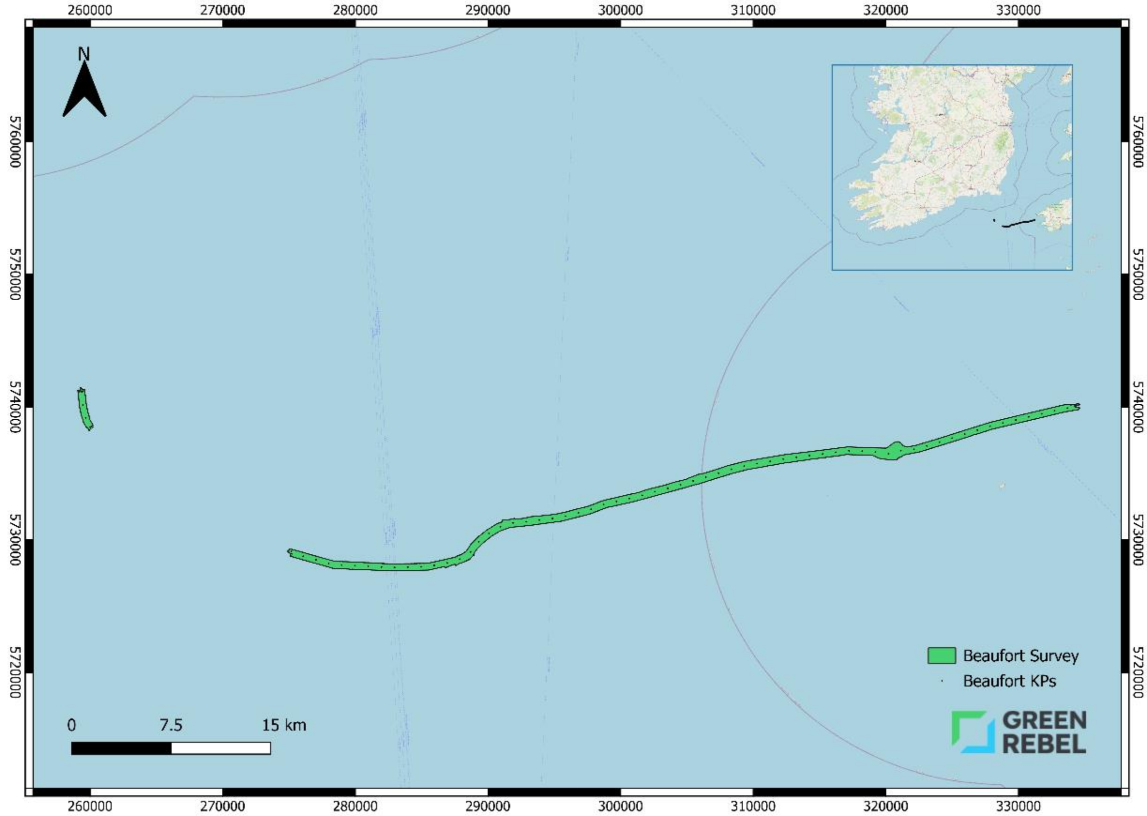

FIGURE 3: MAP SHOWING THE TOTAL AREA SURVEYED IN THE BEAUFORT SURVEY.

2.2.4 Positioning accuracy

The surface positioning quality during field operations met the required project's specifications, as documented in the Mobilisation Report (Table 3) and these data provided positioning for the multibeam. The accuracy of this system is apparent with visual inspections of neighbouring lines in the raw data. This assessment shows consistent vertical alignment of sounding overlap (Figure 4).

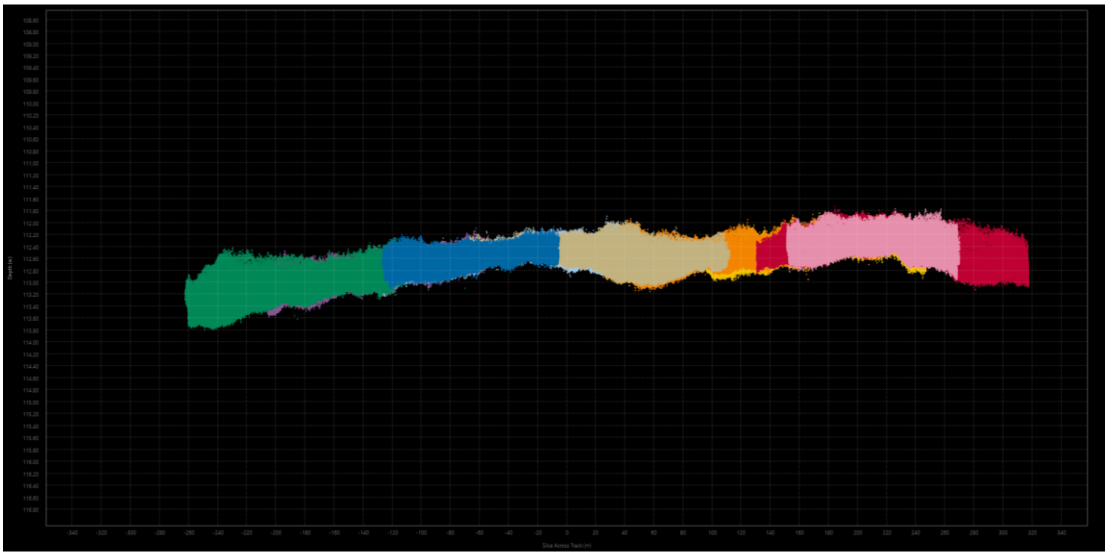

FIGURE 4: PLOT SHOWING ACROSS TRACK BATHYMETRIC SWATH DATA TO HIGHLIGHT THE VERTICAL 'MATCHING'/POSITIONING OF THE RAW DATA ACQUIRED WITH THE PRIMARY GNSS ANTENNA (VERTICAL EXAGGERATION: x40).

2.2.5 Sound velocity control

Sound velocity was measured both at the multibeam transducer as well as through the water column via sound velocity profiles. Sound velocity profile values are required to calibrate the multibeam-derived sounding values for speed of sound in water. These data enabled accurate calculation of bathymetric values.

Sound velocity profiles were recorded at a minimum of every 12 hours or by the discretion of the senior surveyor. A total of 14 sound velocity profile casts were acquired during the survey operations onboard the Glomar Vantage. Surface sound velocity values measured at the multibeam transducer head were continuously measured and monitored by the acquisition software (i.e. QPS QINSy). When QINSy measures a difference between the sound velocity at the transducer (Figure 5) and in the profile, an alarm is set off. When this happens, a new sound velocity profile is recorded. This cautionary procedure ensured that the sound velocity value was updated whenever there was any considerable change in the physio-chemical properties of the underlying water mass. Particular care was taken in environments/situations that were likely to influence sound velocity changes (e.g. heavy rain fall, nearby estuaries, harbours, surface water influx).

Figure 6 shows a sample of typical sound velocity values recorded during the Beaufort survey. Sound velocity profiles measured during the survey period reveal minor fluctuations in these profiles with depth, indicating that local variation is abundant in the upper layers. Note: Profiles that are substantially out of the survey area are (i.e., mobilisation and calibration profiles) excluded from this figure.

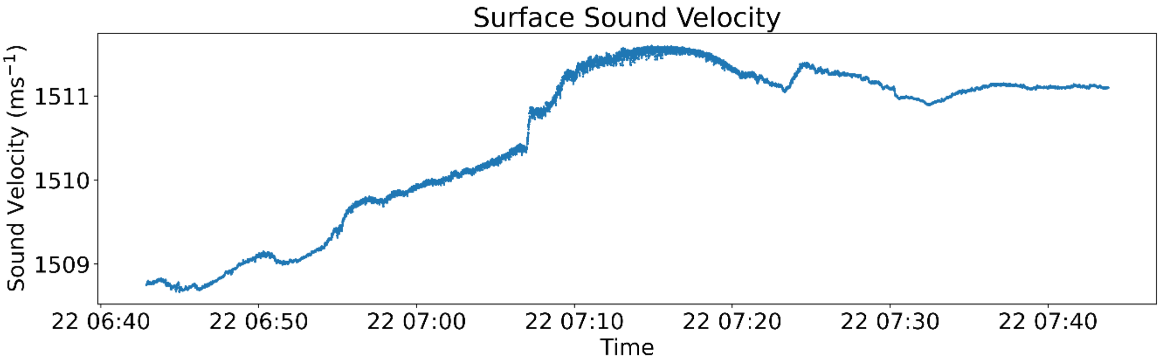

FIGURE 5: REPRESENTATIVE EXAMPLE OF SURFACE SOUND VELOCITY MEASUREMENTS RECORDED DURING SURVEY OPERATIONS (±2 MS-1 VARIATION OVER A SINGLE SURVEY FILE).

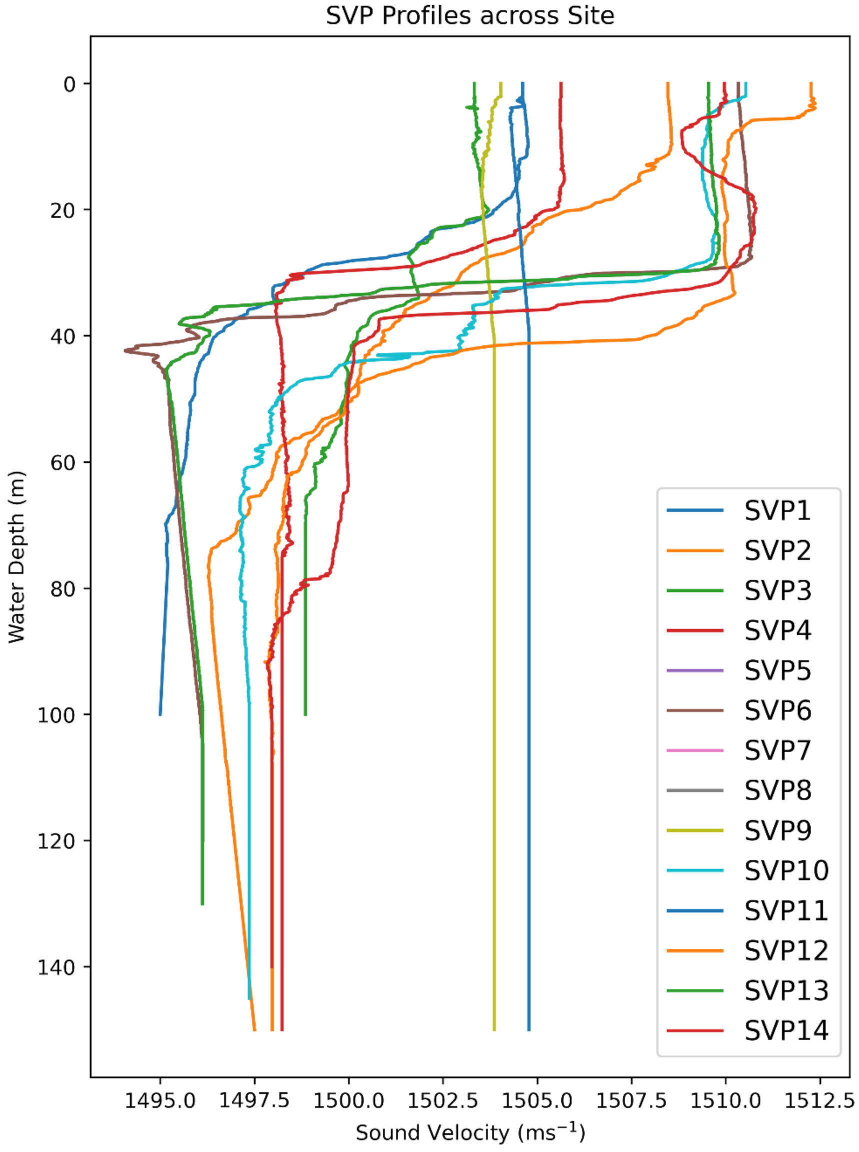

Figure 6: Representative sound velocity profiles acquired during the Beaufort survey.

2.2.6 Sounding quality

Multibeam echosounders transmit and record acoustic energy using a transducer. As such, they are sensitive to noise that can be expressed in the resulting raw data. This is a common phenomenon and can be the result of either direct impact between air bubbles and the transducer when sea states are less favourable, biofouling, or interference by acoustic energy that is similar in frequency to that of the multibeam (400 kHz). Green Rebel has completed testing to optimise survey parameters for minimal across-sounder interference. However, it is impossible to eliminate these artefacts completely. Noise and artefacts expressed in the raw multibeam bathymetric data during the survey operations are uncommon and when they do occur, they are minor (Figure 7). These anomalous soundings are clear and obvious in the raw datasets and can be removed when the data are processed.

One possible measure of multibeam data quality is sounding density. To access this, the density of soundings per 1 m cell were measured and values range from 1 to 4775 soundings per 1 m cell. The mean number of soundings in the raw bathymetric data are 175.41 per 1 m cell. Traditionally, a minimum of 9 soundings per 1 m cell are required for IHO standard Order 1a. As such, sounding density is well within the range to achieve the final product specification after post-processing.

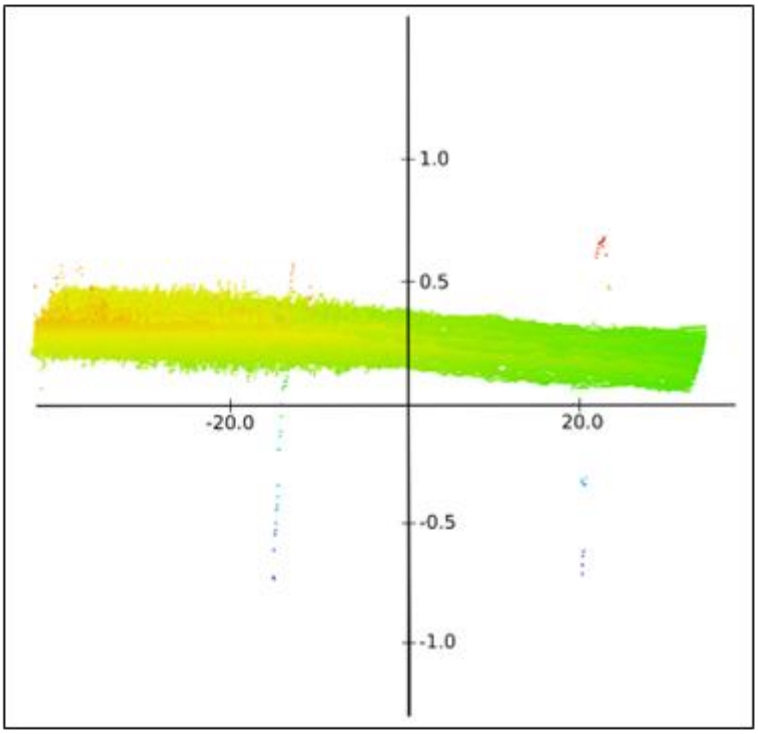

FIGURE 7: SAMPLE OF TYPICAL NOISE ARTEFACTS RECORDED BY THE MULTIBEAM ECHOSOUNDER AND EXPRESSED IN THE SOUNDING DATA. NOTE: UNITS IN METERS AND VERTICAL EXAGGERATION OF X22.78.

2.2.7 Data quality

The processed multibeam echosounder-derived bathymetric data achieves the required specifications IHO Order 1a. Criteria for Order 1a standard include feature search (100%), bathymetric coverage (100%) and maximum allowable total vertical uncertainty (TVU). To calculate TVU, (Equation 1 is utilised:

(EQUATION 1)

$$TVU_{max}(d) = \sqrt{a^2 + (bd)^2}$$

Where *a* is the proportion of the uncertainty that does not vary with depth (0.5 m), *b* is a coefficient which represents that portion of the uncertainty that varies with depth (0.013) and *d* is the measured water depth (m). Table 7 shows the test results used to determine if the data acquired during the Beaufort survey achieved the level of accuracy required for IHO Order 1a. To generate these values, Qimera, the QPS MBES processing software utilises survey crosslines as cross check to evaluate TVU values and other statistics for IHO Standard assessment (Table 7).

TABLE 7: MULTIBEAM BATHYMETRIC DATA IHO ORDER 1 A CROSS CHECK RESULTS.

Attribute	Value
Error Limit	1.15039
Number Rejected	796
P-Statistic	3.95276e-05

Attribute	*Value*
Test	ACCEPTED
Number Of Points	20137852
Grid Cell Size	1.000
Difference Mean	0.042
Difference Median	0.038
Difference Std. Dev	0.151
Difference Range	[-14.079, 14.158]
Mean + 2*Stddev	0.343
Median + 2*Stddev	0.339
Data Mean	-79.654
Reference Mean	-79.696
Data Z-Range	[-133.942, -51.808]
Reference Z-Range	[-134.121, -52.110]

Online quality control inspections were performed during acquisition by a dedicated QC person to ensure a high-density of soundings per 1 m cell. This was confirmed in post-processing where the final sounding grid had a minimum of 1 sounding per 1 m bin (In isolated areas of noise burst or swath edges), a maximum of 4774.9 soundings per 1 m bin, and a mean of 36.93 soundings per cell. For transparency, this is visualised below (Figure 8) and highlights the quality of the final bathymetric data.

Navigation data were logged in standard C-Nav format which were integrated within the raw QINSy database files. Real-time positioning data quality from C-Nav was of sufficient quality to exceed IHO Order 1a standard requirements. Vertical errors within GPS heights were low (± 7 cm) and provide a robust solution for computation of GPS tide. GPS tide was computed using the separation model between World Geodetic System 1984 (WGS84) datum and VORF LAT.

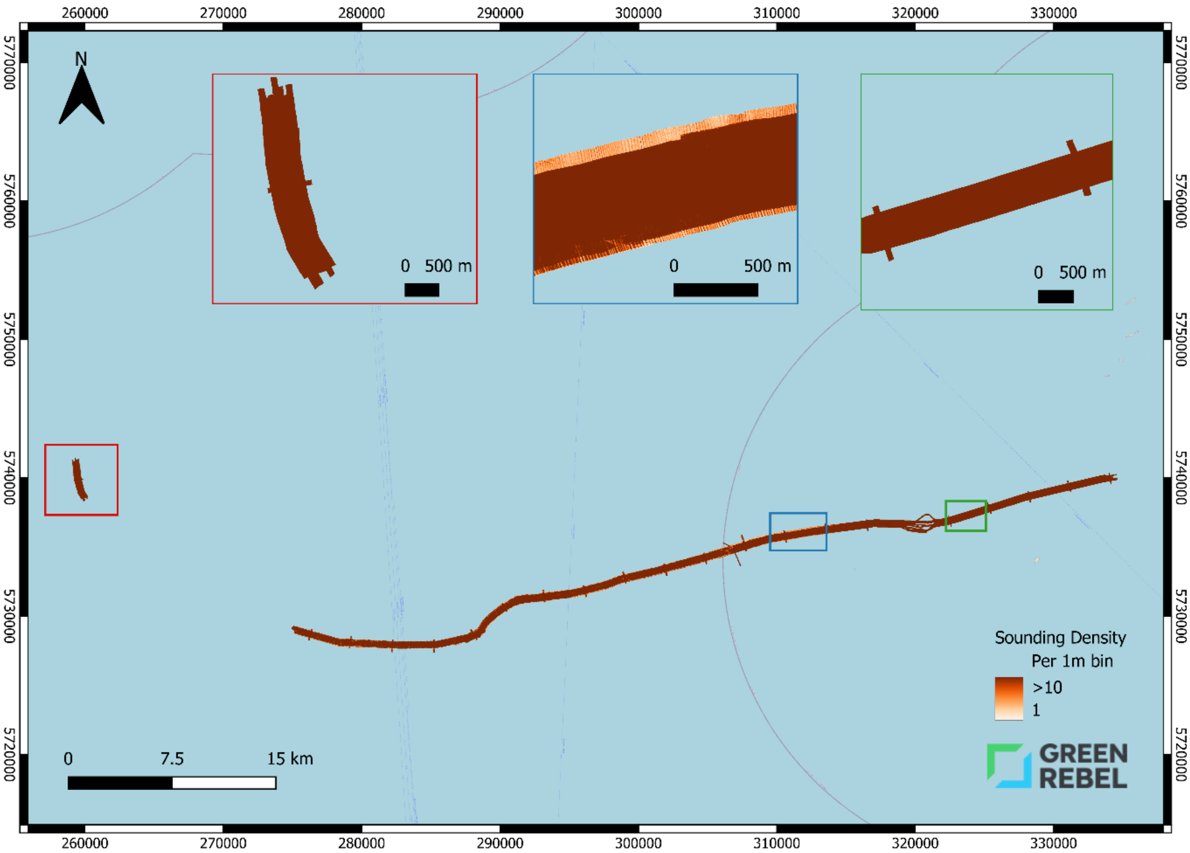

FIGURE 8: MBES SOUNDING DENSITY MAP (SOUNDINGS MEASURED PER 1M BIN) WITH AN INSET IMAGE SHOWING A CLOSE-UP OF LESSER SOUNDINGS ON OUTER BEAMS IN LOCALISED AREAS

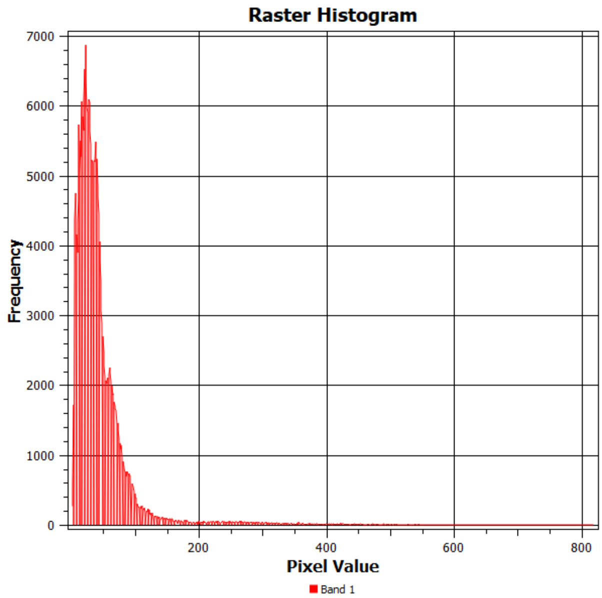

FIGURE 9: HISTOGRAM SHOWING THE NUMBER OF SOUNDINGS PER 1 M CELL (NO. OF SOUNDINGS ALONG X-AXIS).

Overall quality control of the data was completed by generating a QPS Qimera Dynamic surfaces from all MBES sonar data within the Beaufort survey area. The dynamic surface was created with a range of parameters used to assess the data and ensure it falls within specification. The uncertainty at 95% confidence interval was assessed in order to highlight areas where the vertical spread of soundings within a DEM grid are high and checks can be made to determine the cause. Areas within this layer that coincide with high standard deviations can occur where there are sound velocity errors, errors in the navigation, or when acquiring data in heavy weather and where there is a change in seabed relief such as boulder fields. The varying vertical shift tool was utilised to reduce standard deviation in depth values of adjacent lines ensuring an accurate representation of seabed morphology.

Figure 10 shows the uncertainty of the final bathymetric sounding grid at the 95% confidence interval. These data show that the uncertainty is typically < 0.04 m and typically do not exceed 0.1 m although in rare circumstances there are higher standard deviations (up to 4.072 m) around small seabed features that occur in the outer beams where higher beam scattering occurs. Nevertheless, the mean uncertainty is 0.08, which demonstrates the quality and consistency of the overall 1 m grid. This is plotted spatially in Figure 10, which shows the spread of uncertainty data between 0 and 0.4 m. In addition, a longitudinal cross section through the surface shows that the data are vertically well-aligned (Figure 10). The statistical spread of vertical uncertainty is also displayed in a histogram (see Figure 11). No clear and obvious vertical offsets were observed. It is worth noting that survey cross lines are omitted from gridded datasets as they can induce vertical offsets (of up to 2m). While these crossline files increase sounding density, there is sufficient soundings in place. This removes the potential of vertical offsets displaying above the IHO specifications.

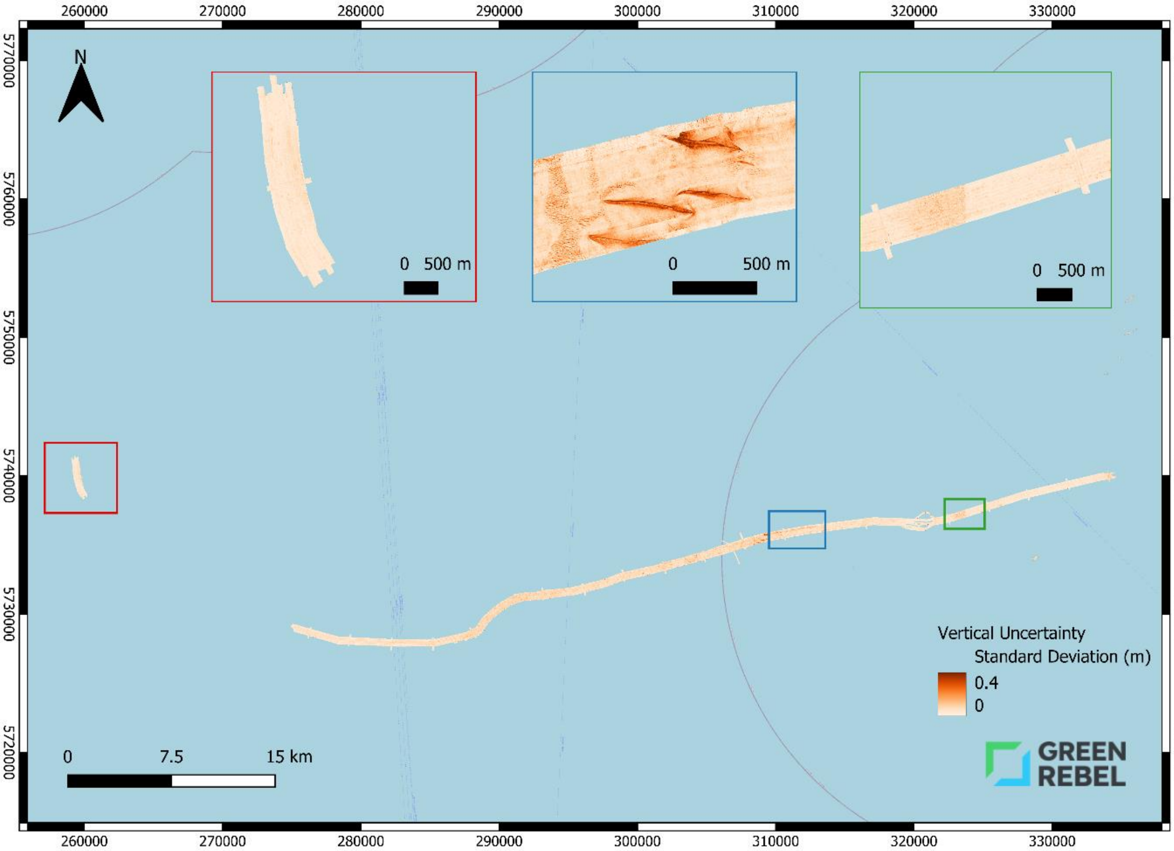

FIGURE 10: MBES UNCERTAINTY RASTER. VALUES ARE HIGHER AT STEEP BATHYMETRIC SLOPES (AS SHOWN IN THE INSET BLUE IMAGE) AND SEDIMENT WAVE CRESTS.

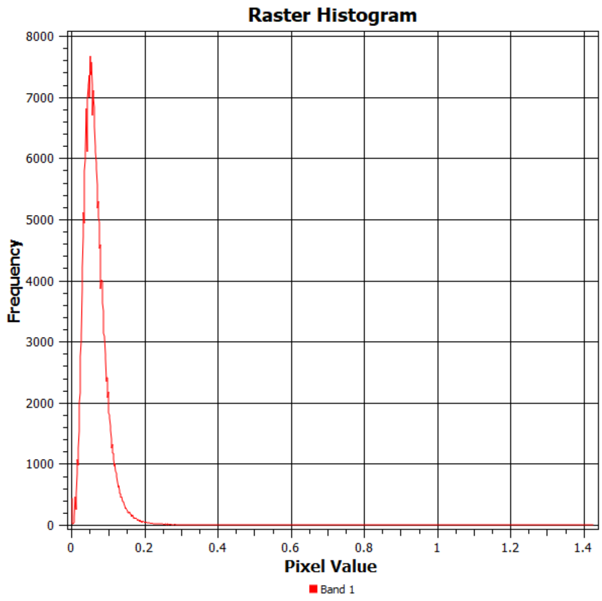

Figure 11: Histogram showing the uncertainty of soundings binned every 1 m within the final bathymetric surface (value of offset in meters along x-axis).

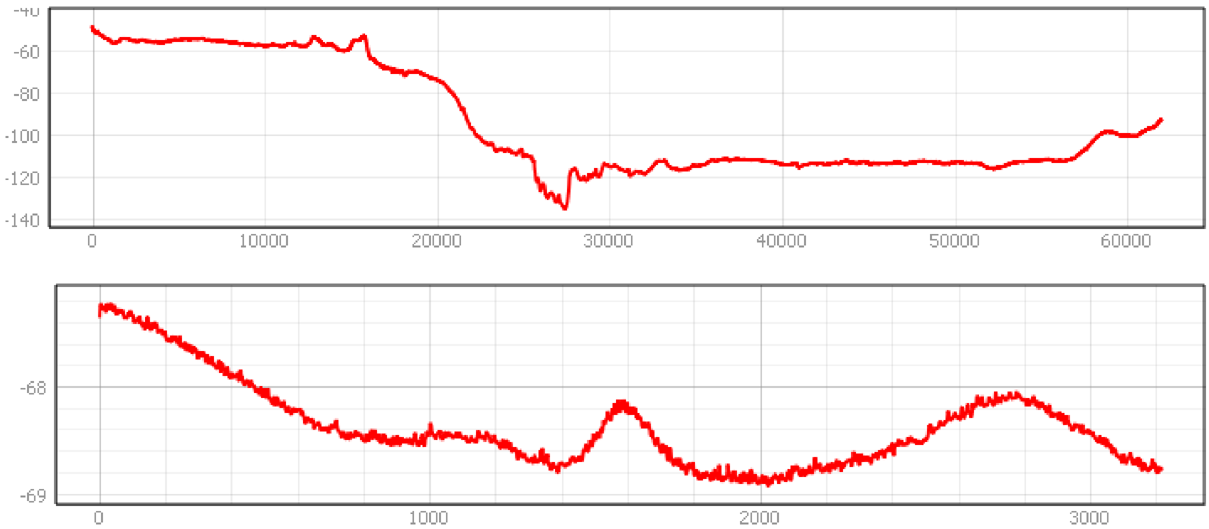

*Figure 12: Cross sections of the MBES data across the Beaufort site: the **top** graph showing a profile starting at KP 0 (larger UK side), ending at KP 62.2 and the **bottom** graph showing a profile starting at KP 0, ending at KP 3.1 (smaller western section).*

Given the high density of soundings, their vertical consistency as shown by low standard deviation and the cross validation with the IHO TVU test as well as the comparison with a well-known and established dataset, these data are deemed of high-quality and fit for purpose.

2.2.8 Final product

The final bathymetric grid was exported at 1 m per pixel as specified in the scope of works. The final bathymetric product was clean, meeting all industry standard tests as previously outlined. No artefacts or issues are observed with the final bathymetry product (Figure 13).

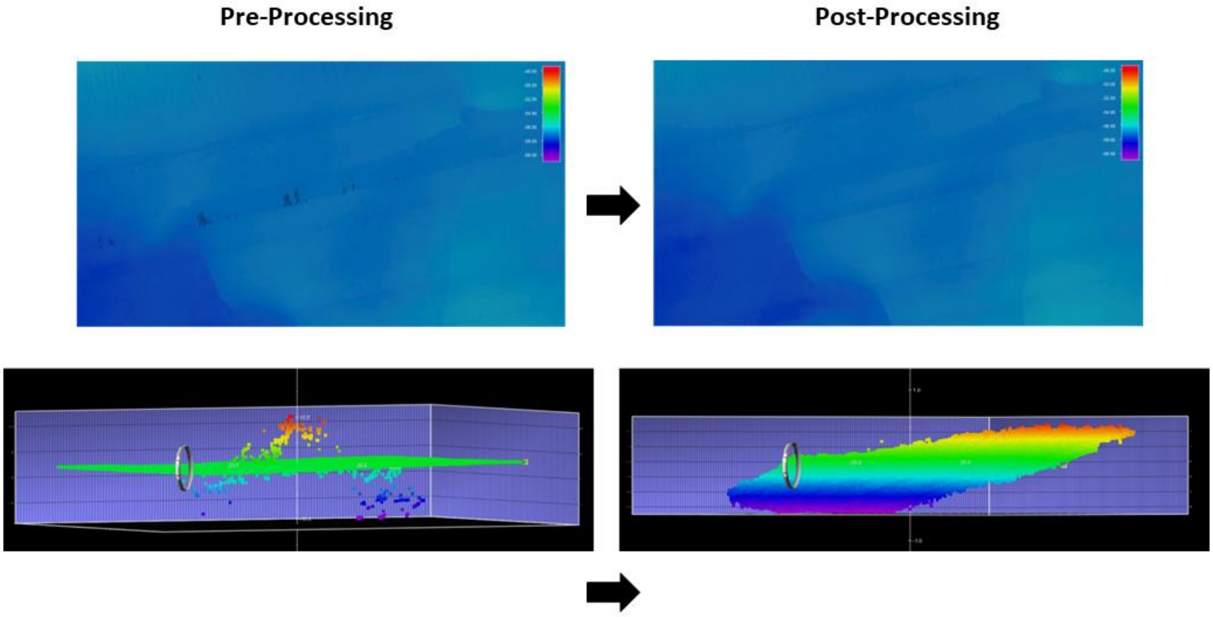

FIGURE 13: COMPARISON OF PRE- AND POST-PROCESSED ON A REPRESENTATIVE BATHYMETRIC SURFACE.

2.3 Multibeam backscatter

2.3.1 Data acquisition

Multibeam echosounder systems captured backscatter intensity data concurrently with bathymetric data to facilitate the geological interpretation of the surface seabed substrates. Backscatter intensity, which varies based on the seabed's hardness and roughness, offers insights into the seabed's composition through the analysis of backscatter values and their spatial patterns. However, raw backscatter data come with inherent artefacts and variations arising from factors such as the beam's angle of incidence and the distance between the seabed and the echosounder, necessitating correction.

2.3.2 Processing workflow

The goal of processing multibeam backscatter data is to integrate sonar data into a coherent backscatter intensity mosaic (measured in decibels, dB) that is compatible with GIS. This process begins with exporting the multibeam .db files as generic sensor format files (.gsf) using Qimera software. These files are then processed with QPS's GeoCoder Toolbox (FMGT), employing the Geocoder algorithms to adjust for acquisition gains and apply radiometric and geometric corrections to the raw acoustic data. This ensures accurate backscatter strength values, correcting for the aforementioned variations. Key sonar acquisition parameters, such as the number of beams and frequency, are defined during this stage. Additionally, any overlapping cross lines are addressed to minimize artefacts in already covered areas of the project. The FMGT software's algorithms analyse the intensity of each sonar ping, normalising them to mitigate variability factors such as beam angles, vessel motion, weather conditions, and along-track variability.

Although this normalization results in a significantly improved dataset, further manual corrections need to be applied if any equipment or acquisition related variations remain in the data. Therefore, after applying the FMGT algorithms, quality control checks are conducted to ensure consistent sediment boundary delineation across survey lines and legs. Particular attention is directed towards correcting any remaining along-line backscatter shifts, whether constant or time-variant. The finalized gridded backscatter mosaic is then exported as GIS-compatible files (*.XYZ and *.tif GeoTiff), providing clean georeferenced, evenly spaced grids of backscatter intensity.

The final, color-coded backscatter mosaic is then imported to GIS and examined for its effectiveness in depicting seabed features and boundary, ensuring suitability for geological interpretation. This report uses "backscatter" to refer specifically to these relative intensity mosaics generated in FMGT from the MBES data.

2.3.3 Seabed Sediment Interpretation

Seabed Sediment interpretation allows for a multifaceted characterisation of the seafloor substrate type while maintaining a non-invasive survey status. In Green Rebel, seabed substrate interpretation is conducted by analysing both MBES backscatter, bathymetry and SSS data. This combination can provide important information and context to planning for subsequent geotechnical survey operations beyond the insights possible from bathymetric or backscatter data alone.

Under this approach sediments were grouped into the most commonly occurring grain size categories based on values derived from backscatter intensity and bathymetric features. These were fine sediments, medium sediments and coarse sediments.

2.4 Side-scan sonar

2.4.1 Data acquisition

Side-scan sonar (SSS) data were acquired with a deep-towed Edgetech 4205 side-scan. The fish was towed at an average depth of 90.5m across the survey area with the aim of averaging a consistent altitude. During acquisition, the fish operated Low and High frequencies simultaneously (230 and 850 kHz, respectively). Positioning for the SSS data on Glomar Vantage was acquired with a Kongsberg uPAP USBL (Ultra Short Base Line). Data acquisition was managed in Edgetech Discovery where range, frequency and file type were controlled. Raw data logging was managed in QINSy where a series of Logfiles were created in addition to *.jsf files storing the raw SSS backscatter data. These *.jsf files include the USBL positioning, vessel position, time, date, cable out and heading information.

2.4.2 Processing workflow

SSS systems measure the intensity of their returning signal. The aim of SSS data processing is to merge all sonar data, apply offsets and navigation correction (as required), and correct the sonar signal (gains and bottom tracking) to create a streamlined sonographic mosaic in a GIS-friendly format. To this end, all SSS data processing was carried out in SonarWiz v7.11.01. The general processing workflow is outlined in Figure 14. All raw SSS data are stored in *.jsf files (Edgetech proprietary file format) which include sonar data, vessel and fish XY position, cable out, fish height and frequency. As a backup, logfiles containing vessel and fish positions were exported in a *.txt file format from QINSy independently. Navigation 300 ping smoothing was applied when files were imported into the SonarWiz project, limiting nav drops and swirls.

SSS *.jsf files were imported to SonarWiz which was set up to correctly read the correct fields from the file (USBL position and heading rather than vessel position). Once the data were imported, they were converted to a CTI proprietary processing file type (*.csf). When preliminary investigation showed that they plot correctly, each line was inspected for navigation. To do this, the navigation for each line was inspected and anomalous spikes were corrected using the interpolating tool in “Z editor”. The lines were inspected to determine the bottom tracking parameters for each line. Manual bottom tracking edits were applied if deemed essential. To enhance the sonographic imagery for subsequent analyses, at this stage, gains could be applied. Typically, Empirical Gain Normalisation (EGN) is applied which creates a dictionary of all amplitude data from all files and assesses them by distance from the sonar. This then creates a signature of the mean sonar signal. When applied to a full suite of survey lines, this is particularly useful for surficial geological features. A traditional, industry-standard black to bronze colour palette, where shadows are illustrated in black is used when visualizing the data.

Geographic accuracy was measured by isolating each line and measuring the linear distance between multiple seafloor features that are seen in both the SSS line and the bathymetric data (collected by Green Rebel's MBES, passing IHO Order 1a). Seafloor features of interest were typically boulders or rocky outcrops with visual characteristics that are easily identified. Attempts were made to ensure that the measurements are equally distributed near both ends of the SSS survey and at several points along the middle when possible. A minimum of 5 points was sought after from each line. However, if an area had little in the way of distinctive seafloor features, fewer points were used. If the average (mean) difference was 2 m or less, the line was considered geographically accurate, and no geographic corrections were required. If the average error was greater than 2 m, map corrections were applied to georeference the SSS data to the bathymetry. After map corrections were made, the accuracy assessment process was repeated, whilst taking care not to measure the same seafloor features that the map corrections were based on. However, in some areas where distinctive seafloor features were rare, this might not be possible. With these amendments, the average difference is now less than 2 m, and the line with map corrections was accepted. If not, further map corrections and subsequent accuracy assessments were made. The processed sonar files were then converted into a grid using the Inverse Distance Weighted algorithm. The final surface was then exported as a geoTiff (*.tif) at a resolution of 0.2m.

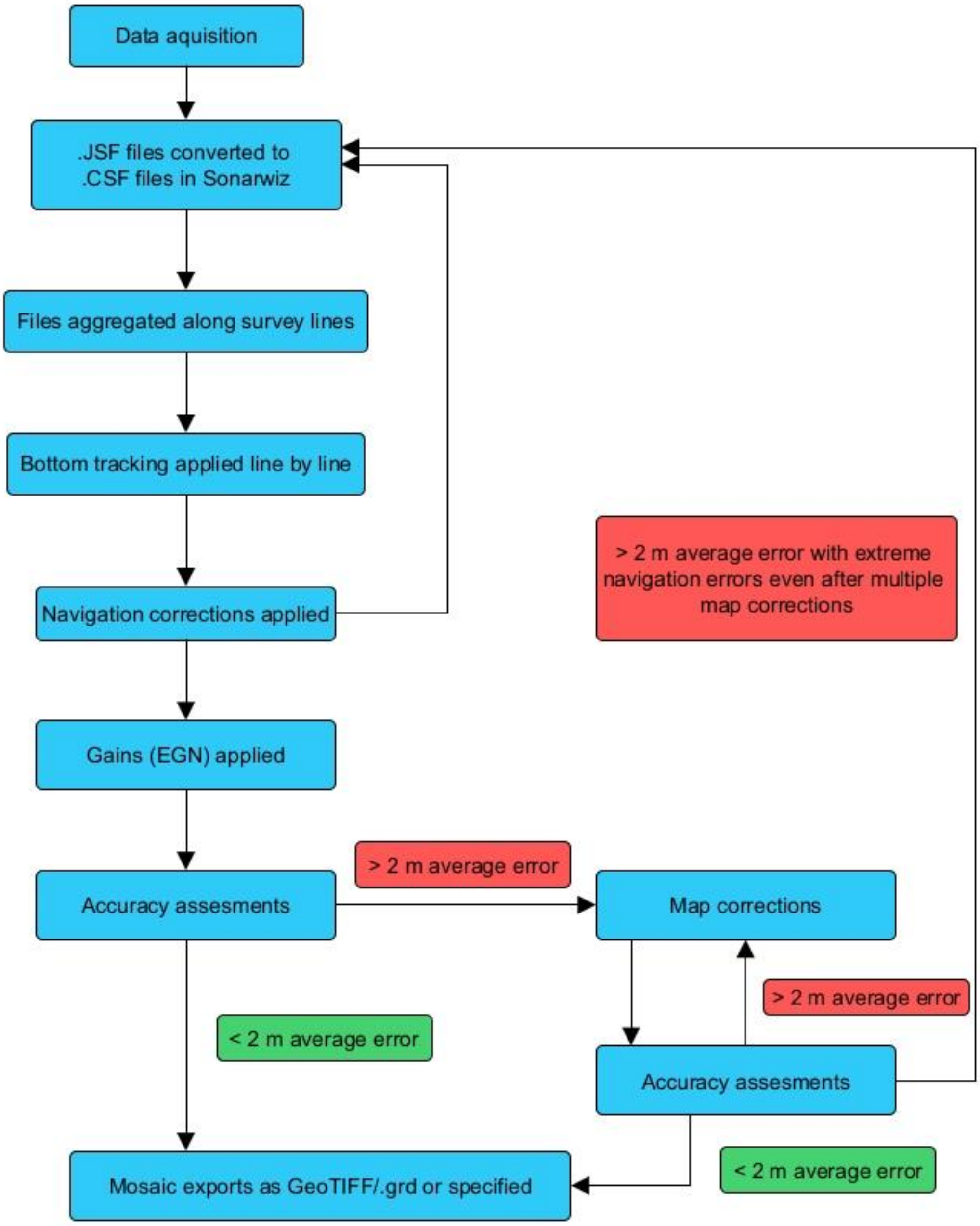

FIGURE 14: GREEN REBEL'S SIDE-SCAN SONAR DATA PROCESSING AND ASSESSMENT STRATEGY.

2.4.3 Accuracy assessment and corrections

The SSS data were positioned with an accuracy of ± 0.44% of the slant range. Overall, the USBL tracked the position of the SSS well, meeting the required specifications. However, isolated, localised deviations were observed; minor navigation wobbles and inconsistencies are common with USBL systems and easily influenced by environmental factors (cf. Li et al., 2018; Figure 15). This is typical and can be rectified in post-processing to ensure that geographic accuracy of 2 m can be attained per project specifications. Minor navigation errors also correlate with rapid change in sensor depth when the cable is retrieved to avoid the fish crashing into a topographic high (anthropogenic and natural), as seen in Figure 16.

Momentary drops in USBL navigation (likely induced by drops in communication between transponder beacons) lead to incorrect interpolation of the data in SonarWiz. This forces the stretching of pixels to bridge the data drops (Figure 17), resulting in mosaic geographic errors over 100 m, in extreme examples. This was rectified in processing steps through the linear interpolation of data within USBL drops resulting in accurate mosaics. In addition, hydrographic conditions on site resulted in "crabbing" of the fish. To amend this, each file was manually adjusted by rotating the port and starboard sonar files, while comparing versus a known medium (i.e. bathymetry). Without any navigation corrections, in areas where no navigation abnormalities were observed, the accuracy of the mosaicked raw data were generally within specification.

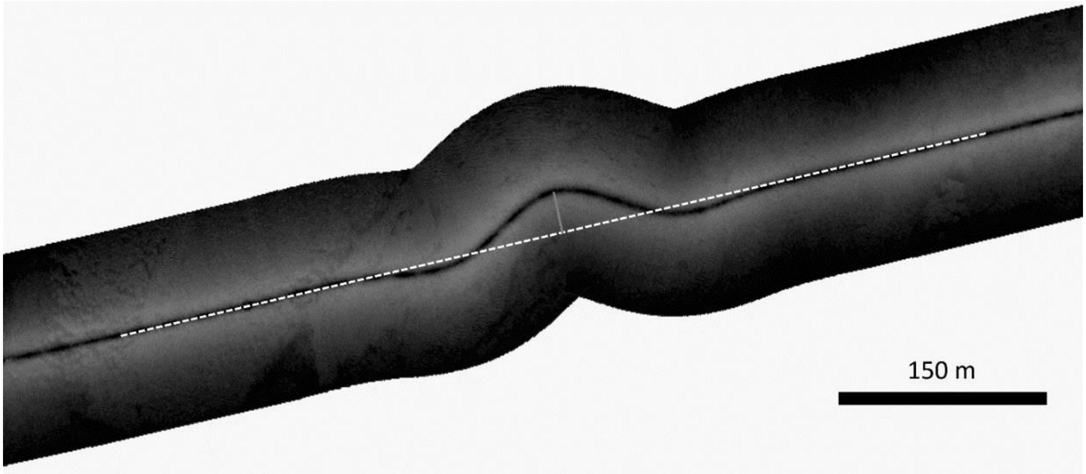

FIGURE 15: A SINGULAR MOSAICED LINE SHOWING POOR NAVIGATION. THE RED LINE INDICATES A 30 M LOCALISED OFFSET WHICH WAS INFREQUENT.

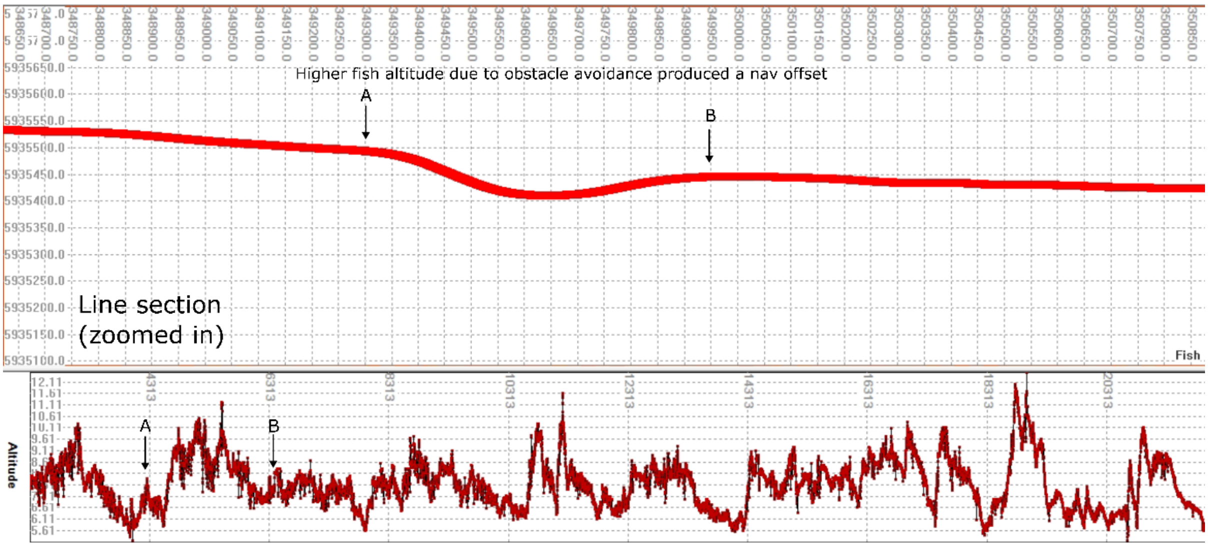

FIGURE 16: NAVIGATION ERRORS SEEN IN THE X Y PLOT (TOP PANEL) BROADLY CORRELATE WITH CHANGES IN FISH DEPTH DUE TO LOCAL TOPOGRAPHY OR CONTACTS PROTRUDING INTO THE WATER COLUMN WHICH PRESENTED A POTENTIAL COLLISION HAZARD (BOTTOM PANEL).

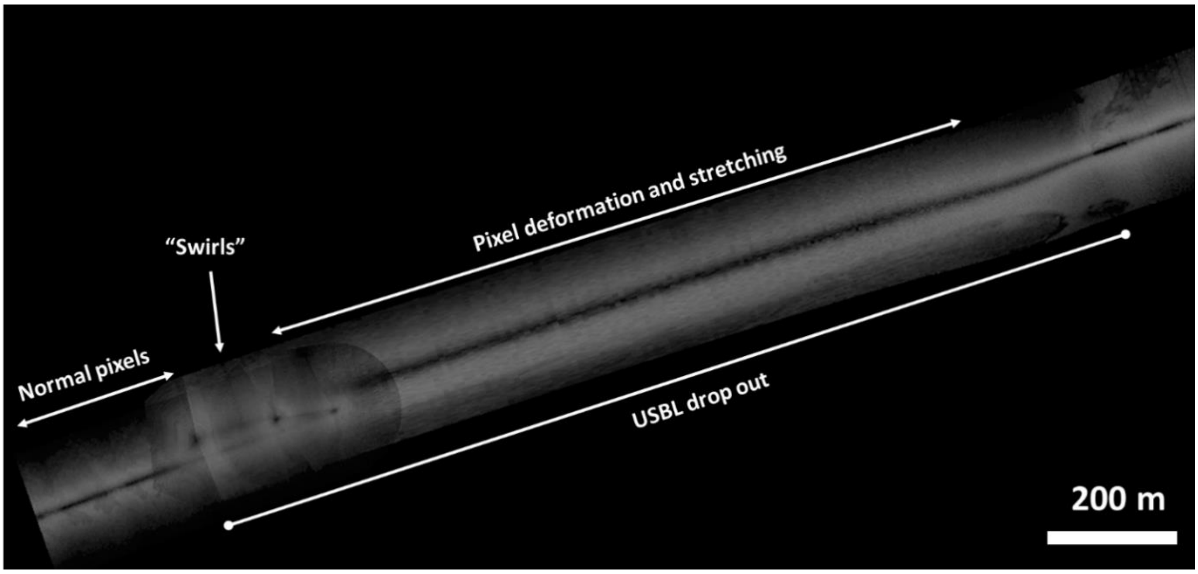

FIGURE 17: USBL NAVIGATION DROPS RESULT IN "SWIRL" PATTERNS AND PIXELS THAT ARE STRETCHED.

2.4.4 Image Quality

The objective of SSS surveying and analysis is to reveal surficial seabed characteristics. Typically, this means delineating/identifying geological features, sedimentary structures, changes in sediment types, boulders, wrecks and geohazards. Features such as boulders and changes in geology are identifiable and well defined, thus, the data were deemed fit for purpose and processing. Noise and interference are typically absent from the data.

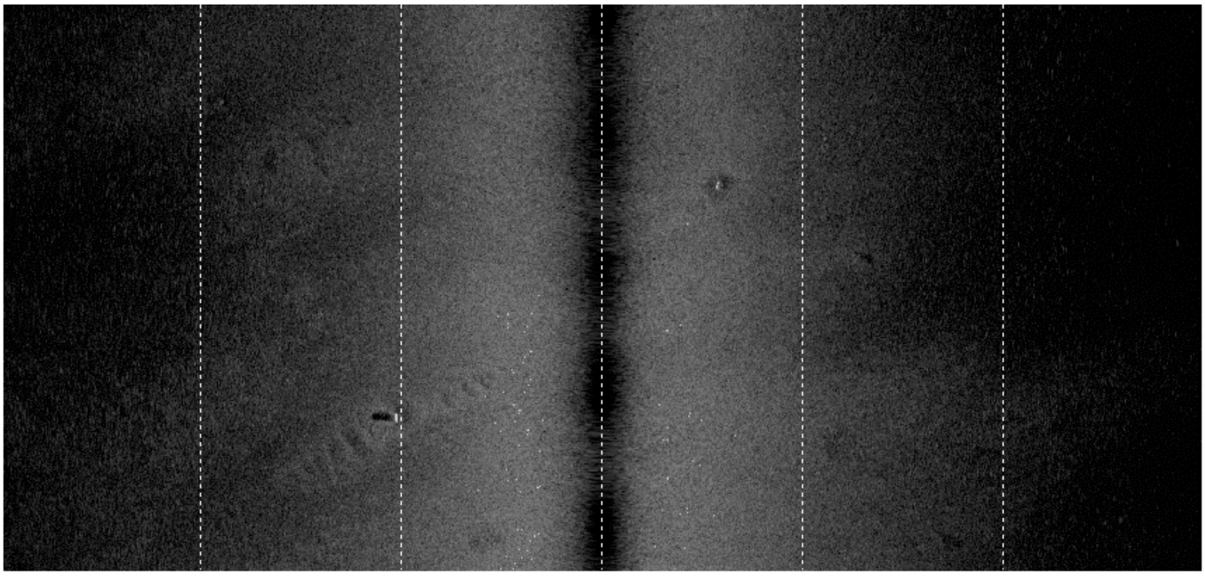

FIGURE 18: UNPROCESSED SIDE-SCAN MOSAIC CLOSE-UP SHOWING TWO BOULDERS.

Bottom tracking was successfully applied (3, 3, 6 for the parameters "Blanking", "Duration" and "Threshold" for seafloor threshold detection), with minimal manual modifications required. The EGN gains improved the peripheral image clarity, resulting in a clear image across the whole swath (Figure 19). The SSS data was of consistently high quality, corroborated by the obvious identification of seafloor objects such as boulders and sediment boundaries (Figure 20). The data had only isolated minor artefacts over the entire area.

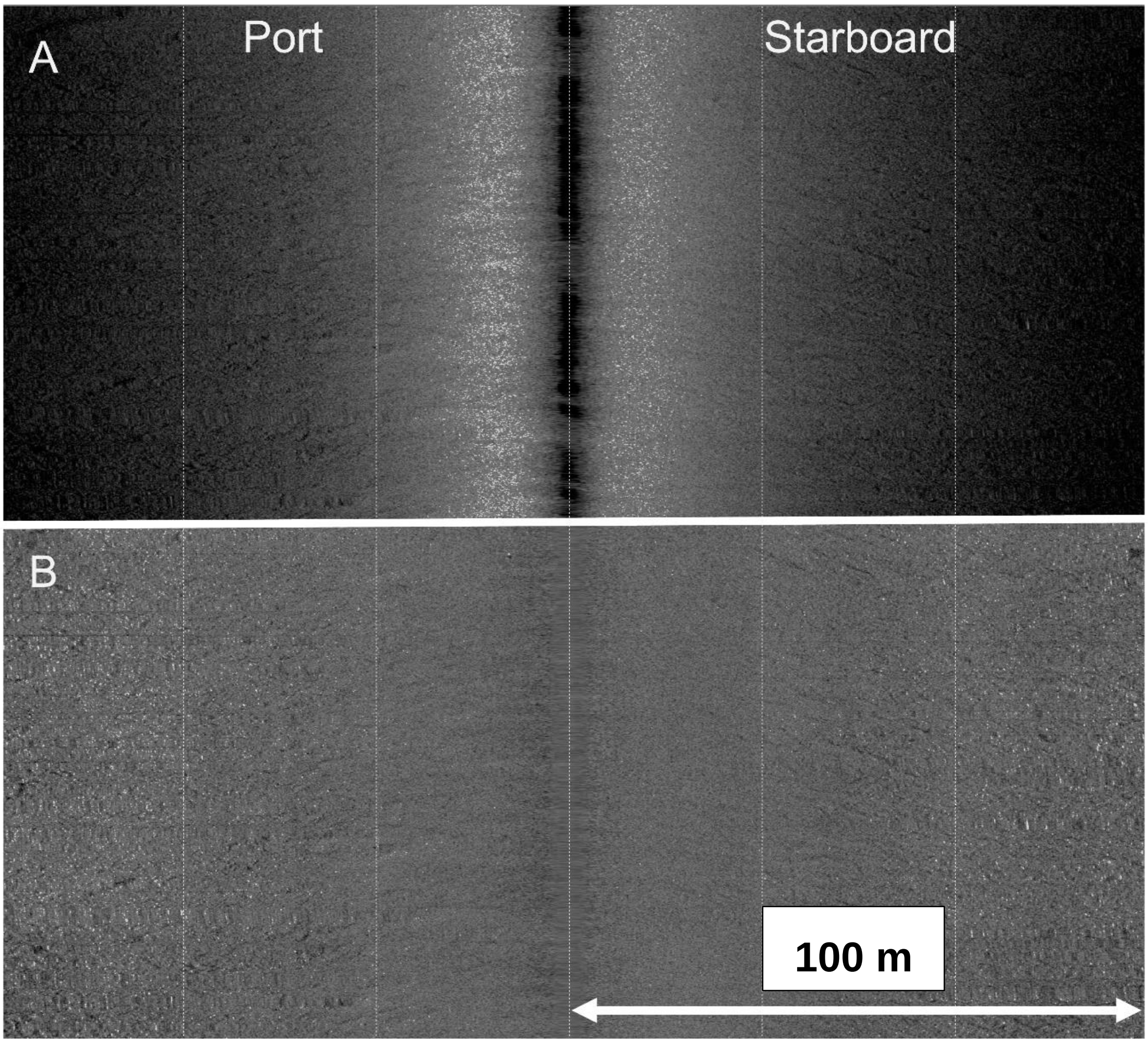

Figure 19: Example of the raw and processed data. The top image shows the raw side-scan, the nadir is visible down the centre of the image and dark edges at the periphery of the swath where sound attenuation influences the visual quality. The bottom image shows the same area with processing parameters implemented (Bottom tracking and EGN gains applied) to improve the visual quality.

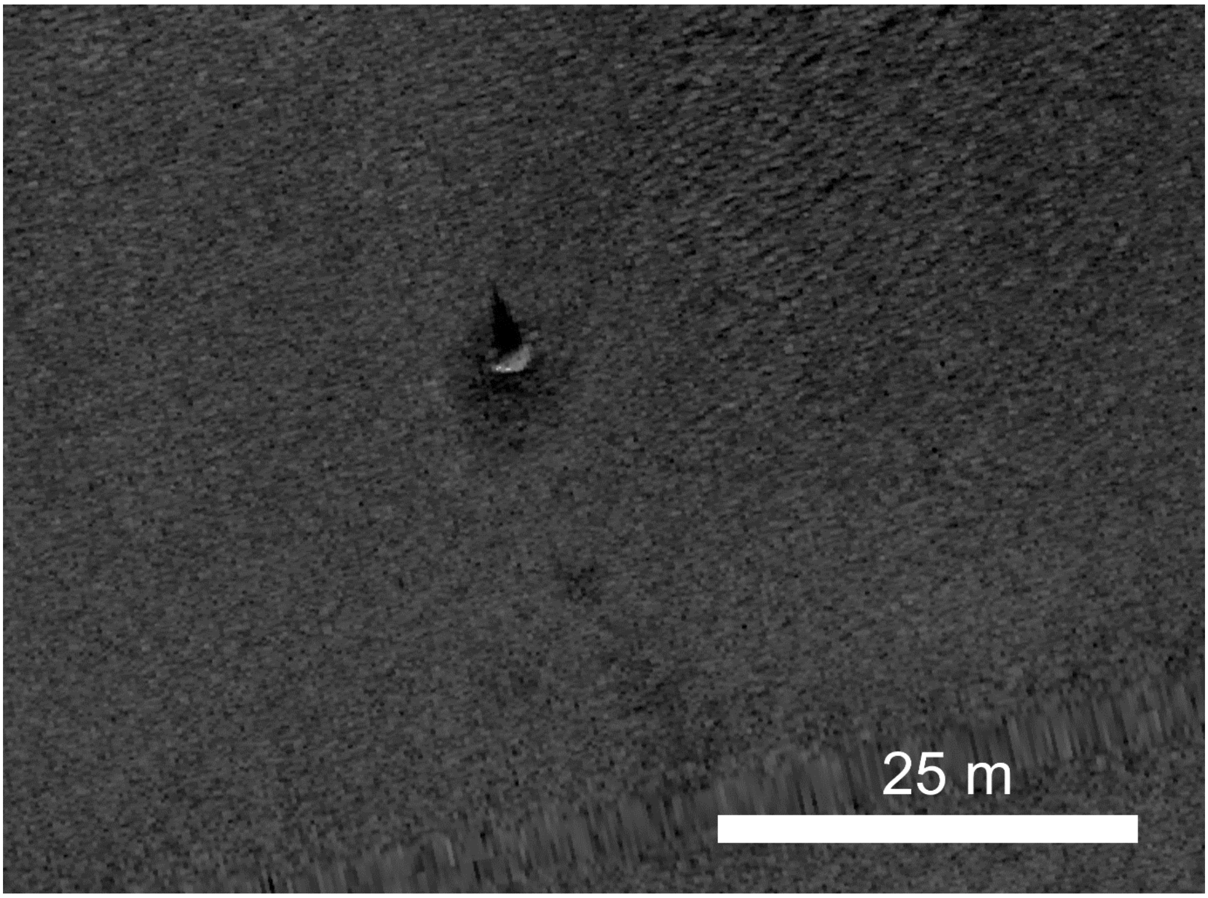

FIGURE 20: IMAGE QUALITY FROM THE LOW-FREQUENCY CHANNEL WITH A BOULDER CLEARLY IN VIEW.

2.5 Magnetometer

2.5.1 Data acquisition and positioning

Magnetometer data were acquired using a single Geometrics G882 Magnetometer which was deep towed at a range of 2.04 m to 50.03 m off the seafloor. The Glomar Vantage (herein GV) vessel was used to collect data across this site. During acquisition, the fish measures the total magnetic field in nT, with a typical sensitivity of 0.02 nT at a 0.1 sec sample interval. Acquisition parameters for each vessel were identical, except for positioning systems. Magnetometer data onboard the GV was acquired with a Kongsberg uPAP USBL and a cNODE Micro (x4) with an accuracy of ± 1.3% of the slant range. Data acquisition was managed in QINSy which created a series of log files with details including USBL positioning, line name, magnetic amplitude, signal strength, altitude, depth, vessel speed. Coverage of the site was attained with an approximate line spacing of 30.00 m (Figure 21).

The USBL system onboard the vessel regionally tracked the position of the magnetometer well. However, local scale variations were observed (1–60 m). Navigation wobbles and inconsistencies are common with USBL systems (cf. Li et al., 2018) and are easily influenced by environmental factors. These variations are normal and were rectified in post-processing through the application of smoothing filters. Very occasional dropouts from the USBL, induced by the magnetometer losing connection with the USBL beacon onboard were noted. This was also corrected in post-processing by interpolating the navigation between the observed error windows. Within the survey the area, approximately 801.14 km of raw magnetometer survey line length was acquired. However, it is worth noting that these values are skewed heavily due to local scale variations and spiking adding significant length to many survey lines.

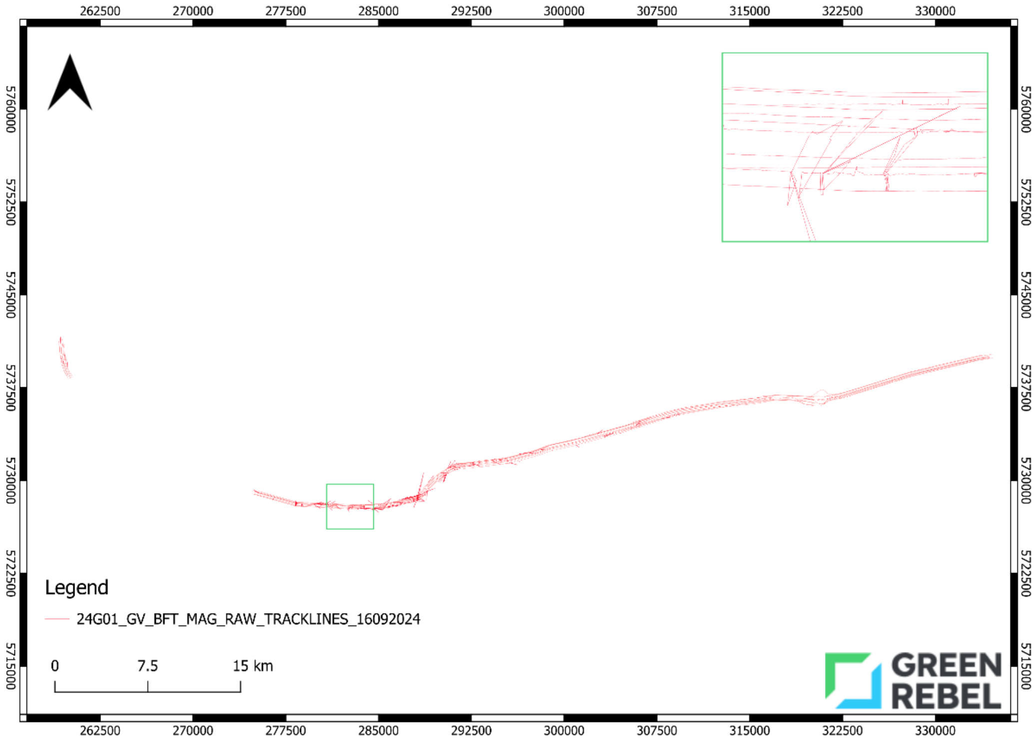

FIGURE 21 : RAW MAGNETOMETER COVERAGE.

2.5.2 Processing workflow

Magnetometer data show the total magnetic field values across the survey area binned per unit area. From this, magnetic anomaly values can be derived. These datasets are useful for the interpretation of seabed feature composition, ferrous object detection (such as wrecks, p-UXO and sub-sea infrastructure) and seabed geology characterisation.

The magnetometer data was logged as a QINSy logfile (*.txt) which includes vessel and fish XY, cable out, fish depth, fish altitude, magnetic amplitude and signal strength. Magnetometer data processing aims to format the data, QC the validity of the traces, correct for erroneous spiking, and calculate and remove the background magnetic amplitude to derive the residual and analytic signal for target isolation. This process begins during logging in QINSy, with each .csv file aggregated via 'Storage DB'. This results in a much cleaner and smoother process when handling raw data, as the number of files handled individually is reduced dramatically.

The treated magnetometer files were then imported to Oasis Montaj 2024.1 for evaluation and processing. File headers were tidied up during the import process. Each file was inspected for navigation-related data errors. Raw navigation XY was displayed and despiked using low-pass filtering. This process was dynamic, allowing line-by-line adjustments. Extreme spiking occurring over five fiducials or less was cleaned using a non-linear filter. The cleaned navigation was then saved as the primary XY of the project. A comparison of unprocessed against processed is visible below (Figure 22).

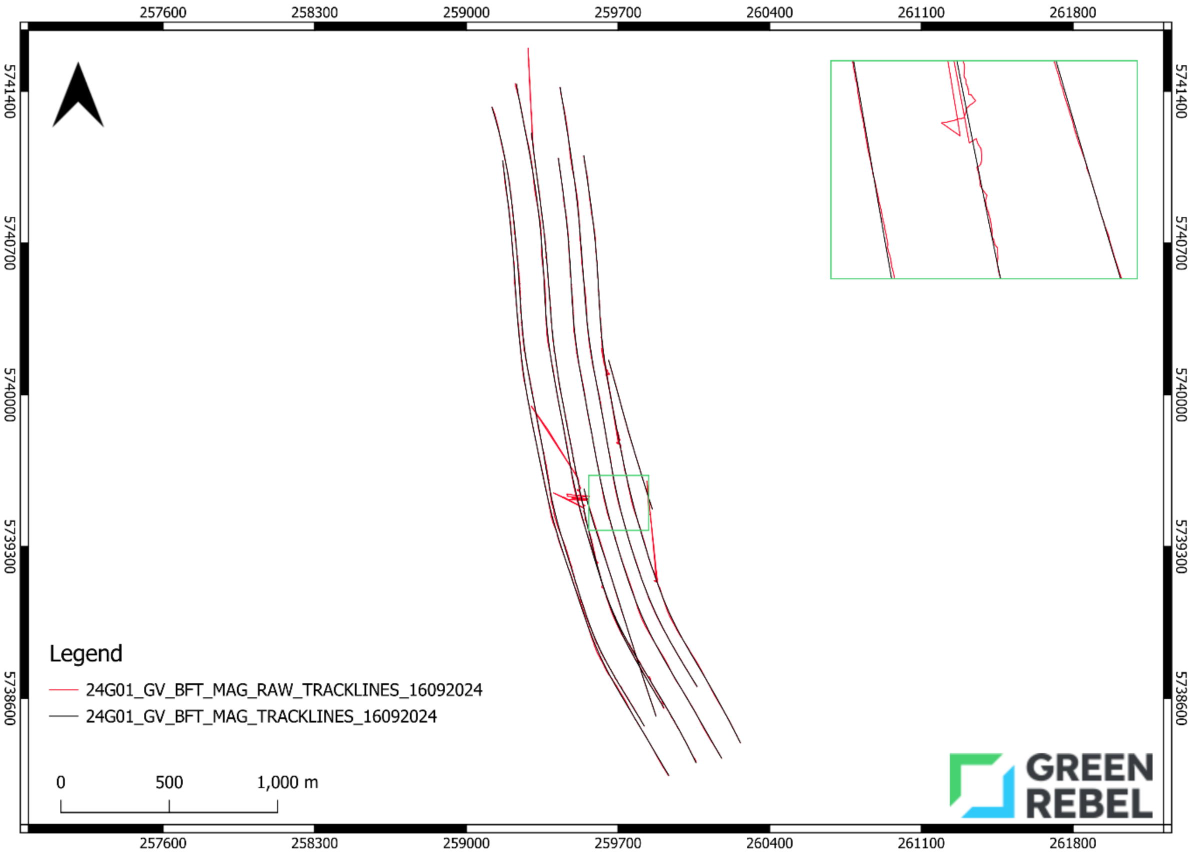

FIGURE 22: RAW VS PROCESSED MAGNETOMETER TRACKLINES.

The raw magnetic gamma values were then inspected, and erroneous spikes were removed through the implementation of an upper and lower threshold limiter filter with a range of approximately 47,000 nT and 52,000 nT. To determine regional background values, a stationary filter (smoothing constant) was applied to the raw magnetic trace (M1). A moving average, low-pass filter was then applied to the cleaned M1 trace, resulting in a background magnetic field calculation (M2). The residual magnetic trace 'K' was subsequently calculated by (Equation 2):

(Equation 2)

$$M1 - M2 = K$$

To identify targets, both the residual and analytic trace were used. The analytic trace identifies only the positive spectrum of an electromagnetic response, thus making it preferred for the picking of monopole targets. The residual trace encompasses both the positive and negative spectrums, allowing for the identification of dipoles and complex targets. Once picked, a target shapefile was then exported and brought into the SSS/SBP/MBES projects, where they were inspected manually over these datasets to determine both their source and the validity of the anomalous reading. When no obvious feature can be observed, other data strings were assessed (e.g., vessel log for nearby vessels, buoys, sudden depth changes) that may have induced spurious data values. Induced anomalies (vessels, buoys, depth changes etc) are removed from the list of anomalies.

2.6 Sub-bottom profiler

The Glomar Vantage is out fitted with an Innomar standard 100 parametric sub-bottom profiler mounted to a plate welded to the moon pool hatch. Time synchronised navigation data and heading and motion data were provided to the system controller by the primary POS MV GNSS and heading and altitude sensors. The primary frequency of 100 kHz was used to determine the bathymetry and the secondary frequency of 8 kHz was used to determine the sub-seafloor strata. Acquisition was managed using Innomar SESWIN software, which visualised raw sub-bottom profiles in real-time. Online data was quality controlled in SESWIN to ensure acquisition parameters were optimised during the survey operations. Raw data were recorded as *.ses3 files, heave-corrected, and subsequently converted to SEG-Y file. Format handling procedure and the relevant trace header byte information are included in Appendix 1. The geophysical lines were surveyed with a line spacing for mainlines of 50 m inside 12nm and 70 m beyond the 12nm and 3000 m for crosslines throughout the area (Figure 23).

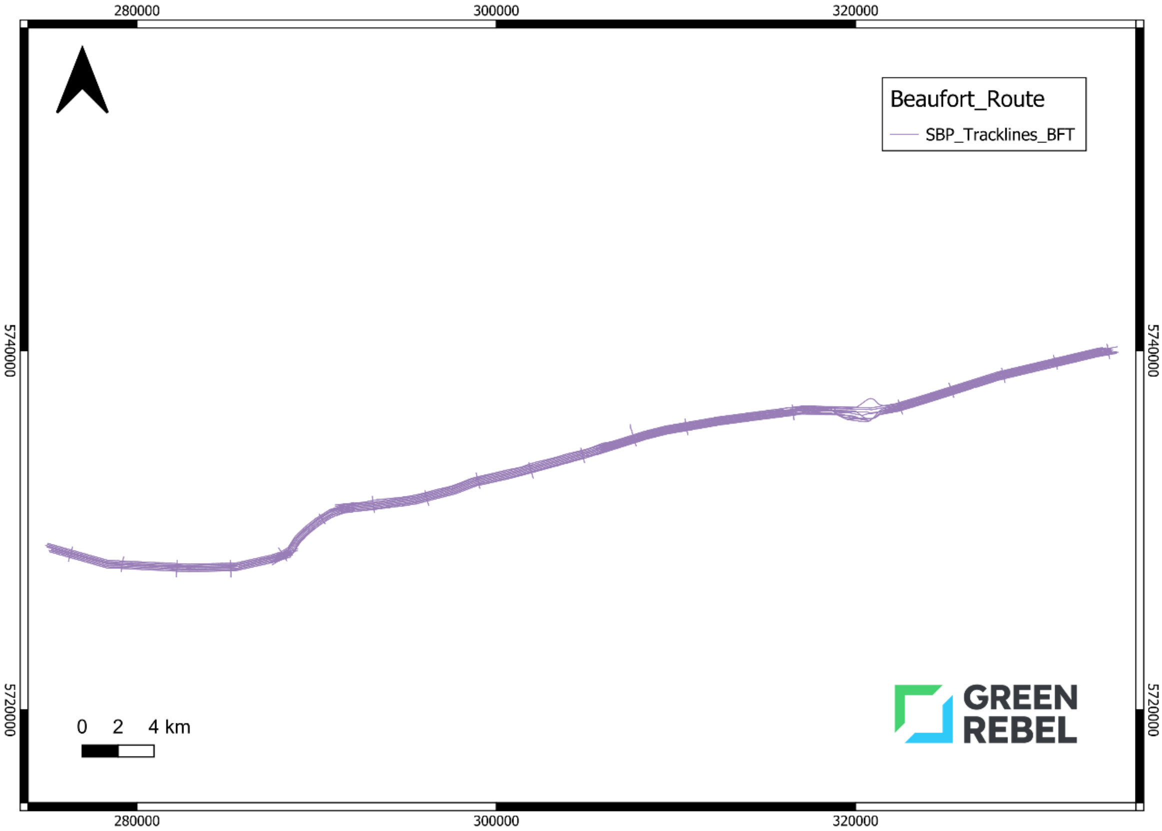

FIGURE 23: SBP TRACK LINES FOR THE GLOMARE VANTAGE.

2.6.1 Processing workflow

Sub-bottom Profilers (SBP) are used to image and characterise the physical properties of the sub-seabed and its internal structure. Sub-bottom profiler processing aims to generate high-resolution images that can aid geological interpretation and characterisation of the study area. The general workflow is outlined in Figure 24.

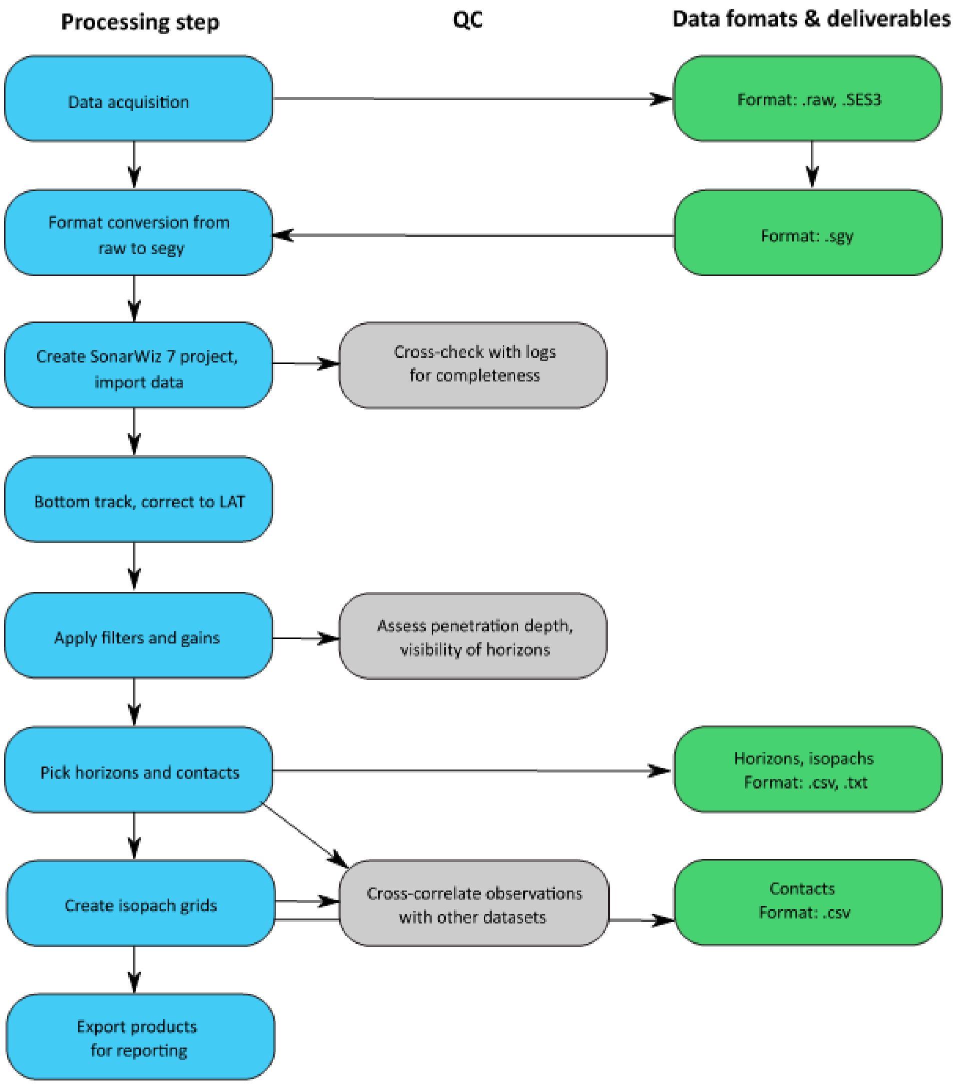

FIGURE 24: GREEN REBEL'S SUB-BOTTOM PROFILER DATA PROCESSING AND ASSESSMENT WORKFLOW.

2.6.2 Tidal and datum control

The sub-bottom profiler was mounted to a plate welded to the lower moon pool hatch and was deployed with a vertical orientation during survey operations. The SBP received its ellipsoidal absolute position from the iXBlue HYDRINS (a Global Navigation Satellite System inertially aided), with centimetric accuracy vertical positioning corrections. Subsequently, the SBP transducer data needed to be reduced to the survey datum: LAT. This was achieved by correcting the bottom-tracked SBP data to datum-corrected bathymetry during post-processing using the SBP vertical offset tool available in SonarWiz.

2.6.3 Resolution and penetration

The theoretical vertical resolution depends on the physical parameters of the used frequency and pulse length. It can be calculated as:

$$\lambda = \frac{vT}{4},$$

Where the pulse length, $T = \frac{1}{f}$, f is the centre transmitted frequency, and v is the sound speed in a medium. The Innomar sub-bottom profiler for Roman Rebel was operated using a transmitted frequency of 8 kHz, thus providing a vertical resolution of up to 0.045 m.

The Innomar medium 100 SBP has a transmit beam width of ±1° (at the reference level of -3dB), which corresponds to the footprint of c. 3.5% water depth. This means that at 1 m water depth, the horizontal resolution is 0.035 m. The average depth at the survey site, calculated from the MBES bathymetry, equals -93.4m. Hence, the mean SBP beam footprint during the survey operations was 3.27 m. The typical sample frequency was 96,000 samples, with a mean of 4480 samples per echo recorded. The signal pulse length was 257 µs.

The range length for the recorded Innomar SBP data was adjusted when needed during the survey operations according to the observed water depth and sub-seabed penetration and spans between 55m and 90m. The parameters above optimise the Innomar sub-bottom profiler to capture a range of up to 10 m below the seabed. However, the penetration depth largely depends on the acoustic properties of encountered substrates.

2.6.4 Data quality and signal processing

Sub-bottom profilers define and characterise sediment structures in the shallow subsurface (i.e., unlithified sediments) but can also detect the surface of the underlying bedrock under the right conditions. Given that the sub-surface features can be well-delineated in the raw data, the Innomar SBP data meet specifications and is fit for purpose. Sub-seabed reflectors are evident and display a strong signal where present across the survey area.

Some data were affected by weather-induced noise, given the sensitivity of the Innomar transducer to collision with air bubbles during less favourable sea states. This phenomenon typically occurs as vertical stripes in the data (Figure 29). Despite these artefacts, seabed reflectors are visible, continuous and can be objectively resolved. The noise unaffected the penetration depth and, as mentioned in the previous subsection, depends on subsurface geology.

The raw data from the Innomar standard show a notable low-frequency noise (Figure 25: Example of a RAW magnitude spectrogram of line GR24G01_BFT_B04B_P140_20240711_094004 Innomar Standard acquired using an Innomar Standard on the Glomar Vantage. Cross talk can be observed between 0 – 20k kHz and -51dB.) recorded (up to -21 dB at < 3000 Hz) and some additional interference at the higher frequency (> 10000 Hz). Similarly, the raw data from the Innomar Standard shows low frequency noise (Figure 26: Example of a RAW magnitude spectrogram of line GR24G01_BFT_B03_P07_20240713_105624 Innomar Standard acquired using an Innomar Standard on the Glomar Vantage.) recorded up to (-12 dB at < 4000 Hz). It is expected that the noise experienced at lower frequencies is ambient noise within the water column and from the vessel (Figure 25: Example of a RAW magnitude spectrogram of line GR24G01_BFT_B04B_P140_20240711_094004 Innomar Standard acquired using an Innomar Standard on the Glomar Vantage. Cross talk can be observed between 0 – 20k kHz and -51dB. and Figure 26: Example of a RAW magnitude spectrogram of line GR24G01_BFT_B03_P07_20240713_105624 Innomar Standard acquired using an Innomar Standard on the Glomar Vantage.), while noise associated with higher frequency is likely introduced from other survey equipment e.g., multibeam echosounder or SSS. This interference can be cleaned and filtered out post-processing by applying a bandpass filter to remove the excess low and high-frequency signal components.

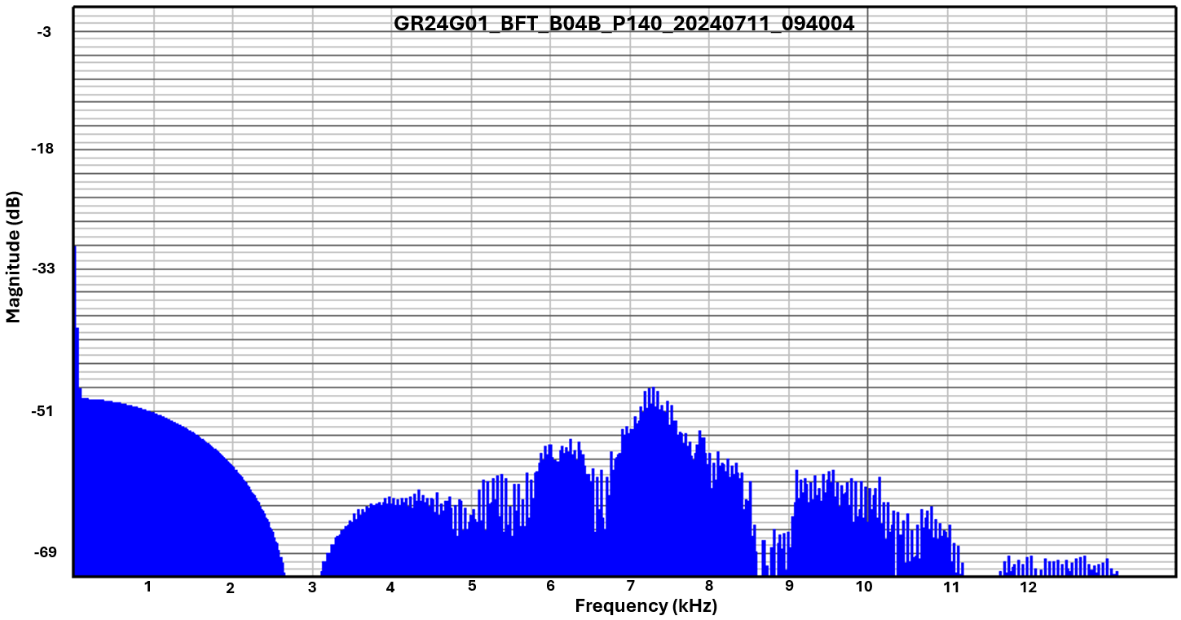

Figure 25: Example of a RAW magnitude spectrogram of line GR24G01_BFT_B04B_P140_20240711_094004 Innomar Standard acquired using an Innomar Standard on the Glomar Vantage. Cross talk can be observed between 0 – 20k kHz and -51dB.

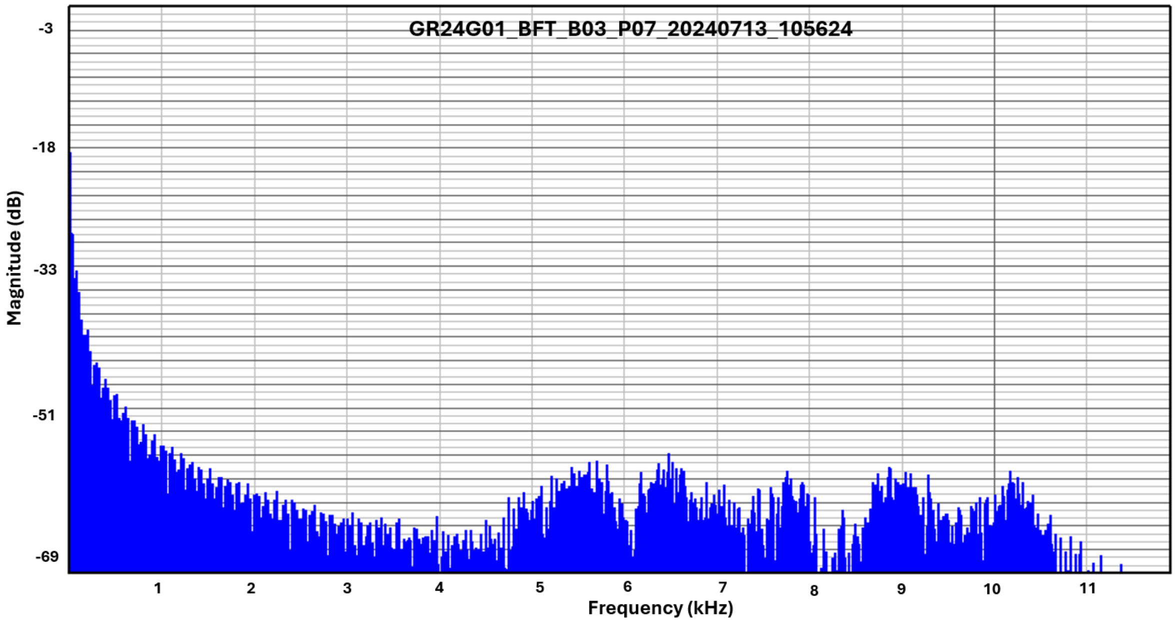

Figure 26: Example of a RAW magnitude spectrogram of line GR24G01_BFT_B03_P07_20240713_105624 Innomar Standard acquired using an Innomar Standard on the Glomar Vantage.

2.6.5 Final product (quality)

Noise artefacts can be corrected and improved during data processing through signal processing, gains and filters. Therefore, after bottom tracking filter parameters were chosen based on frequency distribution of the noise visible in the spectrograms (Figure 27) and applied to the acquired SBP data. Using RadEx Pro software, a minimum phase Butterworth filter was applied to the data. This filter applied a low-cut frequency of 5000 Hz with a 24 dB/octave slope and a high-cut frequency of 10000 Hz with a 24 dB/octave slope. The tapering was set to 10%, and the processing used one thread. Additionally, a burst noise removal filter was applied with a window size of 11 traces for average value calculation, a 75% rejection percentage, and only amplitudes exceeding 5% of the average were modified. Values that exceeded the average more than 3 times were adjusted. Figure 28 and Figure 29 represent the frequency spectrum of raw and processed SBP data, this combination of filters improved the data quality and helped distinguish reflectors within the sub-bottom data.

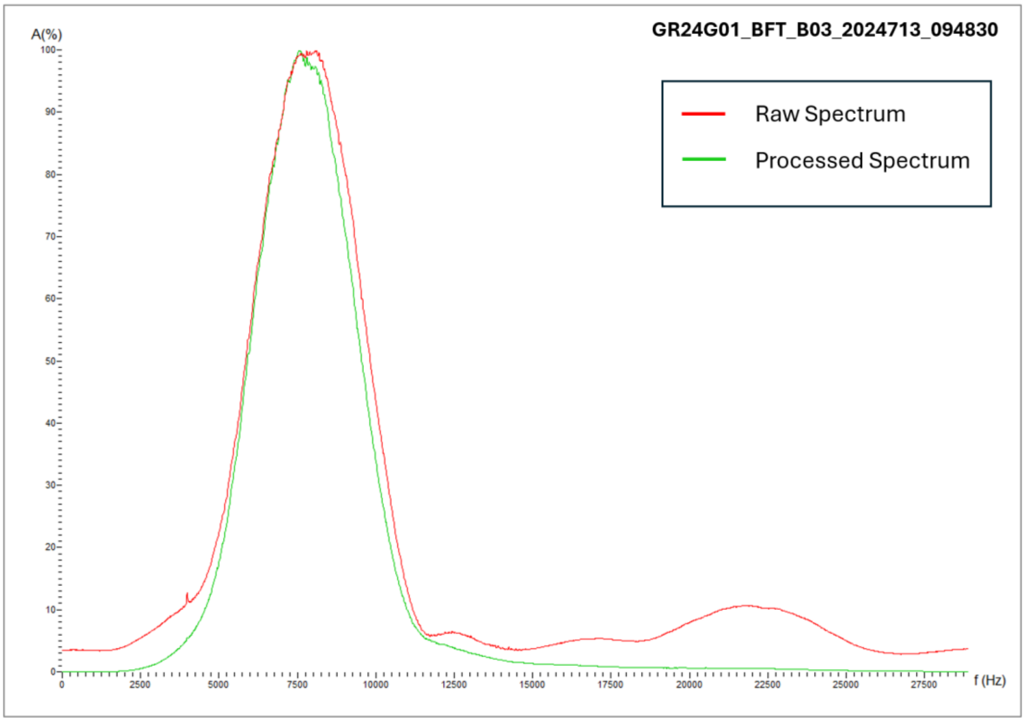

FIGURE 27: RAW VS PROCESSED FREQUENCY RESPONSE SPECTRUM FOR PROFILE GR24G01_BFT_B03_2024713_094830. FOR THE PROCESSED DATA A BUTTERWORTH FILTER AND BURST NOISE FILTER HAVE BEEN APPLIED.

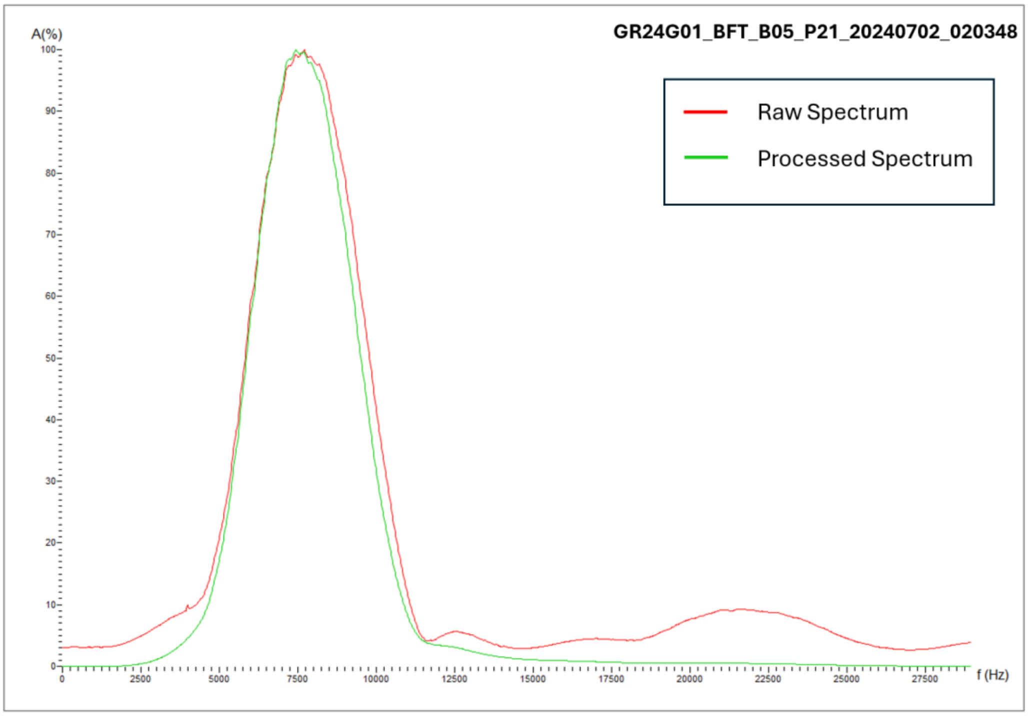

Figure 28: Raw vs Processed frequency response spectrum for profile GR24G01_BFT_B05_P21_20240702_020348. For the processed data a Butterworth filter and Burst noise filter have been applied.

These filters, together with the applied "water column blanking" tool, which eliminates the signal component corresponding to the water column above the seabed, significantly increase the visibility of weaker signals and enhance reflectors (Figure 29).

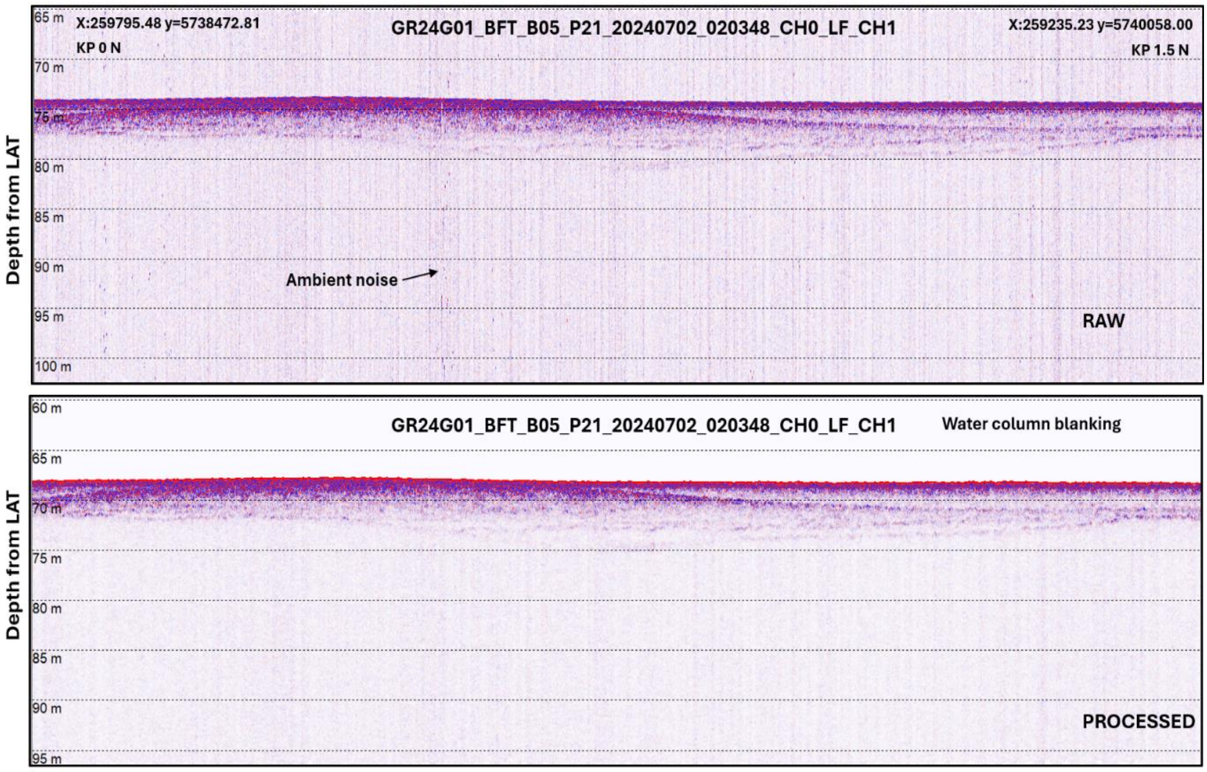

Figure 29: Top image; Raw data uncorrected for heave and with no vertical offsets applied. Bottom image: Processed data displays bottom tracked SBP data that is heave corrected and reduced to the LAT datum. A bandpass filter improves the signal to noise ratio.

3 Classifications

3.1 Inferred Seabed Sediments

Inferred seabed sediments are classified based on their acoustic backscatter response in the MBES backscatter data. The classes include fine, medium, coarse sediments and bedrock outcrops.

3.2 Seabed Targets

Table 8: Types of seabed contacts

Contact type	**Description**
Boulder	Rock >0.5 m
Debris	Small contacts, likely anthropogenic
Outcrop	Bedrock protruding from seafloor
Cable	Linear contact, resembling a cable
Linear Contact	Unknown contact, linear morphology
Sonar Contact	Unknown contact, alternative morphologies
Wreck	Shipwreck

3.3 Sedimentological bedforms

Table 9: Sedimentological bedform categories

Trochoidal sediment waves	Small (0.6 – 5 m length, 0.04-0.25 m height), Medium (5 – 10 m length, 0.25 – 0.44 m height), Large (10-100 m length, 0.5 – 2.8 m height), Very large (>100 m length, >2.8 m height). Symmetrical, trochoidal shape
Sediment waves	Small (0.6 – 5 m length, 0.04-0.25 m height), Medium (5 – 10 m length, 0.25 – 0.44 m height), Large (10-100 m length, 0.5 – 2.8 m height), Very large (>100 m length, >2.8 m height). Unsymmetrical, lee/stoss slope

3.4 Magnetometric Targets

Table 10: Magnetometric target classifications

Monopole	One identifiable positive/negative charge
Dipole	Targets found to have opposing charges due to polarity (both positive and negative)

4 Results

4.1 Multibeam bathymetry

4.1.1 Final Bathymetric product

In line with the project's specifications, the bathymetry was gridded both at 0.25 m and 1 m spatial resolution. The bathymetry of the Beaufort site is diverse, spanning from the shallower coastal waters near Abergele in Wales to the Irish territorial waters, thus extending across the Irish Sea. The seabed surface is covered with diverse geomorphological features typically associated with formerly glaciated margins like drumlins, possible tunnel valleys and iceberg plough marks. Sediment waves, trochoidal sediment waves and ripples of various lengths, heights and shapes are also observed in the bathymetry. Moreover, bedrock outcroppings are observed along the corridor.

The Beaufort bathymetric data is split into two sections: the main corridor and the small cable interconnector area in the west. Water depths across the site range from 46.05 m LAT to 135.66 m LAT.

The eastern extent of the main Beaufort bathymetric data terminates at the overlap zone with the 2023 Geophysical survey coverage of the Tuskar Route near the UK (Wales) in UK territorial waters. Beaufort is characterised by a varying bathymetric gradient associated with prominent trochoidal bedforms in the central area of the main corridor (KP25.8 to KP26.7) flanked by low relief bathymetry to the west and east.

The westernmost section of the Beaufort route covers small cable interconnector with a low relief bathymetric topography.

Any data gaps present in the delivered 0.25 m and 1 m resolution datasets were reviewed and approved by the client representative. Noteworthy, they do not hamper the interpretation requirements and as such can be deemed as fit for purpose.

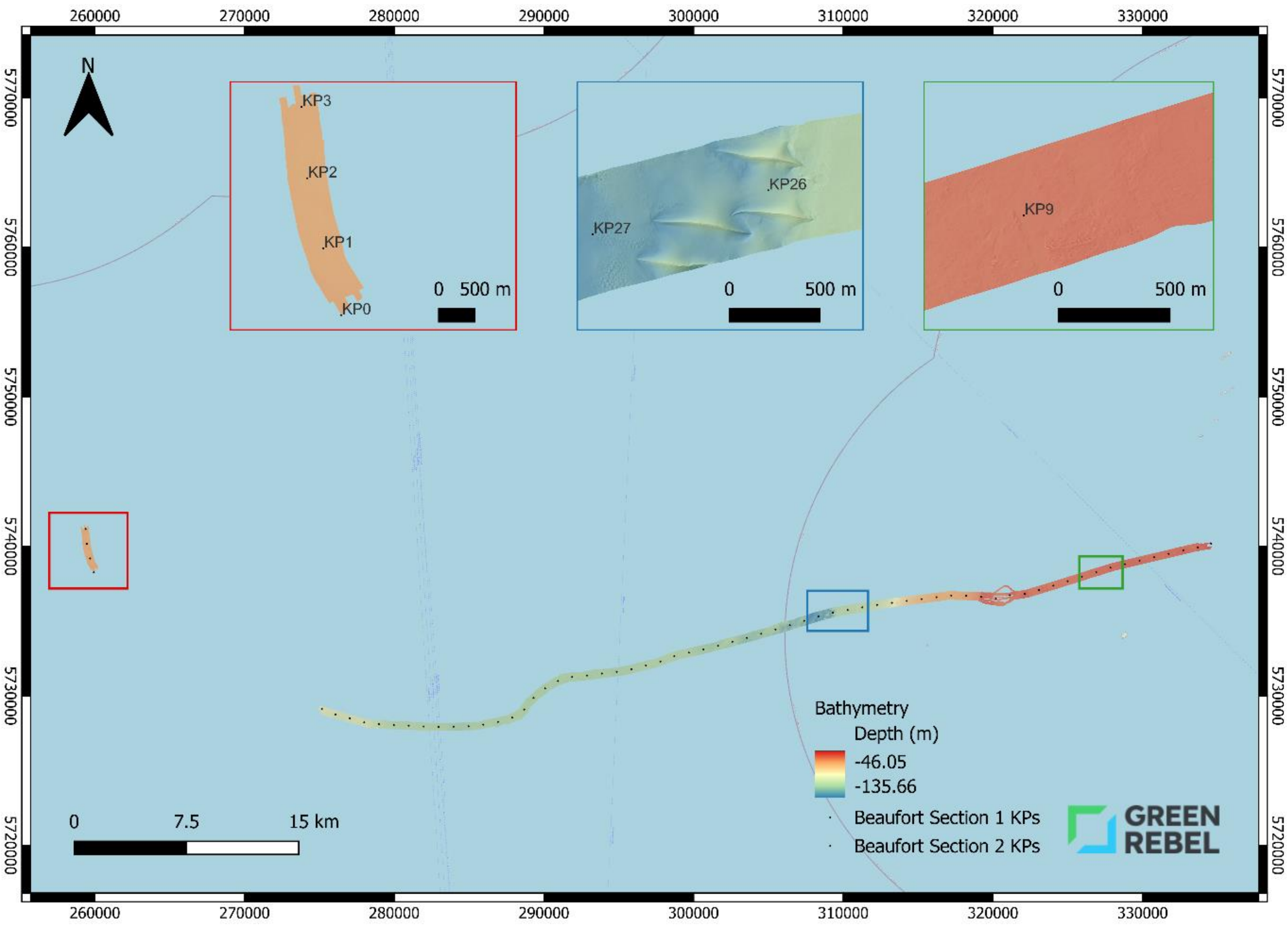

Figure 30: Beaufort MBES Bathymetry (Gridded at 1m resolution, multidirectional hillshade applied). Inset showing trochoidal bedforms (very large sediment waves) between KP26 and KP27 and the western most area highlighted in red.

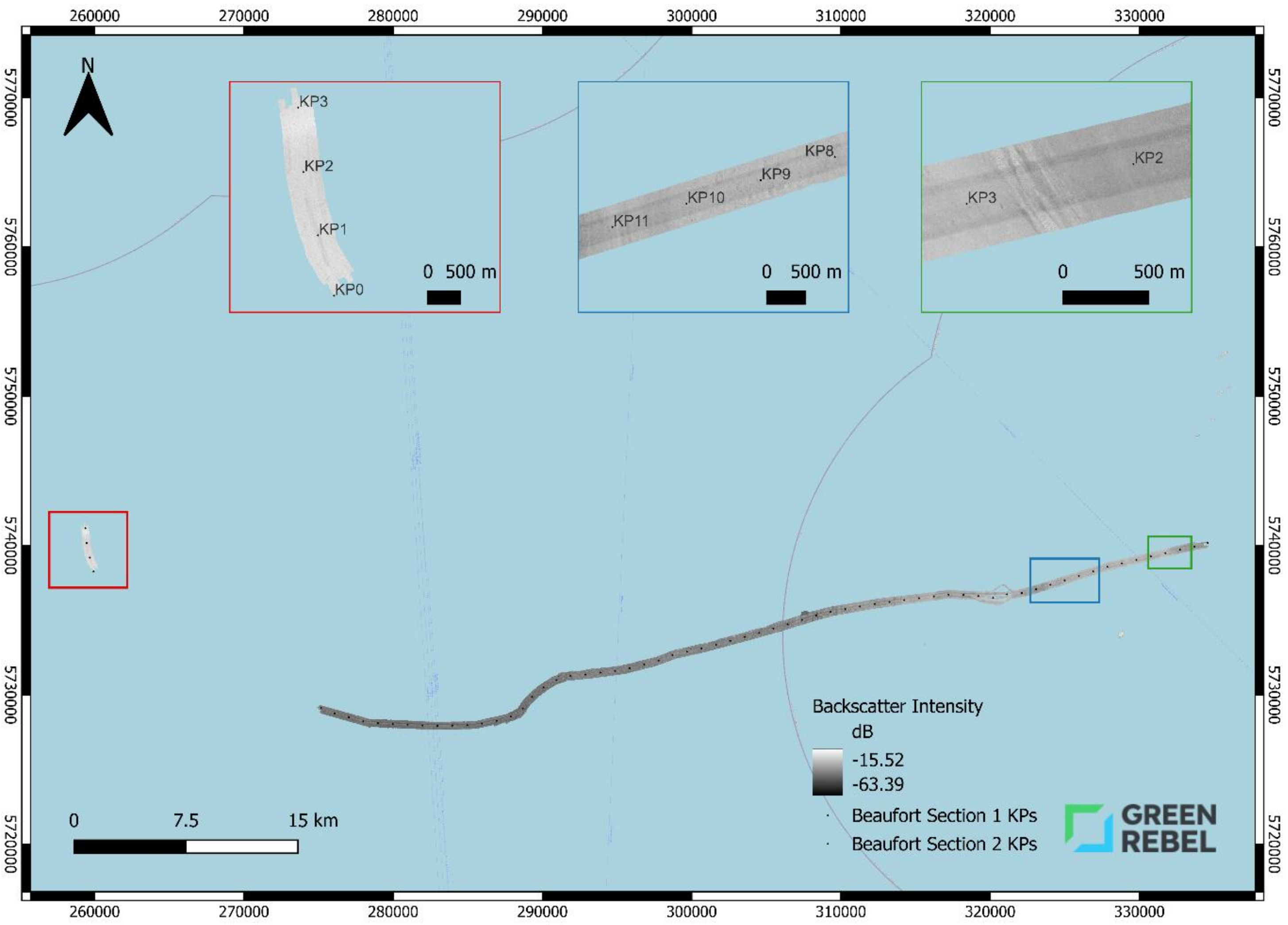

FIGURE 31: FINAL MBES BACKSCATTER PRODUCT (1M RESOLUTION) WITH THE PANELS CORRESPONDING TO SECTIONS WITH VARYING BACKSCATTER INTENSITY.

4.2 Multibeam backscatter

4.2.1 Final backscatter product

The final backscatter data were gridded and exported at 1 m resolution to match the resolution of the coarser bathymetry layer. Backscatter was gridded by colour denoted areas and were also merged into one grid using GIS. See Figure 31 for a combined mosaic of the entire Beaufort survey area which displays the extent of the backscatter coverage.

4.2.2 Seabed sediments

Analysis of the MBES backscatter suggests that the distribution of sediment across the Beaufort survey area shows a mosaic of mostly medium and coarse sediments and their distribution varies across the site (see Figure 32). Localised regions of exposed bedrock outcrops were also delineated (see an example in an inset map in Figure 32).

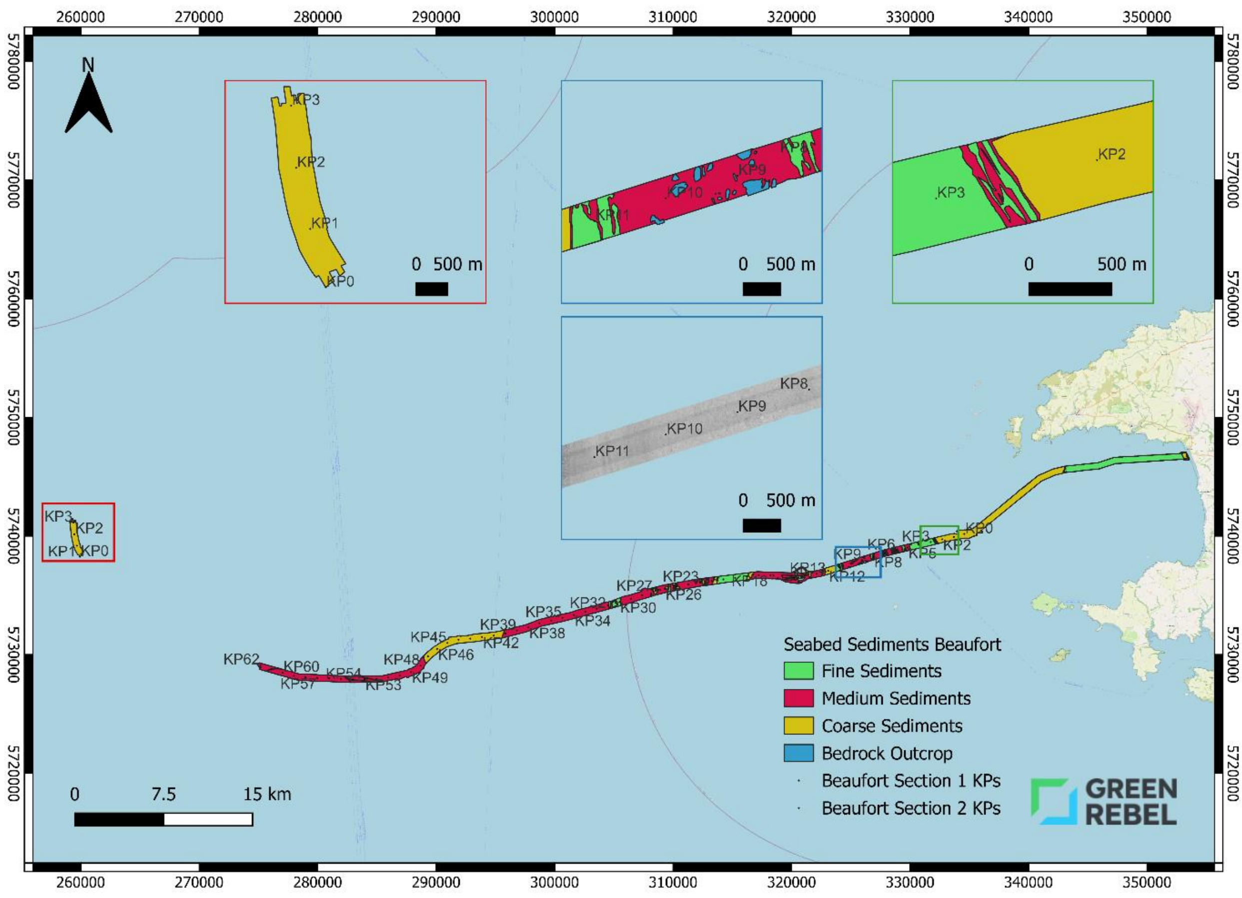

FIGURE 32: BEAUFORT SEABED SEDIMENTS DERIVED FROM MBES BACKSCATTER (NOTE: INSET MAPS SHOWING VARIABLE SEABED LITHOLOGY).

4.3 Side-scan sonar

4.3.1 Coverage

To survey the area approximately 639.62km of SSS data with an swath of 100m wide on either side of the nadir were collected (341.03km low frequency and 298.59km high frequency), including infill lines. This resulted in the insonification of a total area of 43km^2; 23.3km^2 low frequency and 19.7km^2 high frequency. Given the specifications of the survey, most of the site had 300% nadir overlap along the survey lines (Figure 33) with marginal areas receiving 200% overlap or at least 100% coverage along the perimeter. Any lines that were excluded during processing were deemed to be of inadequate quality but did not result in lost coverage.

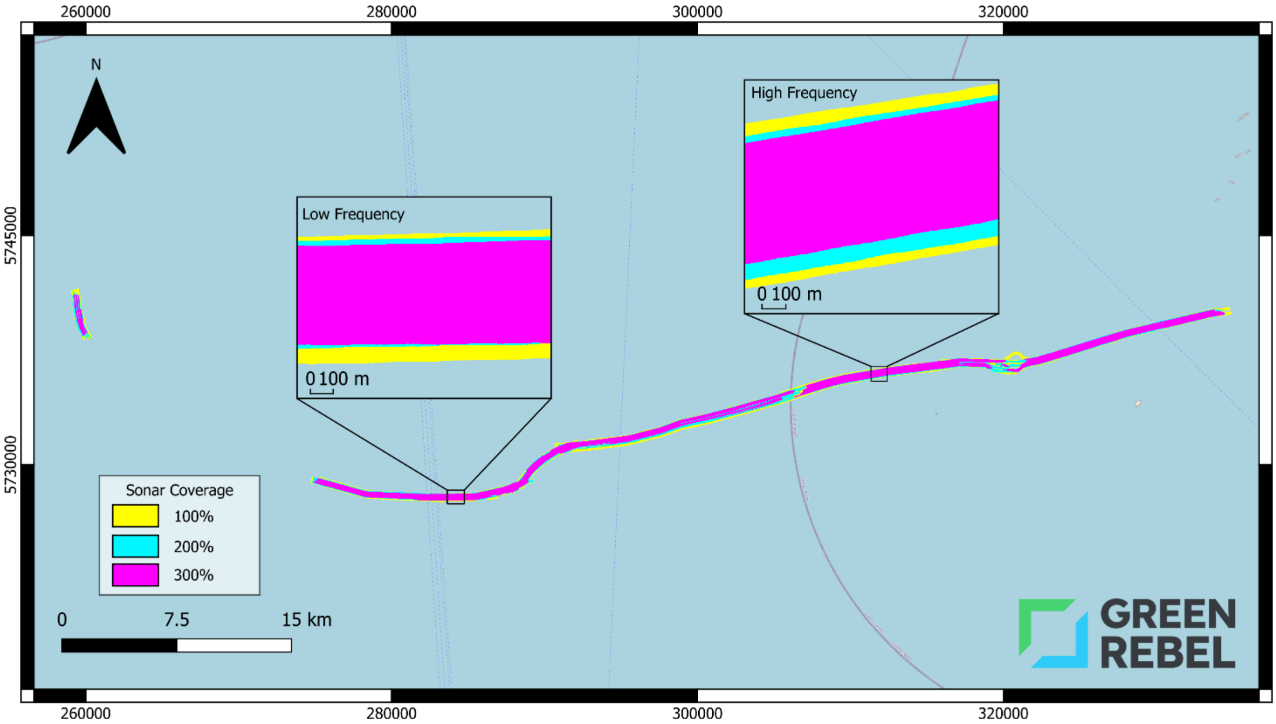

FIGURE 33: SIDE-SCAN MOSAIC COVERAGE (%) TAKEN FROM HIGH AND LOW-FREQUENCY SSS.

4.3.2 Processed accuracy

Although SSS navigation and positional accuracy were adequate throughout the survey, post-processing navigation and map corrections were utilised to improve the whole dataset to reach the desired quality outlined in the scope of works. Figure 34 displays the tracklines of the SSS towfish pre-processing (red), highlighting where navigation is considered “out of spec”, and post-processing (green) where the data have been deemed appropriate. The navigation required modification to remove data gaps caused by USBL dropouts and spatial jumps caused by USBL position. Using interpolation, all navigational spikes and swirls were amended. Accuracy was further increased using port and starboard rotation of each file. Map corrections were then applied across the whole area. The initial average accuracy of the files was greater than the originally specified 2m accuracy, with a final average accuracy of 1.2m calculated from a total of 30 randomly distributed control points.

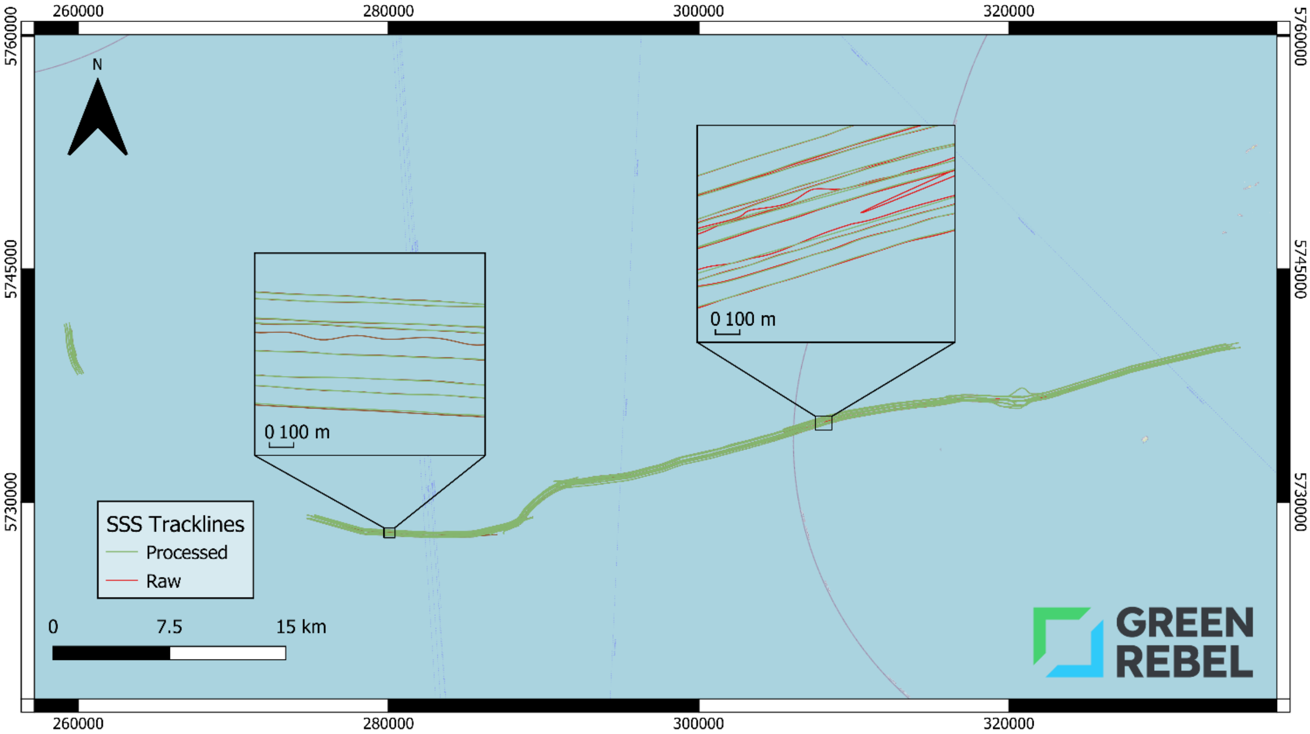

FIGURE 34: MAP OF SSS TRACK LINES BEFORE AND AFTER NAVIGATION CORRECTIONS AND PROCESSING.

4.3.3 Final product

Initially raw SSS data exhibit progressive darkening along the outer swath, representing the attenuation of signal in the water column. This was rectified by applying gains that homogenised the swath data. As per the scope of work a mosaic was then delivered at 0.2 m pixel resolution Figure 35. The mosaic was of very high quality and seafloor features, sand waves and boulders, are clearly discernible, as demonstrated by low and high backscatter. Finally, the .csf files were converted to deliverable format .xtf file type using floating point conversion, to avoid over-compression and maintain 16-bit scaling.

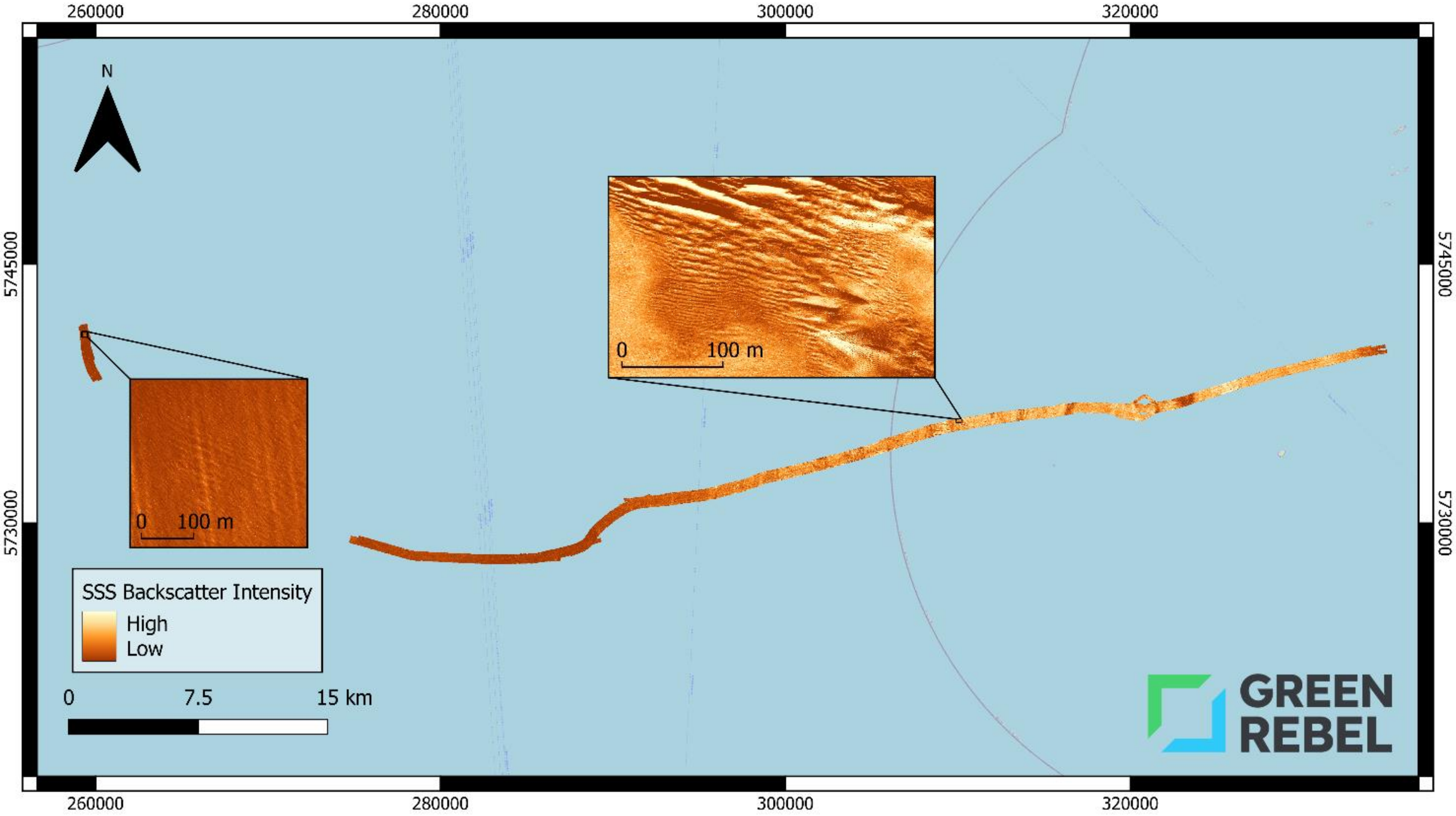

FIGURE 35: FINAL SONOGRAPHIC MOSAIC OF THE SSS DATA EXPORTED AT 0.2 M RESOLUTION.

4.3.4 Sonar Contacts

SSS was employed to capture contacts on the seafloor. In the context of offshore engineering, any anthropogenic objects like wrecks, discarded, lost or snagged fishing gear, potential unexploded ordnance, cables, pipelines and other debris as well as natural seabed features like boulders should be detected to avoid collision with the planned development. Contact picking resulted in the geolocation of 98 and 3052 contacts at the low and high frequency areas respectively. The most commonly occurring contacts, i.e. boulders (Figure 36), are interspersed throughout the survey area. Contacts were correlated with MAG targets, with findings suggesting Contact 238 corresponding with MAG Target 16 and Contact 22 with MAG Target 39.

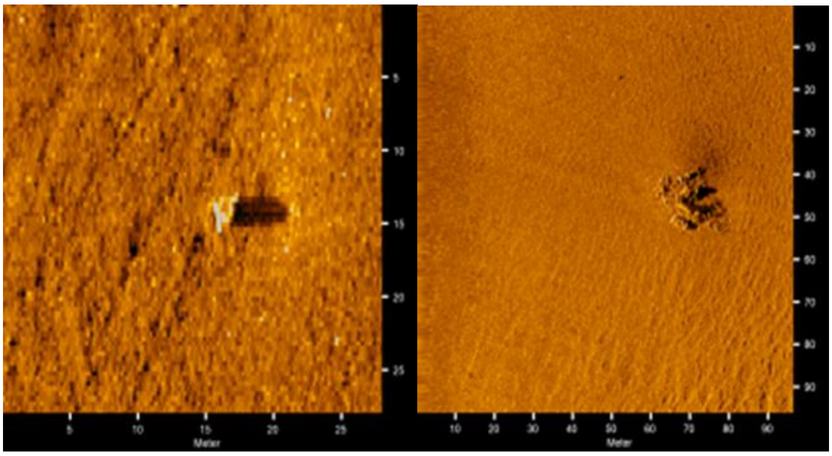

FIGURE 36: EXAMPLES OF SSS CONTACTS (LEFT – BOULDER, RIGHT – DEBRIS ASSOCIATED WITH MAG TARGET 16) ENCOUNTERED AT THE BEAUFORT SITE.

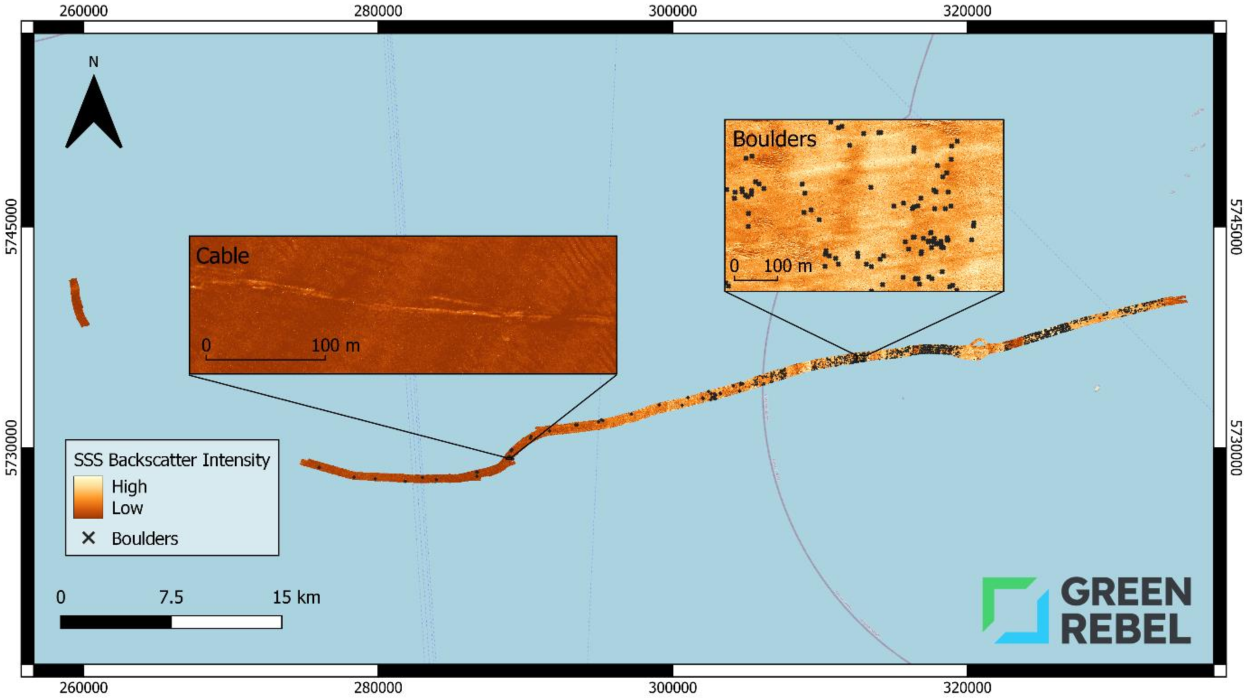

FIGURE 37: SSS CONTACTS FROM THE SITE. NOTE INSET OF A CABLE TO THE WEST (KP 47.74 OF SECTION 1).

4.4 Magnetometer

Overall, the coverage of the dataset was deemed of high quality despite the navigation spikes. Navigational gaps were present when the USBL lost signal to the beacon which was likely weather induced. As a result, given that the raw magnetic signal could not then be parsed with x and y coordinates, these data were rejected based on precautionary principles. This is rectified in post-processing by simply interpolating within the error window. The processed magnetometer data were gridded and covered a line length of approximately 633.48 km (Figure 38).

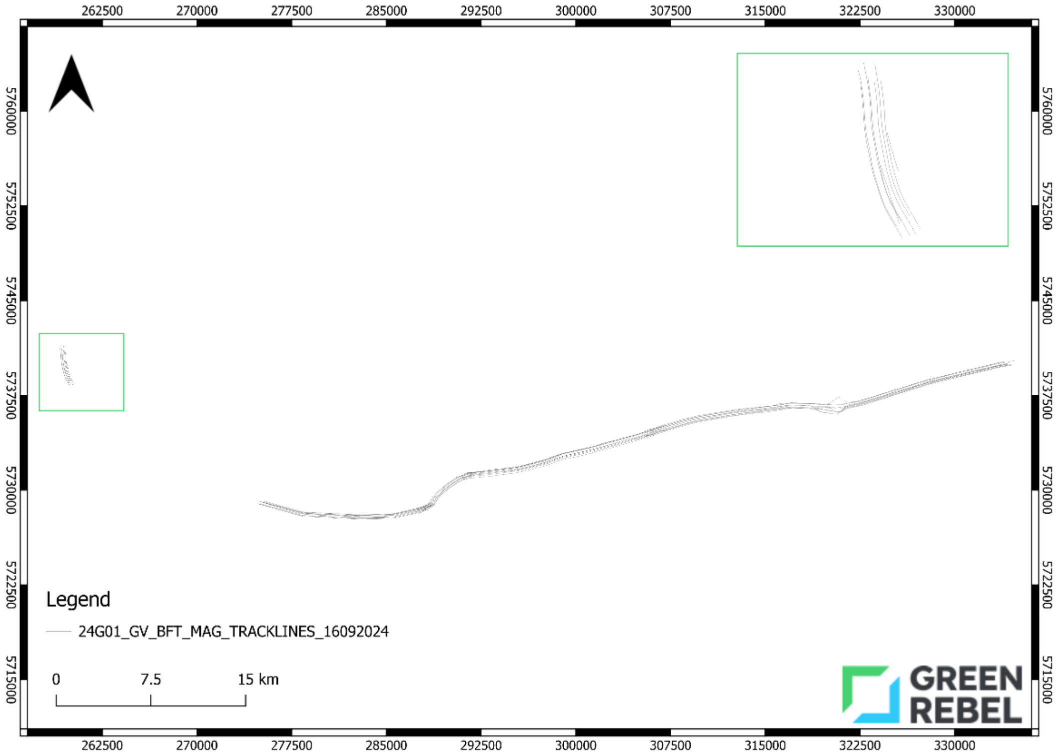

FIGURE 38: PROCESSED MAGNETOMETER TRACKLINES.

4.4.1 Altitude and Depth

The mean survey depth observed was 86.56 m (Table 11). A high standard deviation of 26.283 m reflects variation in water depth across Beaufort. Notably the western corridor often exhibits depths exceeding 100m, whereas the eastern section shallows significantly approaching the east coast of Wales. The mean survey altitude of the fish above the seafloor was 9.29 m. This value is skewed slightly due to the fishing box in the eastern side of the site. A decision was made to acquire as much data as possible around this box, with no time mitigated for rerun later. The maximum altitude of 50.03 reflects this, as altitudes over this feature were heavily inhibited. A right-skewed distribution in the altitude was noted as a result (Figure 39). Both the total field and residual data sets are within the expected value ranges, with symmetrical distribution found in both variables (Figure 40). For these reasons given, the magnetometer data meet the required specifications outlined in the scope of works.

TABLE 11: BEAUFORT MAGNETOMETER STATISTICS

Data	Depth of Mag. (m)	Altitude of Mag. (m)	Total Field (nT)	Residual Amplitude (nT)	Analytic Signal (nT)	*Signal Quality (nT)*
Minimum	3.05	2.04	48828.38	-0.68	0.00	7.00
Maximum	125.54	50.03	49202.14	0.75	19.82	1387.00
Mean	86.56	9.29	48967.67	-0.00	0.06	836.71
Median	102.63	8.46	48963.98	-0.00	0.04	1023.00
Mode	3.05	2.04	48828.38	-0.00	0.00	410.00
St. Deviation	26.283	4.677	31.562	0.004	0.236	393.441

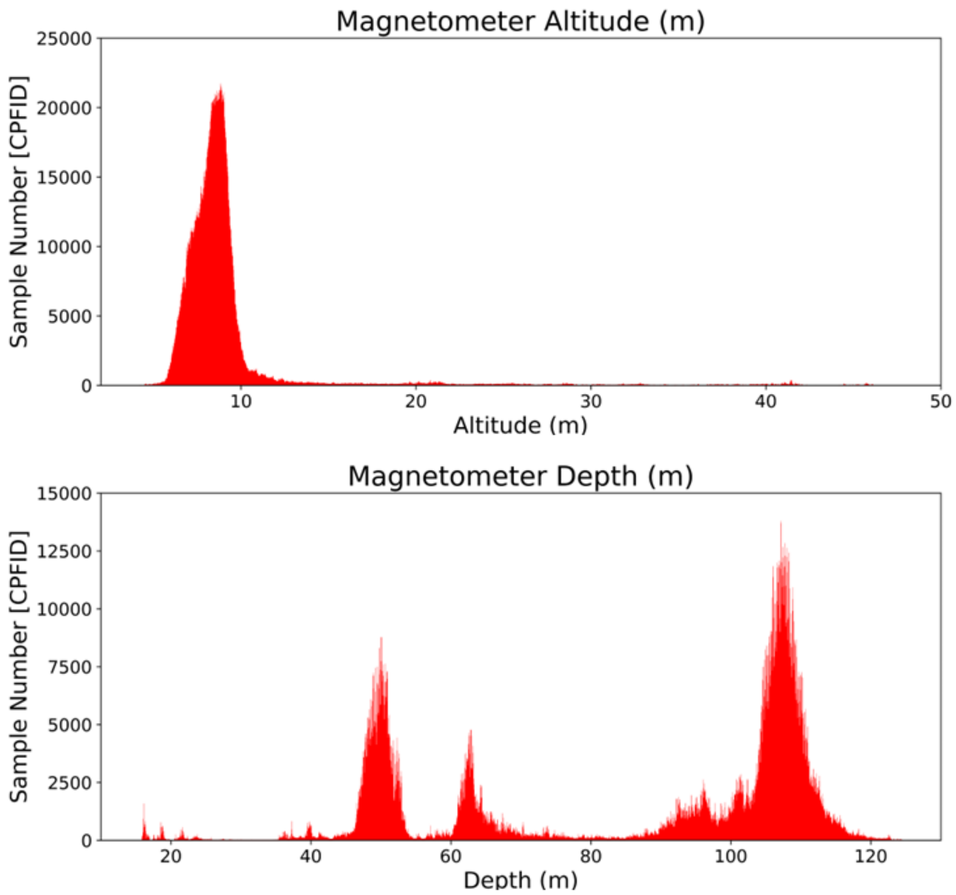

FIGURE 39: ALTITUDE & DEPTH ACROSS BEAUFORT.

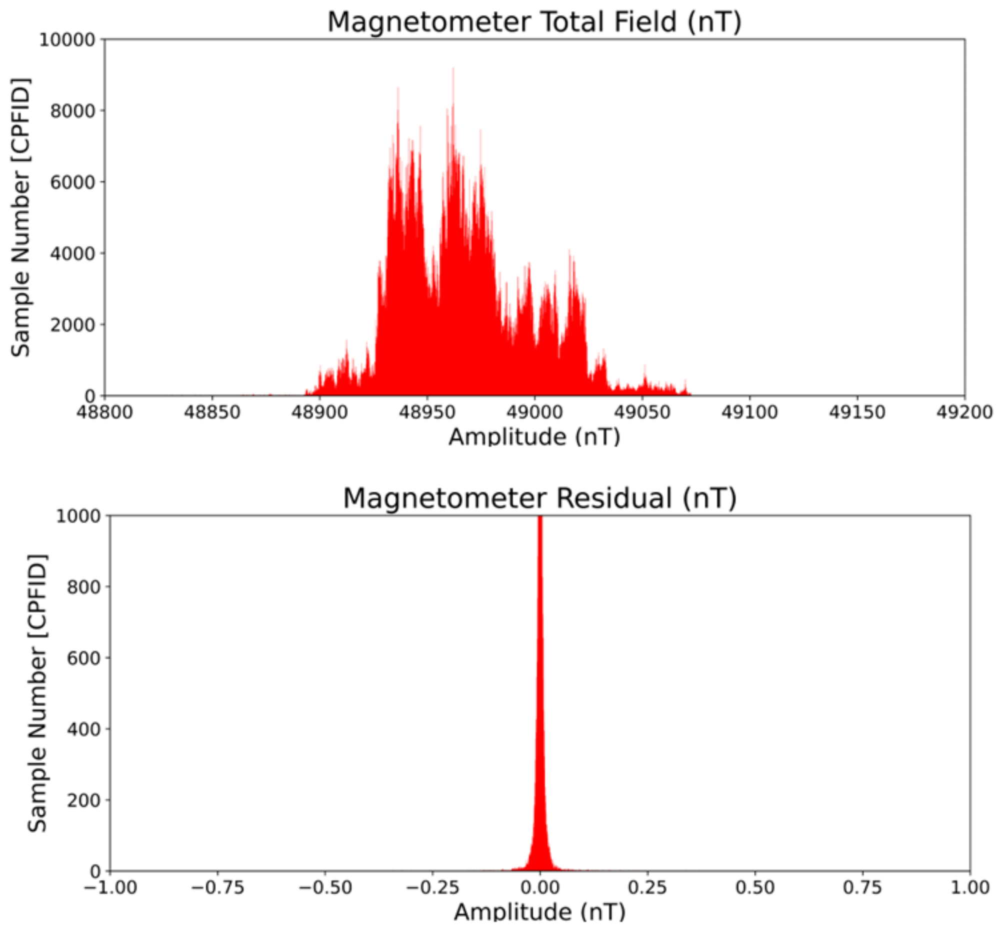

FIGURE 40: TOTAL FIELD & RESIDUAL ACROSS BEAUFORT.

4.4.2 Data quality

All magnetometer data acquisition was managed by QPS QINSy where the raw information was read into a series of *.txt files. To assess the data quality for the magnetometer, an examination of the magnetometer's signal strength across the area was conducted. This parameter is measured in nT and has a typical measurement range of 0 – 1500 nT. The parameter measures the intensity of interference on the magnetometer's caesium sensor. Sources of interference include light penetration, usually an influence during shallow acquisition. A second interference concerns piggyback configuration, in which the tow cable is taut/slack by sudden changes in vessel speed and or/direction. Data of good standard will have signal strength exceeding 250 nT, with exceptional data passing 750 nT. Data collected in shallower environments tends to have lower signal quality, because of surface light and/or interference with sensors on the vessel due to the reduction in cable out length. To assess the quality of the Beaufort site, an investigation into the signal strength was conducted across the GV with results as follows.

Signal quality across the site was defined by two distinct clusters (Figure 41). It was noted across the shallower nearshore zone and the fishing box that the magnetometer signal readings were lower, whereas the deeper offshore waters more suited to magnetometer acquisition returned higher levels of quality data. Navigation over the fishing box was difficult, resulting in an unstable flight in all towed sensors. This in conjunction with the instability in altitude resulted in lower quality data. In the nearshore zone, surface light and the effects of current are likely causations for lower quality data here. Despite this, even the lowest quality data still far exceeds the 200 nT mentioned previously, and this can be contributed to excellent survey design despite the challenges faced.

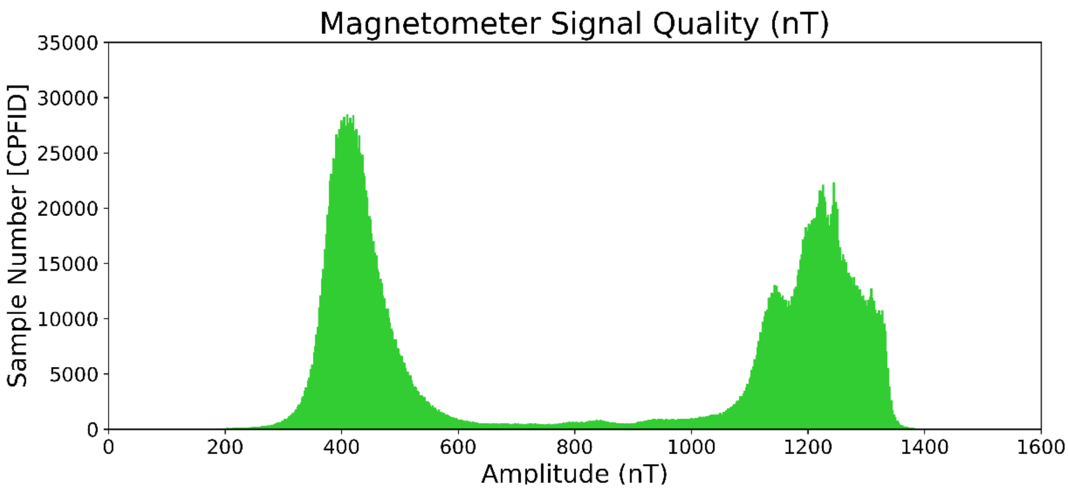

FIGURE 41: SIGNAL QUALITY ACROSS BEAUFORT.

4.4.3 Magnetometer Targets

In total, 49 magnetometer targets were identified across the site (Figure 42). These were classified based on the nature of the residual signal response. Targets with one identifiable positive/negative charge were classified as monopole. Targets found to have opposing charges due to polarity (both positive and negative) were identified as dipole structures. In this site, both monopole and dipole targets were identified.

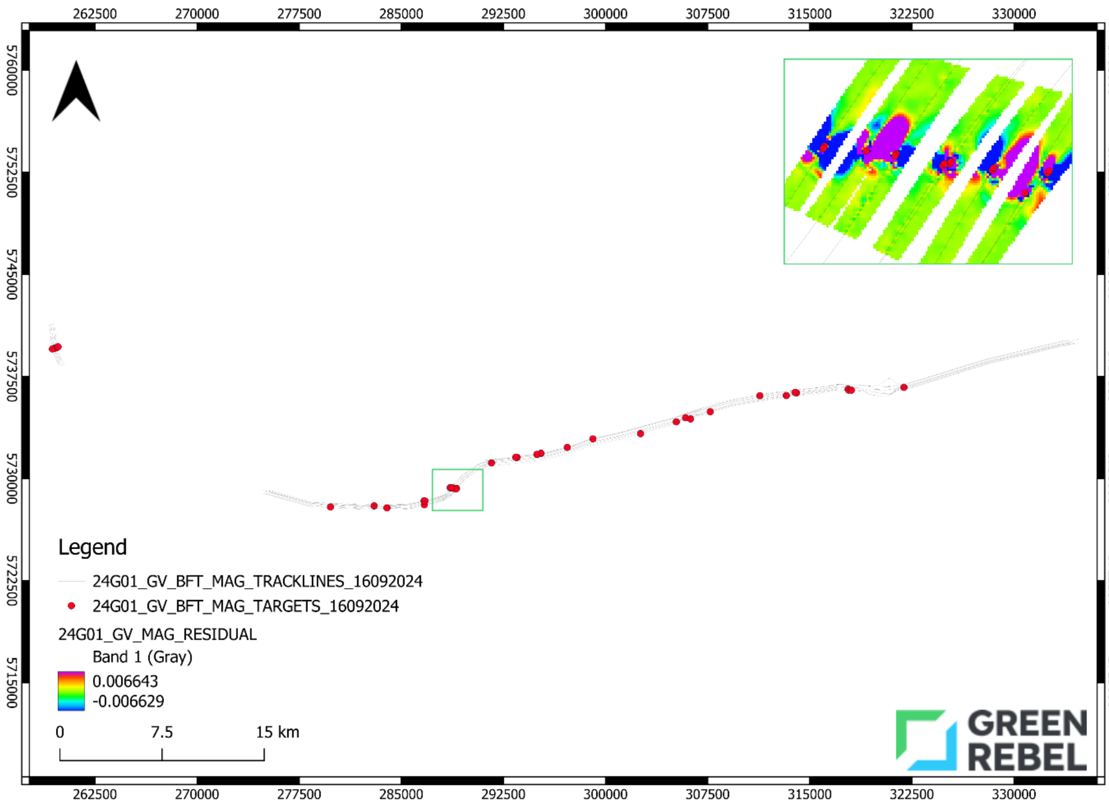

FIGURE 42: MAG TARGETS ACROSS BEAUFORT.

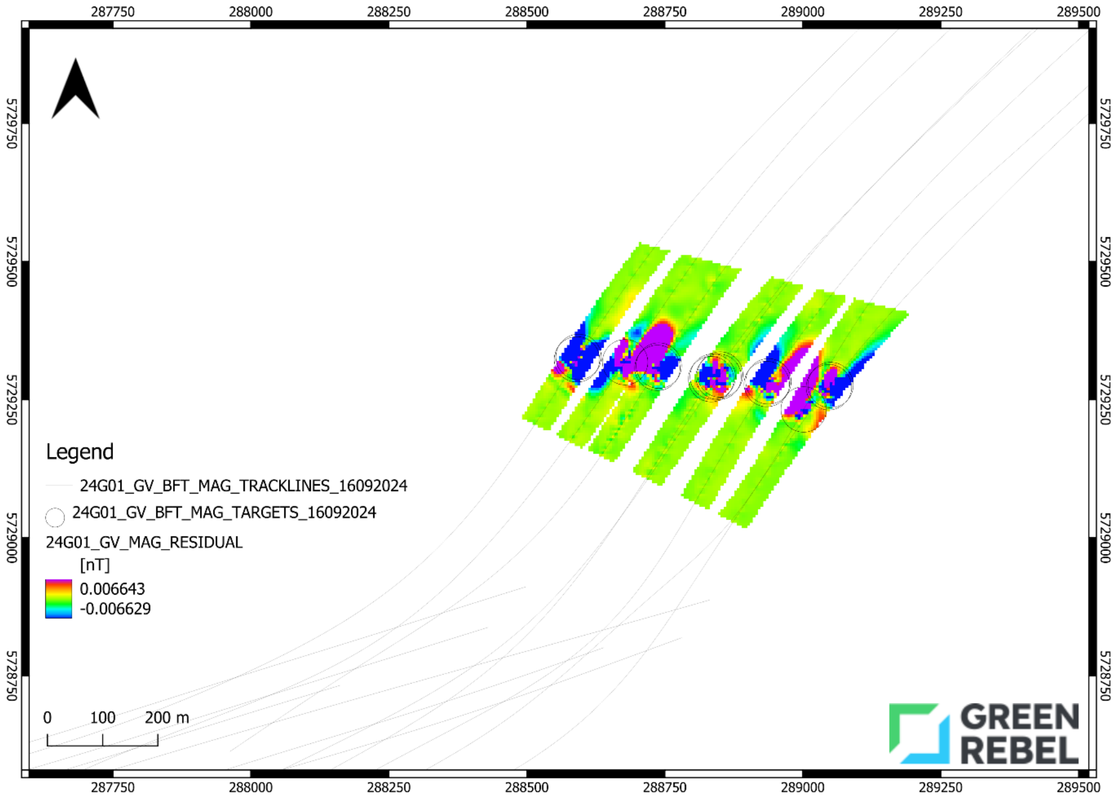

FIGURE 43: LINEAR FEATURE 1.

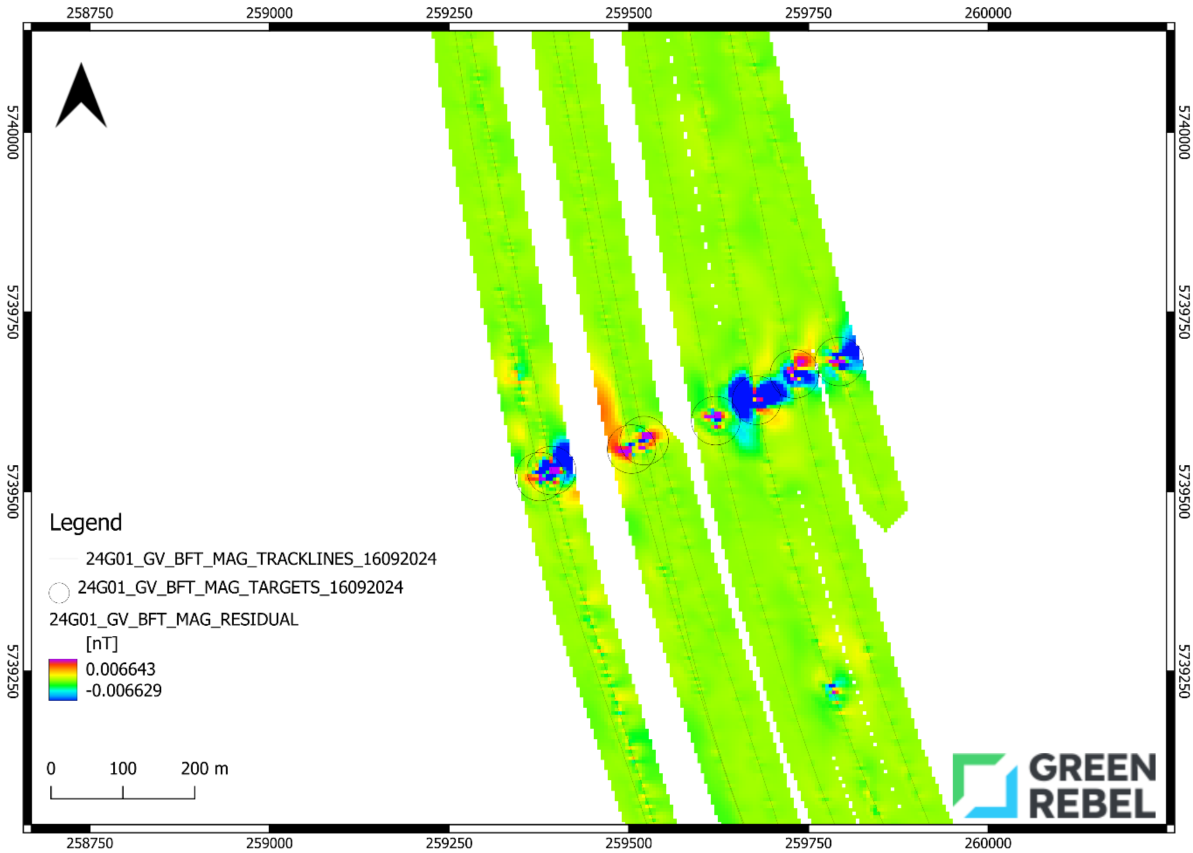

FIGURE 44: LINEAR FEATURE 2.

As noted above, 49 targets were identified from GV data in the survey site (Figure 42). 35 monopoles were identified, with the remaining 14 classified as dipoles. Two linear magnetic assemblages were identified in Beaufort. The first (Figure 42 & Figure 43) which correlate to the Greenlink HVDC Interconnector cable. This behaviour is what we would expect when dealing with buried cable/pipeline systems.. A second linear feature in the north-west isolated corridor exhibits almost identical behaviour magnetically to the first feature, so an assumption can be made that this is also likely to be the Greenlink HVDC Interconnector cable (Figure 44). To reiterate, further analysis is again needed here to assure absolute certainty. A total of 22 targets were correlated to both structures.

4.1 Seismo-stratigraphy

Across the study area, 6 seismic units were identified, and their configuration is described in Table 12. Each unit and its respective horizon are described separately using depth below the seabed. Representative Innomar sub-bottom profiles are included at the end of this section. All horizons were picked to define the top of each stratigraphic unit.

TABLE 12: SEISMO-STRATIGRAPHIC TABLE FOR THE SURVEY SITE.

Seismic Unit	Seismic reflection pattern	Horizon	Reflection Continuity	Amplitude	Reflection configuration	Termination	Geological Interpretation
Seabed	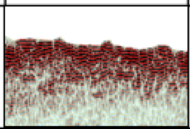	H1 (Seafloor)	Continuous	Very high	-	-	Seabed Surface
SU1	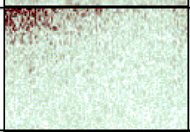	H2	Dis-continuous	Low to moderate	Chaotic	Occasionally Onlap	Holocene marine sands
SU2	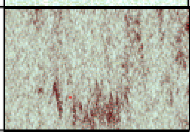	H3	Dis-continuous	Low to moderate	Chaotic	Onlap	Massive sand
SU3	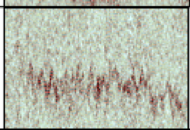	H4	Dis-continuous	Moderate to high	Transparent/ chaotic	-	Reworked till
SU4	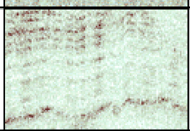	H5	Continuous	Moderate to high	Transparent/ Parallel	-	Stratified sediments
SU5	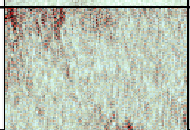	H6	Dis-continuous	Moderate to high	Transparent	-	Glacial Till
SU6	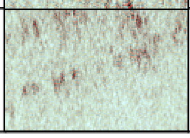	H7	Dis-continuous	Moderate to high	Transparent	-	Till/Bedrock

4.1.1 Seismo-stratigraphic units – description

4.1.1.1 Seabed

The seafloor horizon, denoted as H1, is characterised by strong amplitudes and a continuous reflection (Table 12) with depths ranging from 8.81 m to 135.44 m below LAT (Figure 45). The seafloor morphology exhibits a moderate to high relief topography featuring trochoidal dunes, ripple fields and flat seabed varying throughout the site. Additionally, localised bedrock outcrops (Figure 50) in central and the eastern fringe of the route.

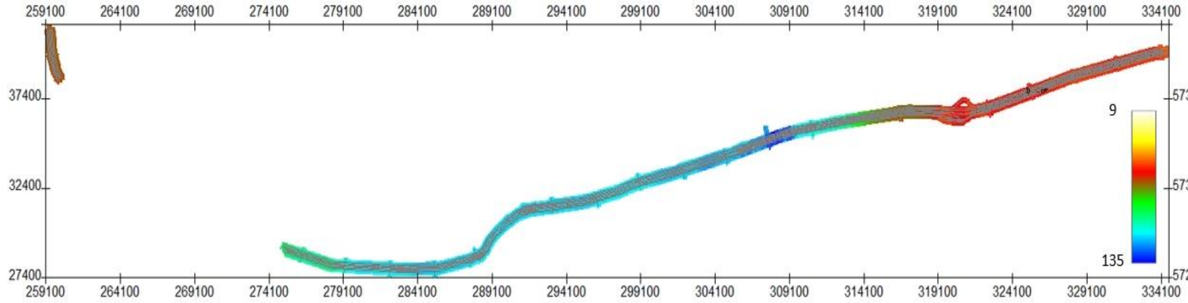

FIGURE 45: SEABED (H1) DEPTH FROM LOWEST ASTRONOMICAL TIDE (LAT) FROM SBP DATA.

4.1.1.2 Seismic Unit 1

Seismic Unit 1, referred to as SU1 (Table 12), is the shallowest (stratigraphically youngest) unit. SU1 is delineated by the discontinuous horizon H2 (top). Acoustically, SU1 is characterised by a high amplitude top reflection i.e.H1, and low to high amplitude base (Figure 46), displaying occasional stratification and cross bedding but typically appears as massive internally. As H2 sits at the seabed surface, it has a depth below seabed value of 0 m (Figure 46).

4.1.1.3 Seismic Unit 2

Seismic Unit 2 (SU2, Table 12) is laterally dis-continuous and is delineated by its top horizon H3 (Figure 46 and Figure 47). Acoustically, SU2 is described as having low to moderate amplitude reflectors with a chaotic internal reflection pattern. SU2 is predominantly found in the west of the site between KP46 – KP62. The depth below seabed values for H3 range from 0.00 - 6.48 m (Figure 46 and Figure 47) with an average depth of 1.24 m and a standard deviation of about 1.20 m.

4.1.1.4 Seismic Unit 3

Seismic Unit 3, referred to as SU3 (Table 12) is discontinuous and is delineated by its top horizon H4. SU3 is characterised as a massive unit of sediment, mostly transparent internally with moderate to relatively low amplitude chaotic reflections. Unit SU3 is similar to SU2, however the erosive top horizon H4 separates the two units marking an unconformity. The depth below seabed values for the top of SU3 (H4) ranges from a 12.93 - 2.68 m, with a mean depth of 8.34 m and a standard deviation of about 2.40 m.

4.1.1.5 Seismic Unit 4

Seismic Unit 4, referred to as SU4 (Table 12), is delineated by the H5 (top) and H6 (bottom) horizons. Internally, SU4 consists of low to moderate amplitude internal reflector displaying a well stratified sediment which appears conformable with the overlying unit SU3 but uncomfortable with SU5 (Figure 47 and Figure 49). The depth below seabed values for the top of SU4 (H5) range from 0.00 – 21.98 m (Figure 46), with an average depth of 12.10 m and a standard deviation of about 5.06 m.

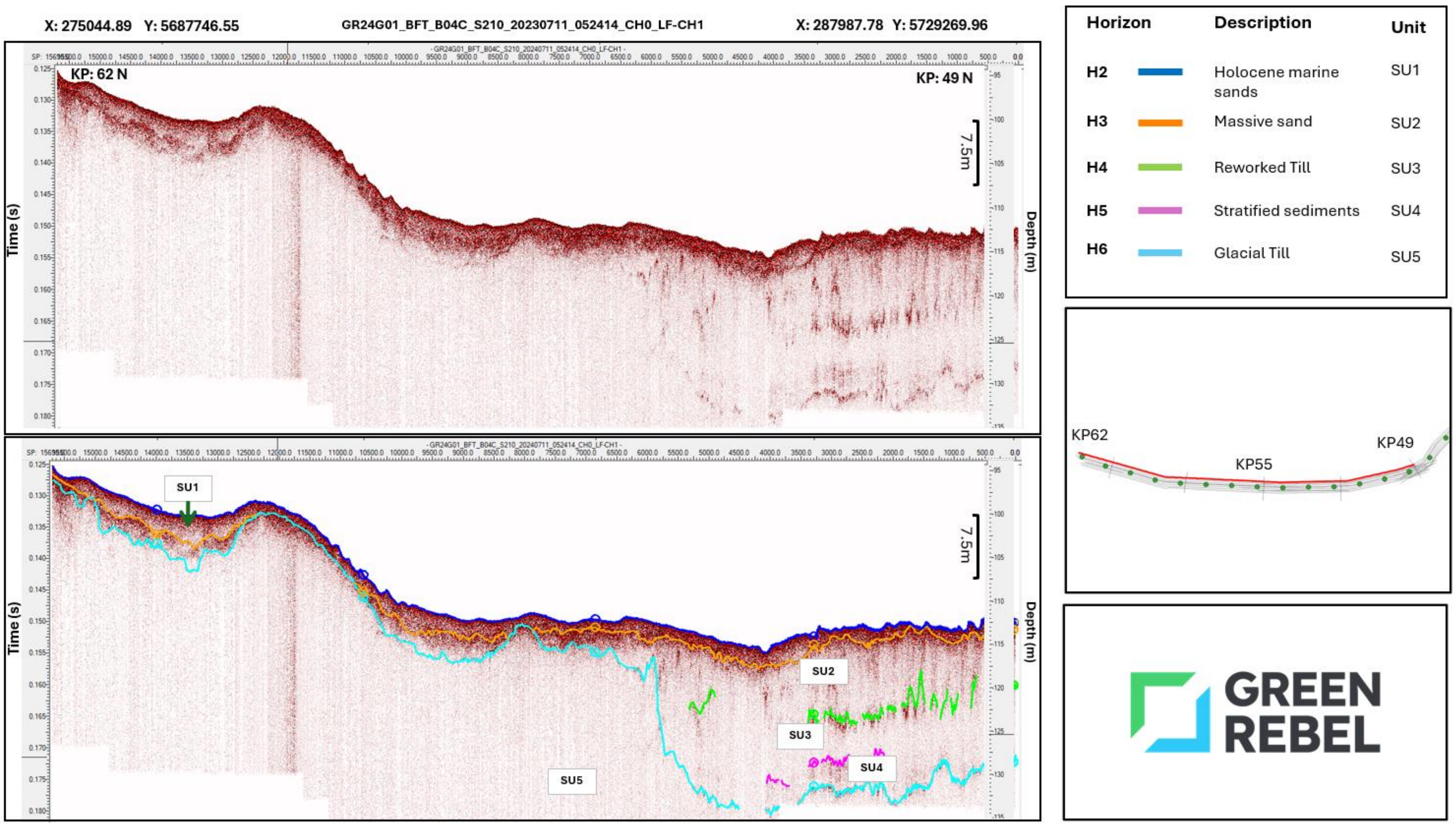

FIGURE 46: REPRESENTATIVE EXAMPLE OF VARIATION IN UNIT THICKNESS AND INTERPRETATION.

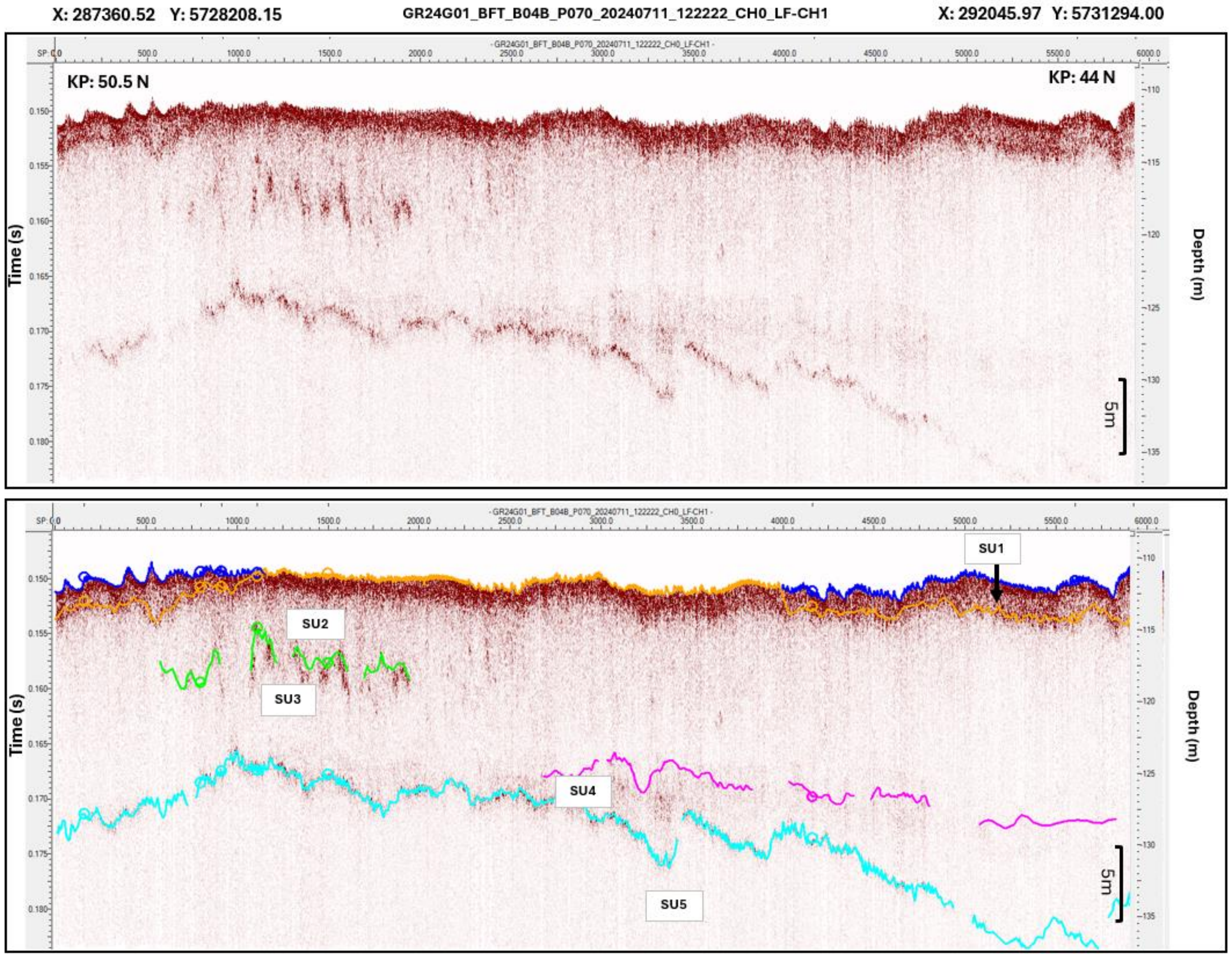

Horizon	Description	Unit
H2	Holocene marine sands	SU1
H3	Massive sand	SU2
H4	Reworked Till	SU3
H5	Stratified sediments	SU4
H6	Glacial Till	SU5

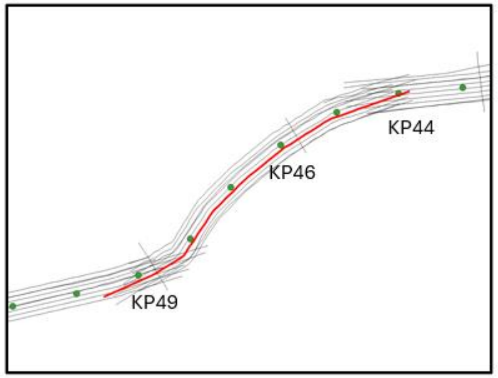

FIGURE 47: EXAMPLE OF STRATIFIED SANDS (SU1) OVERLAYING MASSIVE TO WEAKLY STRATIFIED SANDS (SU2).

4.1.1.6 Seismic Unit 5

Seismic Unit 5, referred to as SU5 (Table 12), is characterised by chaotic reflections (Figure 49) and is delineated by the discontinuous H6 (top) and H7 (bottom) horizons. SU5 is found throughout the survey site. Internally, SU5 displays mostly transparent or chaotic reflectors. SU5 is typically a sub-surface unit, however, it is identified at the seabed in several areas, particularly in the east. The depth below seabed values for the top of SU5 (H6) range from 0.00 - 30.20 m (Figure 49), with an average depth of 9.19 m and a standard deviation of about 7.98 m.

4.1.1.7 Seismic Unit 6

Seismic Unit 6, referred to as SU6 (Table 12), is characterised by the moderate to high amplitude reflection of H7 (top) (Figure 49). Its base is not observed in this survey. Internal reflections within the SU6 are poorly resolved with limited occurrences of low amplitude and chaotic reflections. The depth below seabed values for H7 range from 2.01 – 18.91 m, with an average depth of 6.90 m and a standard deviation of about 3.53 m. From bathymetry and backscatter data, cleavage and bedrock morphology are visible in the east of the site and consequently have been picked as such in the seismic interpretation. Seismic profiles do not display a clear distinction between this outcropping bedrock and the surrounding sediments as there is limited attenuation of seismic signal beneath the surface where this outcrop is identified. Internal reflections within SU6 appear transparent (Figure 51). Bedrock outcrops at the surface between KP 8 and KP 10.

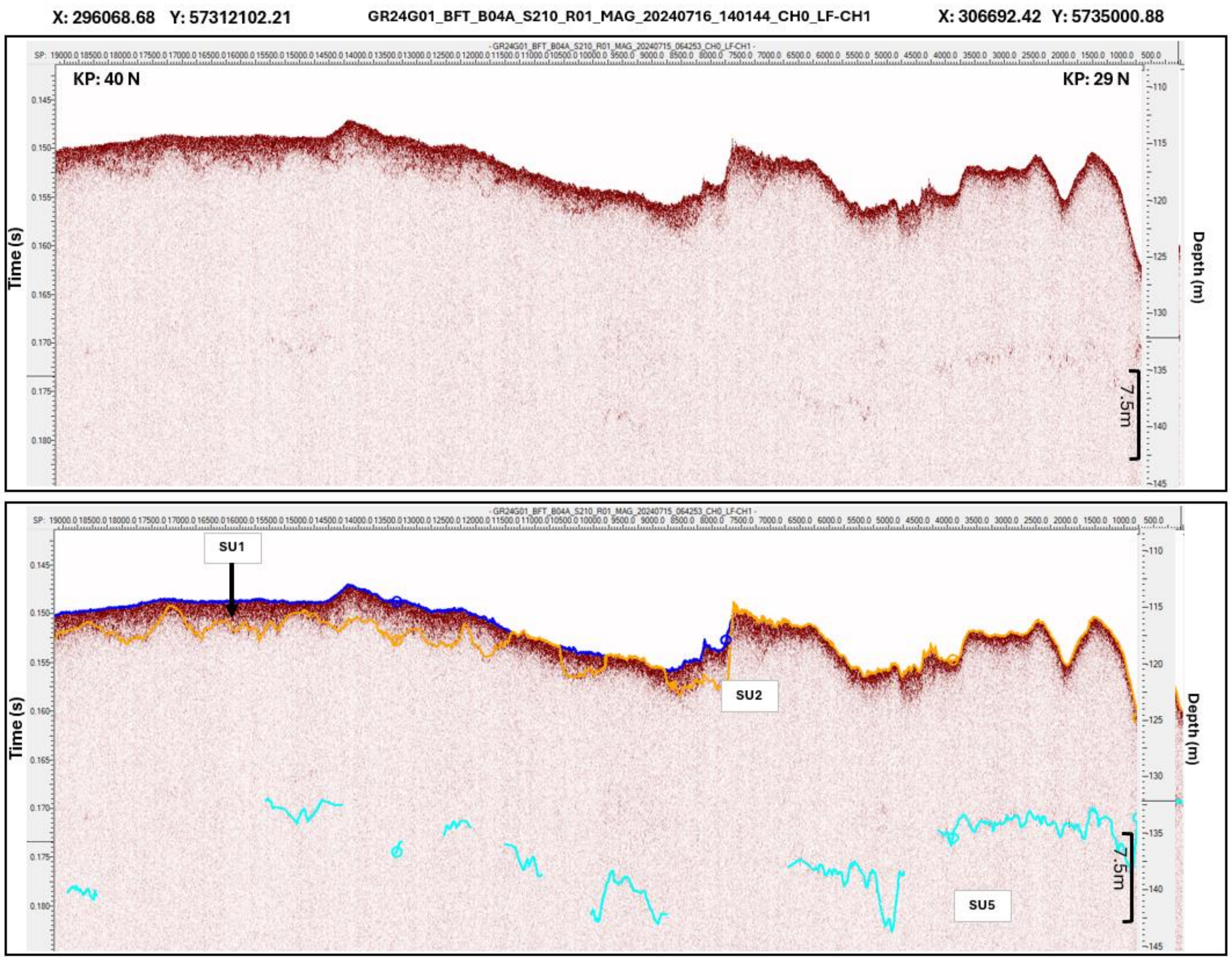

Horizon		Description	Unit
H2		Holocene marine sands	SU1
H3		Massive sand	SU2
H6		Glacial Till	SU5

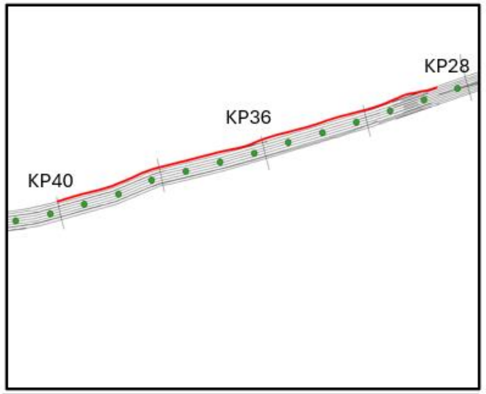

Figure 48: Example of SU1, SU2, and SU5. interaction where SU1 Holocene sands overlies Massive sediment/reworked till SU2.

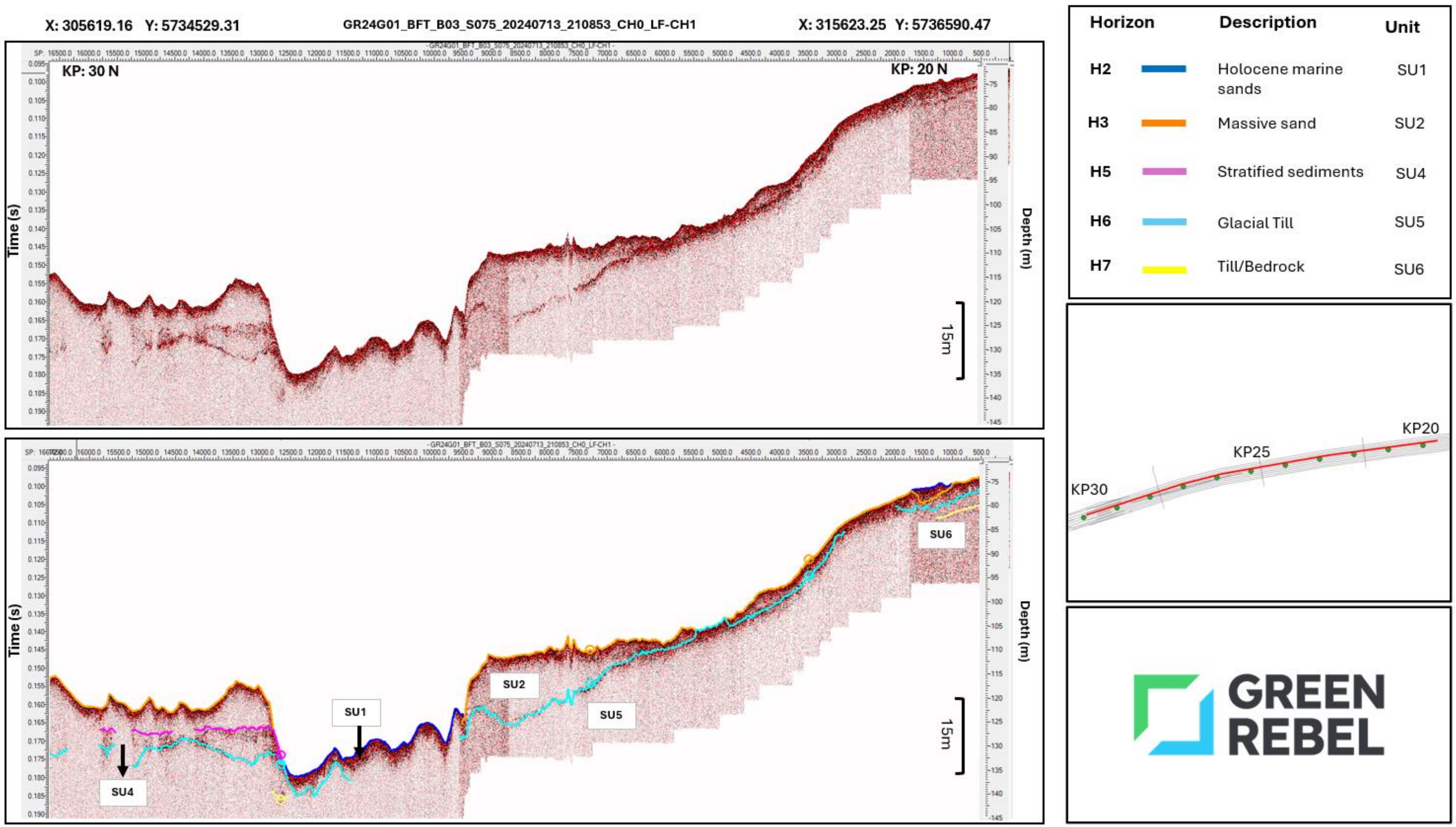

FIGURE 49: EXAMPLE OF MAIN HORIZONS REACHING THE SEABED SURFACE AS WELL AS THE CONFORMABLE CONTACT BETWEEN SU4 AND SU3.

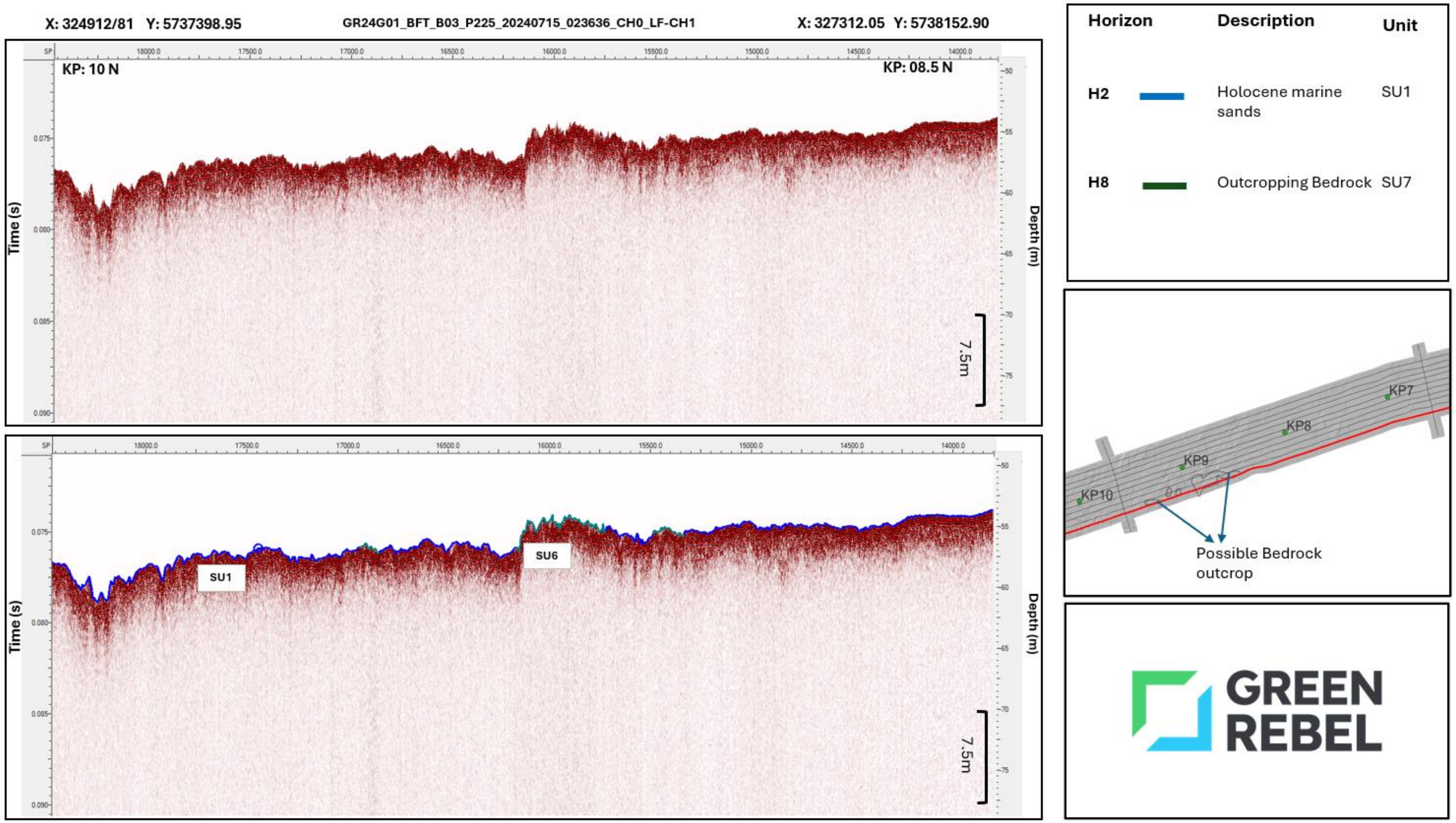

FIGURE 50: EXAMPLE OF BEDROCK OUTCROP SU6 IN SEISMIC SECTION.

4.1.2 Seismo-stratigraphic units – Interpretation

Based on the multibeam backscatter (see section 4.2.2) data and previous scientific investigations (Tóth et al., 2020, Scourse et al., 2019, Emodnet, 2021), the seabed sediment is interpreted as dominant in fine-grained sediments (muds to very fine sands) in the western and eastern sections, with medium and coarse-grained sediments also present but less dominant in the central sections. There are localised occurrences of bedrock outcropping between KP 8 - KP 10. Seven geological substrates (Table 12) are identified in the area including Holocene marine sediment, Quaternary sands and mud deposits, reworked till and till facies overlying pre-quaternary bedrock (Emodnet, 2021). Ground truthing these substrates lies beyond the scope of this body of work. The site is an open marine setting throughout the site with evidence of active sedimentation and transport visible from both surface and subsurface observations.

Seismic Unit 1 (SU1) is stratigraphically the shallowest unit observed in the west of the survey site. Its internal structure and acoustic characteristics (Section 4.1.1) are consistent with recent Holocene sands. Stratification within the unit may be the result of tidal or seasonal variations to sediment supply or current competencies (Figure 47). SU1 is consistent with the presence of a massive, fine - coarse grained sand deposit influenced by the coastal dynamics, tides and currents of the region. SU5 is therefore interpreted as a Holocene marine sands deposit.

Seismic Unit 2 (SU2) is found throughout the survey site typically underlying SU1, occasionally being identified at the seabed surface. This unit typically has an erosional top (H3) with chaotic or transparent internal bedding structures, however due to limited signal attenuation, it is difficult to observe internal structures. The absence of a bedding pattern differs from that of overlying marine sediments and when considered along with the erosional top of H3, SU2 indicates variations in sediment depositional setting or time. Consequently, SU2 may have been deposited as a (de)glacial massive sand deposit during the Weichselian glaciation and is interpreted as a massive sand unit.

Seismic Unit 3 (SU3) is found in the west of the survey site and consists of massive sediment, likely comprised of silt, sand and gravel underlying SU2 and SU3 and overlying SU4. This unit exhibits little internal structure and is demarked by the erosional top H4. Its base appears conformable with SU4 indicating a deposition after SU4 resulting from a change in depositional environment or energy. Considering how consistently H4 appears throughout the surrounding survey lines in the area, and as it is conformable with SU4, SU3 has been separated from SU2 as a distinct unit. Such a deposit is compatible with interpretations of glacial outwash or periods of reworking and winnowing of fine-grained deposits. Consequently, SU3 may have been deposited as a (de)glacial deposit of reworked till during the Weichselian glaciation and is interpreted as a possible reworked till unit.

Seismic Unit 4 (SU4) is a geographically discrete unit localised to the centre of the survey site. Its seismic character is consistent with interbedded muds and sands (see section 4.1.1). Considering the glacial history of the Irish Channel, the relative stratigraphic position of the unit, and the stratified nature of these mud and sand deposits, these sediments were likely deposited during the last (de)glaciation of the Irish Sea. The stratification observed in SU4 (Figure 46) is compatible with a glacial or ice-proximal setting where seasonal changes affect sediment delivery to fluvial, lacustrine, and marine environments. This is consistent with some Weichselian deposits previously identified in the Irish Sea (Scourse et al, 2019). SU4 is interpreted as stratified sediments associated.

Seismic Unit 5 (SU5) has transparent internal reflectors due to the unsorted and massive composition of the sediment limiting seismic attenuation. Overlying SU5 are Holocene (SU1), and three glacial associated sediments (SU2, SU3 and SU4). Consequently, SU5 is likely composed of glacial till consistent with previous interpretations of the Irish Sea (Mellet et al., 2015; Fugro, 2021.,) of glacial till overlain by reworked till (south of Tramore by Tóth et al., 2020, or north of Anglesey by Scourse et al., 2019. Glacial till is formed because of multiple glacial advances and retreats, particularly in the last major glaciation, known as the Late Devensian or Weichselian glaciation lasting from ~30 to 22 Ka (Hubbard et al, 2009).

Seismic Unit 6 (SU6) is observed throughout the site. The transparency and lack of internal reflectors makes it difficult to interpret the composition of this unit. Where bedrock is identified as outcropping, previously interpretations have identified this bedrock as Cambrian-Silurian mudstone (Emodnet, 2021). From bathymetry and backscatter analysis, there is evident bedding structures exposed at the surface in the east of the surveyed area despite not being readily visible from the seismic profiles. No other occurrence of outcropping bedrock was observed. Although SU6 is picked in other areas throughout the site, it may not represent bedrock in those areas. In some instance this may represent other units of glacial till or bedrock, however due to the transparent nature and depth of these horizons, it is not possible to infer their composition. SU6 is therefore interpreted as probable bedrock or glacial till.

4.2 Potential Engineering Geohazards

4.2.1 Surface Geohazards

4.2.1.1 Gradients and sediment mobility

High gradients are generally present around outstanding seabed obstacles. The highest slope values at the Beaufort site are observed where sediment waves and other surface geomorphological features of various scales occur (Figure 51). Elsewhere, the site exhibits a gently sloping/flat seabed.

Locally, the site displays enhanced sediment mobility in the form of migrating sediment waves of various scales (from small to very large). This indicates that tidal currents are capable of mobilizing sediments and initiating bedload transport. Considering the scale of some of the very large trochoidal bedforms observed at the site (Figure 52), which reach up to 20 m in height above the surrounding seabed and more than 200 m in width, the tidal currents magnitude can be assumed as significant and may induce additional risk for further operations. Although the largest sediment waves may be relict features produced by past hydrodynamic regimes, the interaction between new cable infrastructure and any observed sediment waves should be considered, as seabed feedback in the form of enhanced erosion (scour) and sediment redeposition may occur after installation.

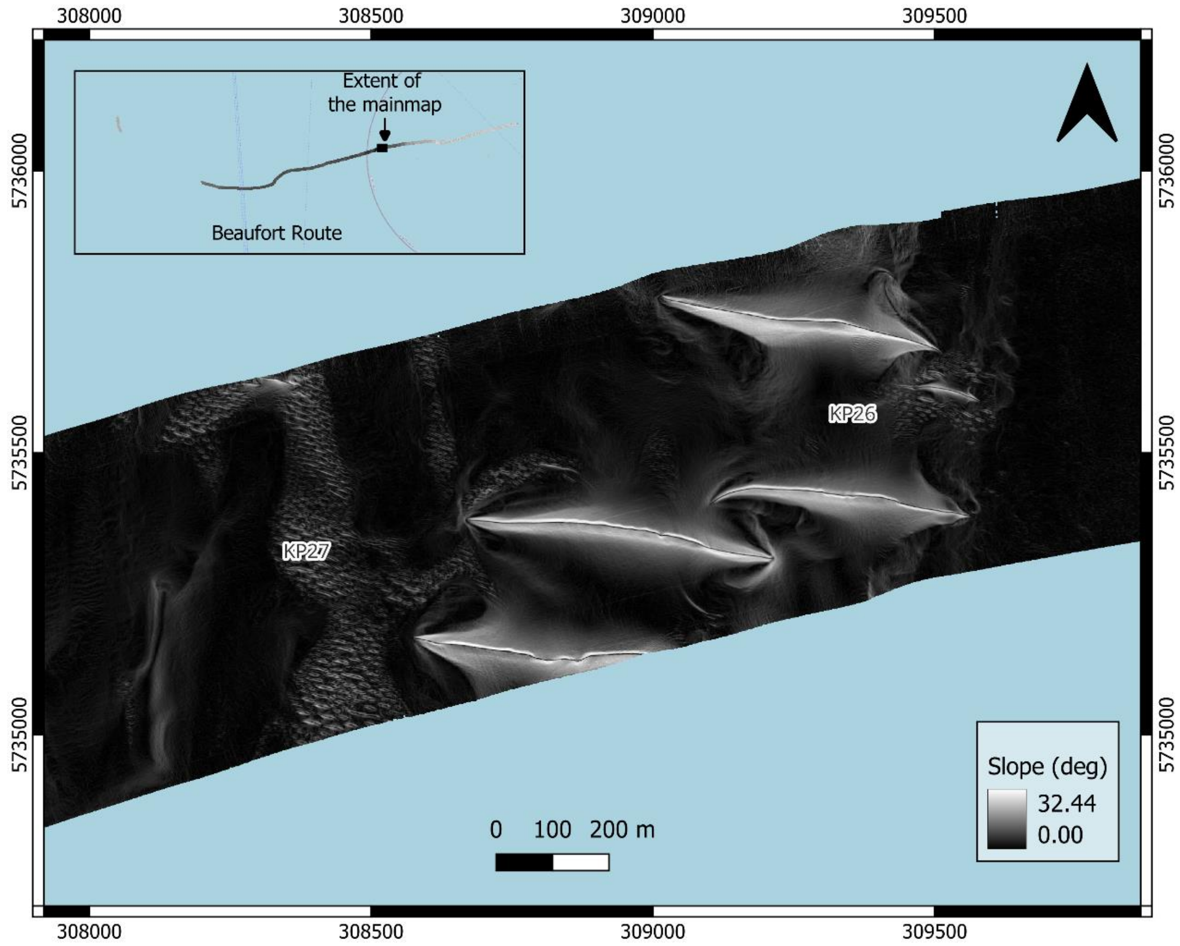

Figure 51: Gradients (slope) are high near sediment waves present at the site. Slope values are expressed in degrees.

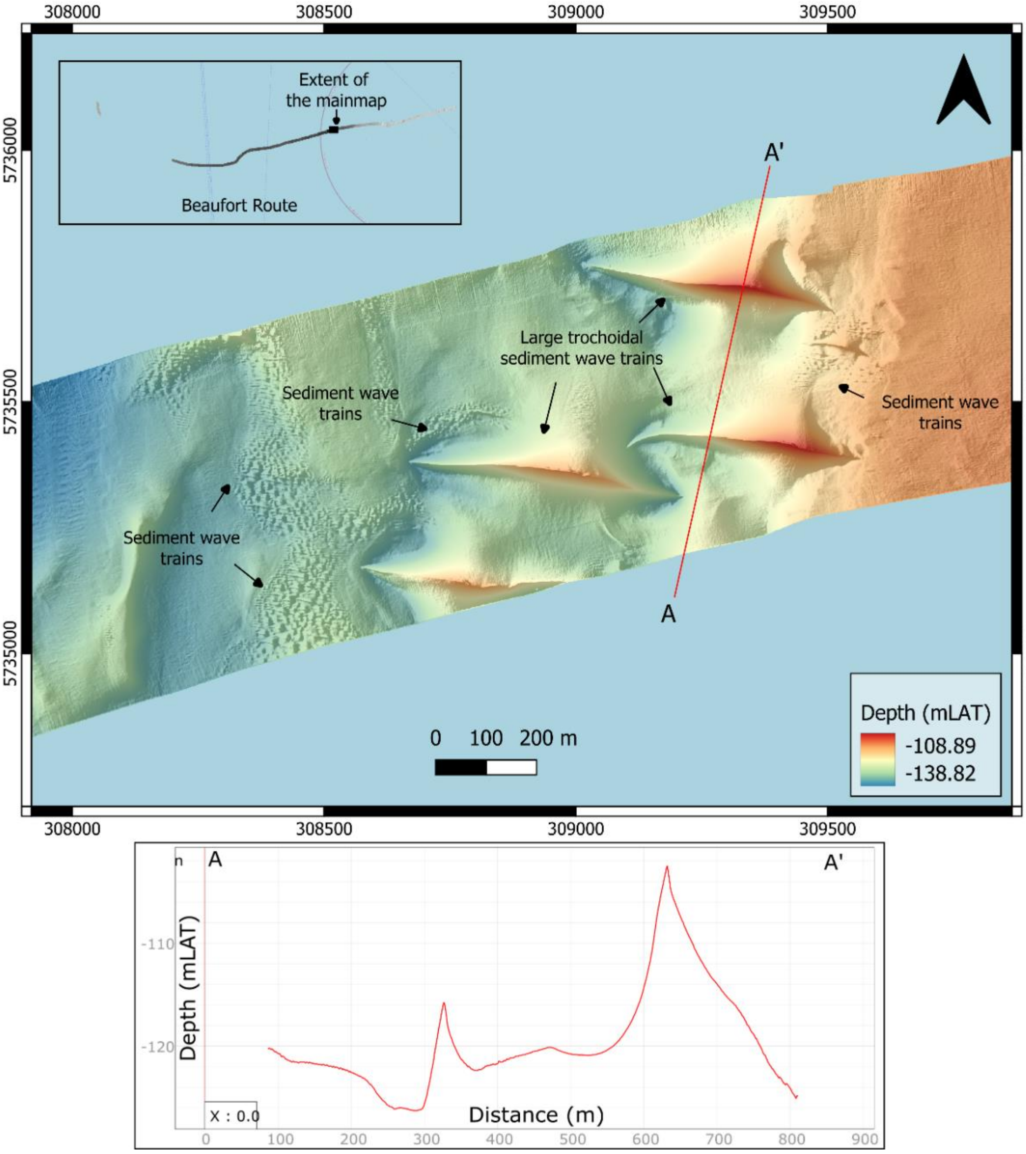

FIGURE 52: SEDIMENT WAVES OF VARIOUS SCALES PRESENT NEAR KP26 OF THE SECTION 1. THE CROSS SECTION PROFILE BELOW THE MAIN MAP FIGURE SHOWS A BATHYMETRIC PROFILE DENOTED BY A – A'.

4.2.1.2 Boulders

Altogether, 3072 boulders were observed across the Beaufort site in the SSS waterfall display. Their locations and individual attributes are delivered in the contacts shapefile layer.

4.2.1.3 Anthropogenic

Anthropogenic targets like wrecks, unexploded ordnance or other manmade debris can pose significant risks to subsea developments, hence special care is taken during contact picking to detect them. At KP 1.414 of the

Section 2, a linear feature can be observed throughout all the acquired datasets (Figure 53). Although its identity cannot be confirmed, it is most probably a subsea cable. The Greenlink HVDC Interconnector cable runs through/nearby the survey area according to the developer's website (EirGrid), suggesting that this linear feature could be interpreted as that cable.

Additionally, trawl marks are observed to intersect the cable (Figure 53). Bottom-contact fishing can be hazardous to subsea infrastructure and this evidence of trawling should be considered when planning the cable route. Noteworthy, trawl marks are uniquitous across the survey area.

The Greenlink HVDC Interconnector cable was also observed at KP 47.74 of Section 1 in all the datasets (see section 4.3.4; Figure 37 for the sidescan image). Its identity could not be confirmed using open-source cable infrastructure information available online (ArcGIS Hub; EMODNet Human Activities).

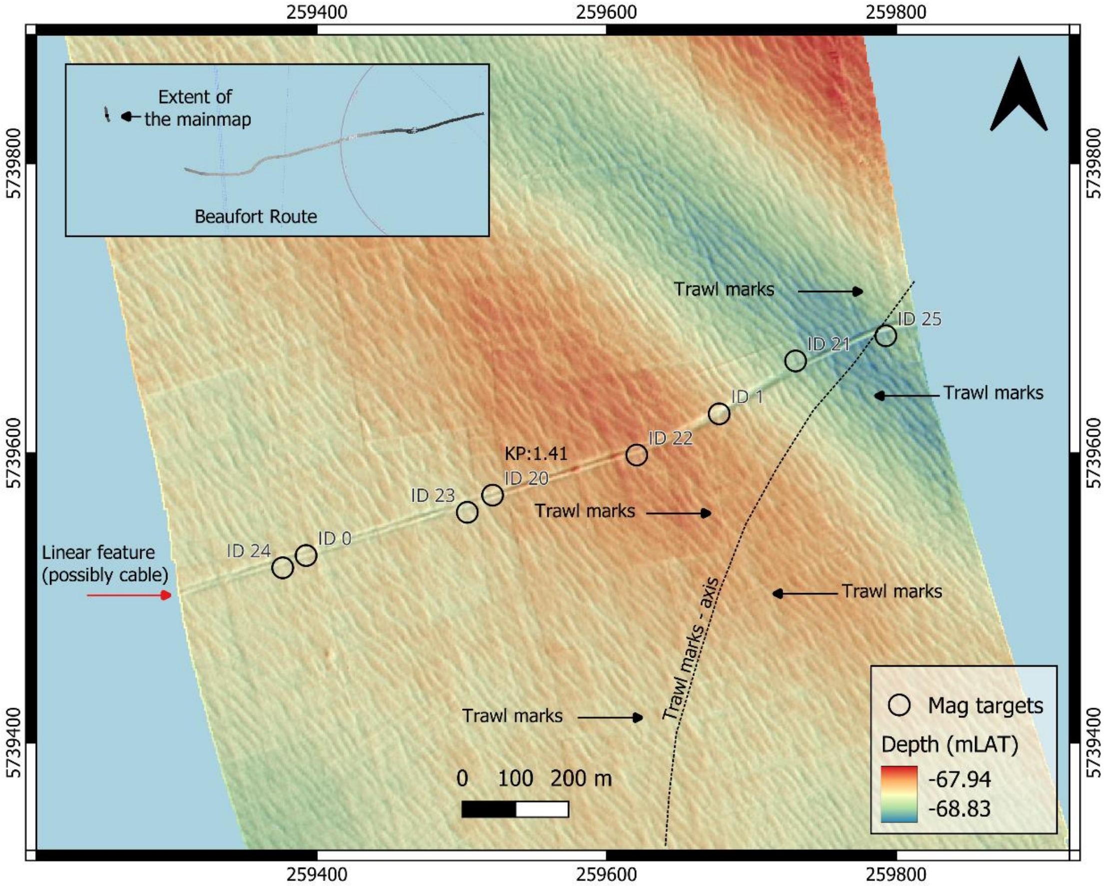

FIGURE 53: LINEAR FEATURE VISIBLE AT KP: 1.41 (SECTION 2) THROUGHOUT THE DATASETS WHICH IS INTERPRETED AS A CABLE CROSSING THE SURVEY AREA. SEDIMENT WAVES AND TRAWL MARKS ARE OBSERVED IN IMMEDIATE VICINITY OF THE LINEAR FEATURE.

4.2.2 Subsurface Geohazards

There were no evident seismic geohazards identified across the survey.

5 Conclusions and Recommendations

MBES Bathymetry data provided a high-resolution insight into the topographic variability of the site, characterized by high and lows associated with sediment wave fields, flat seabeds and high slopes related to trenches. MBES backscatter reveals fine-, medium- and coarse-grained sediments with some bedrock outcrops present along the Beaufort corridor. A targeted geotechnical survey campaign will help providing greater confidence in the surface and sub seabed substrate estimations. SSS contact picking highlight the prevalence of glaciomarine deposition in the region. A high concentration of boulders is present in some sectors of the site and should be considered during the further cable infrastructure planning and development. The magnetometer data helped ascertain regions of anomalous magnetic properties.

Sub bottom profiler data provided detailed insight into the stratigraphy and complexity of the subsurface of the site. From seismo-stratigraphic analysis, six seismic units with distinct acoustic signatures were identified indicating varying depositional environments and processes. The seabed, marked by a continuous reflection, is characterised by trochoidal dunes, rippled fields and bedrock outcrops observed in both the central and eastern sections. Seismic Unit 1 (SU1), the shallowest layer, is consistent with Holocene sands while Seismic Unit 2 and 3 suggest a glacial setting associated with the Weichselian glaciation. SU4, found in the central area, contains interbedded muds and sands consistent with a glacial-proximal environment. Deeper units, SU5 and SU6, exhibit characteristics of glacial till and bedrock, with SU6's transparent reflection suggesting bedrock outcropping or deep glacial deposits. Future ground-truthing surveys, including geotechnical sampling, will help refine substrate composition and support infrastructure planning by confirming sediment stability and bedrock positioning.

6 Appendices

6.1 Appendix 1

Seismic data handling

Raw Innomar sub-bottom *.ses3 data were converted to SEGY before importing into SonarWiz. SEGY is a universal sonar format that can be edited and viewed in various software and programs. By importing the SEGY format, the trace headers were adjusted and edited within the software with additional gains, offsets and filters applied to the original file. Information pertaining to the handling of seismic data is provided below.

Relevant bytes for the processed Innomar SBP .sgy data

SEG-Y bytes	***Property***
All co-ordinates, depths and times multiplied by a scalar equal to 100. Big Endian byte order, IEEE Float 32 Bit	
1-4	Trace sequence number
9-12	Original Field Record Number
73-76	Source X co-ordinate, scalar=100
77-80	Source Y co-ordinate, scalar=100
109-110	Delay recording time (storing vertical corrections for the time domain data), scalar=100
49-52	Source depth (storing vertical corrections for the depth domain data), scalar=100 Velocities used for TWT/Depth conversion: 1500 m/s water, 1600 m/s sediments

Relevant SIS strings for the Innomar SBP .raw/.ses3 data

SIS string	***Property***
SIS 1	Time
SIS 7	Easting
SIS 8	Northing

Opening the data in SonarWiz

The project data can be viewed in SonarWiz should access have been granted via a project *.mml file within CTI SonarWiz. The project file is all encompassing and self-contained so by ensuring that the project files are kept together in the same folder and unedited or moved, it will open with all project features and files.

When importing the data into a new SonarWiz project the features and sonar files must be imported with the correct coordinate system. SonarWiz digitiser can only read water column data within the profile viewer. As such, to plot the digitised reflectors correctly, the sound and sediment velocity values must be the same. For example, this can be done by changing the water velocity figure (1500 ms^{-1}) to match the sediment velocity (1600 ms^{-1}) of the file. This process requires that you make the edits in the properties window for the file which is located under the Project Explorer tree.

Interpolating horizons to elevation and isopach grids

The delineated horizons were exported from SonarWiz as ASCII files with x,y,z values corresponding to easting, northing and meters below LAT, respectively. The exported data were examined for outliers using QPS Qimera. Subsequently, the ASCII files were imported to Surfer v23.3., where the kriging algorithm with sector search was implemented to produce elevation grids. To produce the depth below seabed grids, the grids corresponding to the delineated horizons were subtracted from the elevation grids representing the seabed surface horizons H1.

Creation of the isopach grids for the relevant units involved two steps. Firstly, the elevation grids corresponding to the units overtopping every reference unit were merged using spatial analyst mosaicking tools available in ArcMap v.10.8.1. For example, to create an isopach for the unit 4, elevation grids for the units 1, 2 and 3 were merged. Merging was performed to ensure that thickness of every reference unit is calculated. This allowed to create the thickness rasters (i.e., isopachs) by subtracting the reference units from the merged grids comprising the closest overtopping unit elevations.

The resulting isopach and depth below seabed grids contained outliers (negative values), suggesting intersection of the units with their overtopping counterparts. These false values arise from localised interpolation errors and were corrected for using QGIS Desktop v. 3.22.6. Additional smoothing and artefact corrections were applied using grid editing tools in Surfer v23.3

References

ArcGIS Hub, Global Submarine Cables, https://hub.arcgis.com/datasets/EsriOceans::global-submarine-cables-1/explore?layer=1&location=52.856047%2C-2.763853%2C5.82, last accessed 28.10.2024.

EMODNet, 2021. https://emodnet.ec.europa.eu/en/geology, last accessed 28.10.2024.

EMODNet Human Activities. Human Activities | European Marine Observation and Data Network (EMODnet), last accessed 28.10.2024.

Fugro, 2021, 003700854 03, WPM2 & WPM3 ECR East A & B-Seafloor and Shallow Geological Results Report, Awel Y Môr Offshore Windfarm Ltd. Available at: https://infrastructure.planninginspectorate.gov.uk/wp-content/ipc/uploads/projects/EN010112/EN010112-000230-6.4.2.5.1_AyM_ES_Volume4_Annex2.5_GeologicalResultsECC_vFinal_Part1.pdf

Hubbard, A., Bradwell, T., Golledge, N., Hall, A., Patton, H., Sugden, D., Cooper, R. and Stoker, M., 2009. Dynamic cycles, ice streams and their impact on the extent, chronology and deglaciation of the British–Irish ice sheet. *Quaternary Science Reviews*, *28*(7-8), pp.758-776. https://www.sciencedirect.com/science/article/abs/pii/S0277379109000201

Li J, Gu Q, Chen Y, Sun G, Huang H. 2018. A Combined Ray Tracing Method for Improving the Precision of the USBL Positioning System in Smart Ocean. Sensors (Basel). **18(10)**:3586. https://doi.org/10.3390/s18103586

Mellet C., Long D., Carter G., et al (2015) Geology of the seabed and shallow subsurface: the Irish Sea. British Geological Survey Commissioned Report, CR/15/057. 52pp

Scourse, J.D., Saher, M.H., Landeghem, K.J., Lockhart, E.A., Purcell, C., Callard, L., Roseby, Z.A., Allinson, B., Pieńkowski, A.J., O'cofaigh, C., Praeg, D., Ward, S.L., Chiverrell, R.C., Moreton, S.G., Fabel, D., & Clark, C.D. (2019). Advance and retreat of the marine-terminating Irish Sea Ice Stream into the Celtic Sea during the Last Glacial: Timing and maximum extent. Marine Geology, **412**, 53–68. https://doi.org/10.1016/j.quascirev.2009.08.009

Tóth, Z., Mccarron, S., Wheeler, A. J., Wenau, S., Davis, S., Lim, A. & Spiess, V. 2020. Geomorphological and Seismostratigraphic Evidence for Multidirectional Polyphase Glaciation of the Northern Celtic Sea. Journal of Quaternary Science, **35**, 1–14. http://dx.doi.org/10.1002/jqs.3189